

Final Report Compilation for Night Ventilation with Building Thermal Mass

TECHNICAL REPORT



October 2003
P-500-03-096-A9



Gray Davis, *Governor*

CALIFORNIA ENERGY COMMISSION

Prepared By:
Architectural Energy Corporation
Vernon A. Smith
Boulder, CO

Purdue University
James Braun
West Lafayette, IN

CEC Contract No. 400-99-011

Prepared For:
Christopher Scruton
Contract Manager

Nancy Jenkins
PIER Buildings Program Manager

Terry Surles
PIER Program Director

Robert L. Therkelsen
Executive Director

DISCLAIMER

This report was prepared as the result of work sponsored by the California Energy Commission. It does not necessarily represent the views of the Energy Commission, its employees or the State of California. The Energy Commission, the State of California, its employees, contractors and subcontractors make no warrant, express or implied, and assume no legal liability for the information in this report; nor does any party represent that the uses of this information will not infringe upon privately owned rights. This report has not been approved or disapproved by the California Energy Commission nor has the California Energy Commission passed upon the accuracy or adequacy of the information in this report.

Acknowledgements

Jim Braun and Zhipeng Zhong of Purdue University conducted this research project. Todd Rossi and Doug Dietrich of Field Diagnostic Services, Inc., provided data collection services and field support. Lanny Ross with Newport Design Consultants provided field support as well.

Preface

The Public Interest Energy Research (PIER) Program supports public interest energy research and development that will help improve the quality of life in California by bringing environmentally safe, affordable, and reliable energy services and products to the marketplace.

The Program's final report and its attachments are intended to provide a complete record of the objectives, methods, findings and accomplishments of the Energy Efficient and Affordable Commercial and Residential Buildings Program. This attachment is a compilation of reports from Project 3.2, *Night Ventilation with Building Thermal Mass*, providing supplemental information to the final report (Commission publication #P500-03-096). The reports, and particularly the attachments, are highly applicable to architects, designers, contractors, building owners and operators, manufacturers, researchers, and the energy efficiency community.

This document is one of 17 technical attachments to the final report, consolidating two research reports from Project 3.2:

- [*VSAT – Ventilation Strategy Assessment Tool. \(Aug 2003\)*](#)
- [*Development and Evaluation of a Night Ventilation Precooling Algorithm \(Aug 2003\)*](#)

The Buildings Program Area within the Public Interest Energy Research (PIER) Program produced this document as part of a multi-project programmatic contract (#400-99-011). The Buildings Program includes new and existing buildings in both the residential and the nonresidential sectors. The program seeks to decrease building energy use through research that will develop or improve energy-efficient technologies, strategies, tools, and building performance evaluation methods.

For the final report, other attachments or reports produced within this contract, or to obtain more information on the PIER Program, please visit www.energy.ca.gov/pier/buildings or contact the Commission's Publications Unit at 916-654-5200. The reports and attachments, as well as the individual research reports, are also available at www.archenergy.com.

Abstract

Project 3.2, *Night Ventilation with Building Thermal Mass*

As an alternative to leaving HVAC equipment off during unoccupied hours, this project examined ventilating with cool air during night and early morning hours to lower the temperature of the building mass. Taking advantage of the thermal storage capabilities of the building structure, this technique can shift a significant portion of a building's on-peak cooling requirements to off-peak periods, reducing both energy and demand costs. The goal of the project was to develop a simple, low-cost algorithm that could be integrated within a controller for packaged air conditioners with economizers, such as rooftop units.

- The algorithm was tested in simulations and a retail building located in southern California. The simulated building types included small office buildings, sit-down restaurants, retail stores, and schools (spaces including classroom wing, auditorium, gymnasium, and library).
- The greatest savings were predicted for buildings in coastal climates. Significant savings were also predicted for hot inland climates.
- The electrical energy savings varied between zero and about 8%. The electrical demand cost savings associated with night ventilation varied between zero and about 28%, whereas the total electrical cost savings ranged from zero to about 17%.

This document is a compilation of two technical reports from the research.

VSAT – Ventilation Strategy Assessment Tool

Submitted to

California Energy Commission

As Deliverables 3.1.2, 3.2.1, and 4.2.2

Prepared by

**James E. Braun and Kevin Mercer
Purdue University**

Revised August 2003

Table of Contents

SECTION 1: INTRODUCTION	1
SECTION 2: BUILDING MODEL	3
2.1 Model Description	3
2.1.1 Exterior Walls and Roofs	3
2.1.2 Floor Slabs	7
2.1.3 Interior Walls	7
2.1.4 Windows	8
2.1.5 Infiltration	9
2.1.7 Internal Gains	10
2.1.8 Zone Loads	10
2.1.9 Solar Radiation Processing	11
2.2 Prototypical Building Descriptions	11
2.3 Model Validation	20
2.3.1 TYPE 56 and VSAT Building Model Assumptions	20
2.3.2 Case Study Description	21
2.3.3 Results for Constant Temperature Setpoints	22
2.3.4 Results for Night Setback/ Setup Control	24
2.3.5 Conclusions	26
SECTION 3: HEATING AND COOLING EQUIPMENT MODELS	27
3.1 Vapor Compression System Modeling	28
3.1.1 Mathematical Description	28
3.1.2 Prototypical Rooftop Air Conditioner Characteristics	33
3.1.3 Heat Pump Heat Recovery Unit (Energy Recycler[®])	35
3.2 Primary Heater	40
3.3 Enthalpy Exchanger	40
3.3.1 Mathematical Description	40
3.3.2 Prototypical Exchanger Descriptions	43
SECTION 4: AIR DISTRIBUTION SYSTEM AND CONTROLS	45
4.1 Ventilation Flow	45
4.1.1 Fixed Ventilation	45
4.1.2 Demand-Controlled Ventilation	46
4.1.3 Economizer	46
4.1.4 Night Ventilation Precooling	47
4.2 Mixed Air Conditions	48
4.3 Equipment Heating Requirements	49
4.3.1 Heat Pump Heat Recovery Unit	49
4.3.2 Primary Heater	49
4.4 Equipment Cooling Requirements	50
4.4.1 Heat Pump Heat Recovery Unit	50
4.4.2 Primary Air Conditioner	50
4.5 Supply, Ventilation, and Exhaust Fans	51
4.6 Zone Controls – Call for Heating or Cooling	52

<u>SECTION 5: WEATHER DATA, SIZING, AND COSTS</u>	53
<u>5.1 Weather Data</u>	53
<u>5.2 Equipment Sizing</u>	54
<u>5.3 Costs</u>	54
<u>SECTION 6: SAMPLE RESULTS AND COMPARISONS WITH ENERGY-10</u>	57
<u>6.1 Sample Results</u>	57
<u>6.2 Comparisons with Energy-10</u>	59
<u>SECTION 7: REFERENCES</u>	64

SECTION 1: INTRODUCTION

This report describes a simulation tool (VSAT – Ventilation Strategy Assessment Tool) that estimates cost savings associated with different ventilation strategies for small commercial buildings. A set of prototypical buildings and equipment is part of the model. The tool is not meant for design or retrofit analysis of a specific building. It does provide a quick assessment of alternative ventilation technologies for common building types and specific locations with minimal input requirements.

Figure 1 shows a schematic of a small commercial building and HVAC system. The buildings currently considered within VSAT include a small office building, a sit-down restaurant, a retail store, a school class wing, a school auditorium, a school gymnasium, and a school library. All of these buildings are considered to be single zone with a slab on grade (no basement or crawl space). VSAT considers only packaged HVAC equipment, such as rooftop air conditioners with integrated cooling equipment, heating equipment, supply fan, and ventilation. Modifications to the ventilation system are the focus of the tool's evaluation. A basic ventilation system (shown within the box of Figure 1) consists of ambient supply, exhaust, and return ducts and dampers. The different ventilation strategies that are considered by VSAT are: 1) fixed ventilation rates with no economizer, 2) fixed ventilation rates with a differential enthalpy economizer, 3) demand-controlled ventilation with an economizer, 4) fixed ventilation rates with heat recovery using an enthalpy exchanger, 5) fixed ventilation rates with heat recovery using a heat pump, 6) night ventilation precooling, 7) night ventilation precooling with an economizer, and 8) night ventilation precooling with demand-control ventilation and an economizer. Details about these strategies are given in later sections.

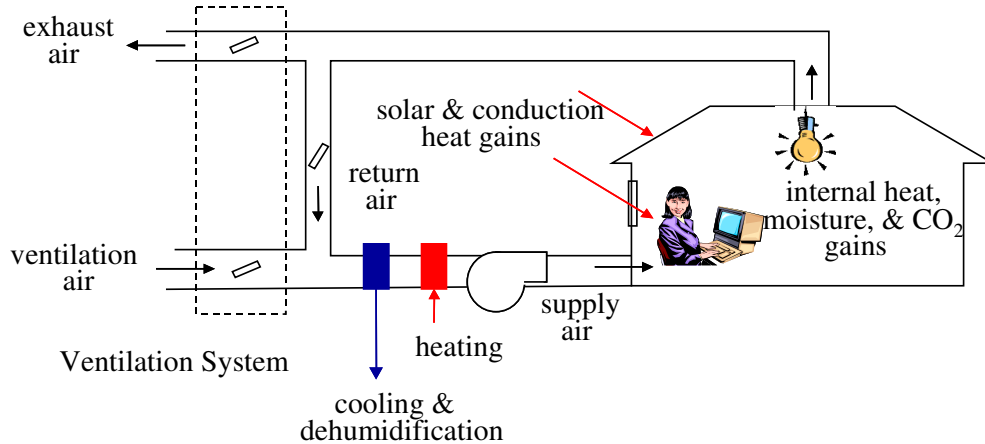


Figure 1. Schematic of a Small Commercial Building and HVAC System

VSAT is derived from a simulation tool that was developed by Braun and Brandemuehl (2002) called the Savings Estimator. It performs calculations for each hour of the year using fairly detailed models and TMY2 or California Climate Zone weather data. The goal in developing VSAT was to have a fast, robust simulation tool for comparison of ventilation options that could consider large parametric studies involving different systems and locations. Existing commercial simulation tools do not consider all of the ventilation options of interest

for this project.

Figure 2 shows an approximate flow diagram for the modeling approach used within VSAT. Given a physical building description, an occupancy schedule, and thermostat control strategy, the building model provides hourly estimates of the sensible cooling and heating requirements needed to keep the zone temperatures at cooling and heating setpoints. It involves calculation of transient heat transfer from the building structure and internal sources (e.g., lights, people, and equipment). The air distribution model solves energy and mass balances for the zone and air distribution system and determines mixed air conditions supplied to the equipment. The mixed air condition supplied to the primary HVAC equipment depends upon the ventilation strategy employed. The zone temperatures are outputs from the building model, whereas the zone and return air humidities and CO₂ concentrations are calculated by the air distribution model. The equipment model uses entering conditions and the sensible cooling requirement to determine the average supply air conditions. The entering and exit air conditions for the air distribution and equipment models are determined iteratively at each timestep of the simulation using a non-linear equation solver. Details of each of the component models are described in later sections.

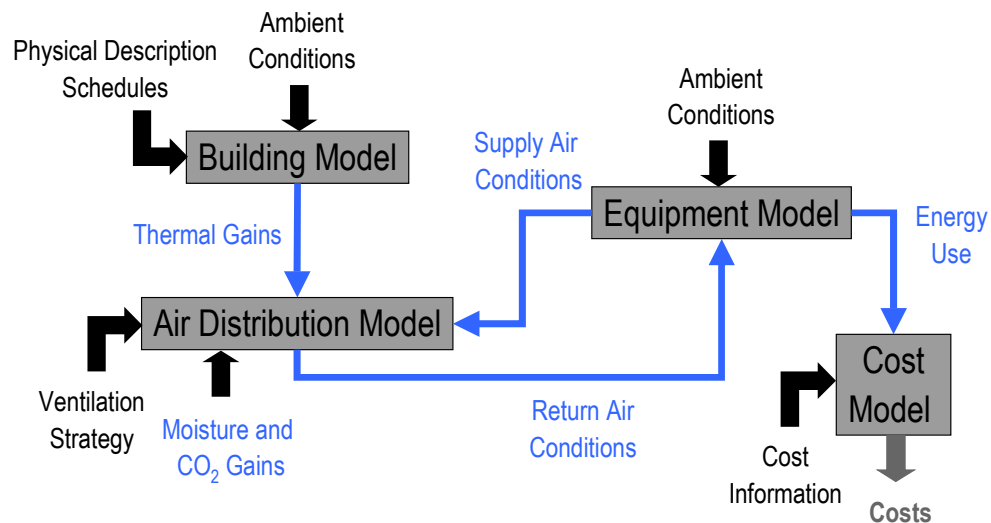


Figure 2. Schematic of VSAT Modeling Approach

SECTION 2: BUILDING MODEL

The space loads are based on the building physical characteristics, operating schedule, occupancy patterns, and space setpoints. The total sensible loads are calculated from an energy balance on the zone air for a given temperature setpoint with individual heat gains from walls, roof, floor, windows, internal gains, and infiltration. The following sections describe individual models for each of these elements and the overall strategy for estimating sensible cooling and heating requirements for the building.

2.1 Model Description

2.1.1 Exterior Walls and Roofs

Figure 3 shows the heat transfer rates and nomenclature associated with an external wall or roof (j^{th} wall). One-dimensional heat transfer is assumed. The symbols \dot{Q} and T denote heat transfer rates and temperatures, respectively. The subscripts i and o refer to conditions at the inside and outside of the wall, respectively. The subscript c refers to convection, whereas r denotes radiation. The subscript s refers to conduction within the wall at the surface (inside or outside).

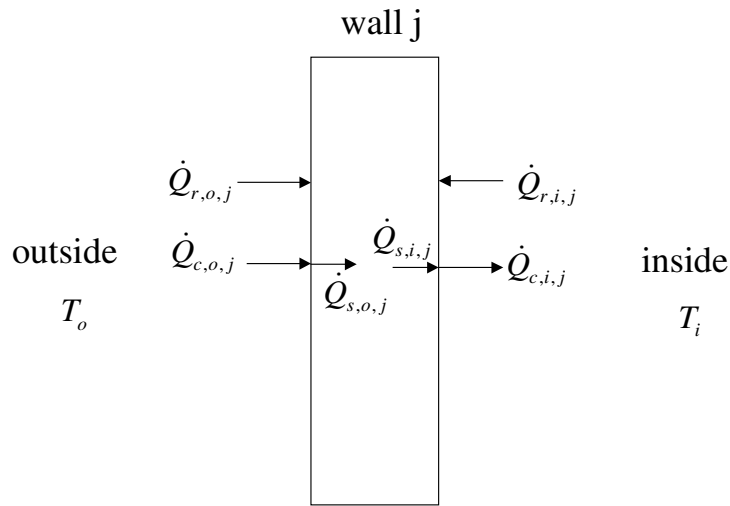


Figure 3. Heat transfer rates for an external wall

Radiation at the outside of the wall is due to solar (short-wave radiation) and long-wave radiation exchange with the sky and other surfaces. Long-wave radiation is assumed to occur between the wall surface and other surfaces that are at the ambient temperature (T_o). Furthermore, the radiation is linearized so that a radiation heat transfer coefficient is determined at a representative mean temperature. The long-wave radiation is combined with the convection using a combined convection and long-wave radiation heat transfer coefficient. With these assumptions, the effective outside convection (convection and long-wave radiation) and radiation (short-wave only) for wall j are calculated as

$$\dot{Q}_{c,o,j} = h_o A_j (T_o - T_{s,o,j}) \quad (2.1)$$

$$\dot{Q}_{r,o,j} = \alpha_o A_j I_{o,j} \quad (2.2)$$

where h_o is the outside heat transfer coefficient (convection and long-wave radiation), A is wall surface area, α_o is the absorptance for solar radiation of the outside surface, I_o is the instantaneous radiation incident upon the outside surface. The outside heat transfer coefficient and absorptance are assumed to be constant, independent of operating conditions (e.g., wind speed).

The conduction at the outside surface of the wall is equal to the sum of the convective and radiative gains. In order to simplify the transient heat transfer calculations, an equivalent outside air temperature is defined that would give the correct heat transfer rate in the absence of the solar radiation gains. This is commonly referred to as the sol-air temperature and is calculated as

$$T_{eq,o,j} = T_o + \frac{\alpha_o I_{o,j}}{h_o} \quad (2.3)$$

With this definition, the conduction heat transfer rate at the outside surface is

$$\dot{Q}_{s,o,j} = h_o A_j (T_{eq,o,j} - T_{s,o,j}) \quad (2.4)$$

A similar approach is followed for the inside surface: long-wave radiation is assumed to occur between each wall surface and other wall surfaces that are at the inside air temperature (T_i); long-wave radiation exchange with other surfaces is linearized so that a radiation heat transfer coefficient is determined at a representative mean temperature; long-wave radiation is combined with convection using a combined convection and long-wave radiation heat transfer coefficient; an equivalent inside air temperature is defined that would give the correct heat transfer rate in the absence of the internal radiation gains (from solar through windows and internal sources). With these assumptions, the conduction heat transfer rate at the inside wall surface is

$$\dot{Q}_{s,i,j} = h_i A_j (T_{eq,i,j} - T_{s,i,j}) \quad (2.5)$$

where

$$T_{eq,i,j} = T_i + \frac{\dot{q}_{g,r}}{h_i} \quad (2.6)$$

and where h_i is the inside heat transfer coefficient (convection and long-wave radiation) and $\dot{q}_{g,r}$ is the absorbed radiation flux due to internal sources and solar radiation transmitted through windows.

The transient heat transfer problem for a wall can be represented using an electrical analog. Figure 4 shows a simple two-node representation (two state variables) for a wall subjected to time-varying temperature boundary conditions. Outside and inside radiation gains are handled

with an equivalent air temperature. In this representation, R represents a thermal resistance and C is a thermal capacitance. The total thermal resistance ($R_1 + R_2 + R_3$) includes the thermal resistance between the outside air and the wall (combined convection and long-wave radiation), the conduction resistance within the wall and the thermal convection resistance between the wall and the building interior. The capacitors incorporate the total capacitance of the wall material. For this simple representation, the physical location of the nodes has a significant effect on the model predictions. Chaturvedi and Braun (2002) found that 2 or 3 nodes were sufficient to provide accurate transient predictions if the location of the nodes were optimized. For best results, the outside and inside resistances should include the air resistance and a portion of the material within the wall.

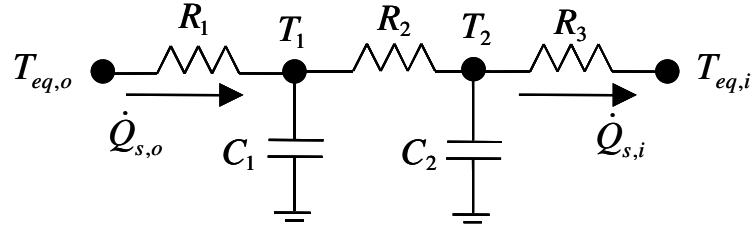


Figure 4. Thermal network representation of an external wall

The electrical circuit can easily be represented in state-space form as

$$\frac{d\bar{x}}{d\tau} = \hat{A}\bar{x} + \hat{B}\bar{u} \quad (2.7)$$

$$y = \bar{c}^T \bar{x} + \bar{d}^T \bar{u} \quad (2.8)$$

where \bar{x} = vector of state variables
 \bar{u} = vector of inputs
 y = output variable
 \hat{A} = constant coefficient matrix
 \hat{B} = constant coefficient matrix
 \bar{c} = constant coefficient vector
 \bar{d} = constant coefficient vector
 τ = time

For a wall, the desired output variable is the rate of conduction heat transfer at the inside surface ($\dot{Q}_{s,i}$). The state vector contains temperatures of “nodes” within the structure of the wall, the input vector consists of the equivalent inside and outside air temperatures ($T_{eq,i}$ and $T_{eq,o}$), and coefficient matrices and vectors contain the physical characteristics of the wall (i.e., the R 's and C 's).

The state-space formulation could be solved at each timestep of a simulation. However, the computation can be significantly reduced if the state-space formulation is converted to a transfer function representation. Seem et al. (1989) presented a technique for determining an

equivalent transfer function representation from the state-space representation that involves the exact solution to the set of first-order differential equations with the inputs modeled as continuous, piecewise linear functions. This approach is used within VSAT for a one-hour timestep to determine a transfer function equation at the beginning of the simulation. After the transfer function has been developed, then the solution for the output at any time t is of the form

$$y(t) = \sum_{k=0}^{N_{state}} \vec{S}_k^T \cdot \vec{u}_{t-k\Delta\tau} - \sum_{k=1}^{N_{state}} e_k \cdot y(t - k\Delta\tau) \quad (2.9)$$

where N_{state} = number of state variables
 \vec{S}_k = vector containing transfer function coefficients for the input vector k timesteps prior to the current time t
 e_k = transfer function coefficient for the zone sensible load for k timesteps prior to the current time t
 $\Delta\tau$ = time step (one hour for VSAT)

At the beginning of the simulation, the vectors \vec{S}_k for $k = 0$ to N_{state} are determined as

$$\begin{aligned} \vec{S}_0 &= \vec{c}\hat{R}_0\Gamma_2 + \vec{d} \\ \vec{S}_j &= \vec{c}\left[\hat{R}_{j-1}(\Gamma_1 - \Gamma_2) + \hat{R}_j\Gamma_2\right] + e_j\vec{d} \quad \text{for } 1 \leq j \leq (N_{state} - 1) \\ \vec{S}_{N_{state}} &= \vec{c}\hat{R}_{N_{state}-1}(\Gamma_1 - \Gamma_2) + e_{N_{state}}\vec{d} \end{aligned} \quad (2.10)$$

where

$$\begin{aligned} \Gamma_1 &= \hat{A}^{-1}(\Phi - \hat{I})\hat{B} \\ \Gamma_2 &= \hat{A}^{-1}\left[\frac{\Gamma_1}{\Delta\tau} - \hat{B}\right] \end{aligned} \quad (2.11)$$

where \hat{I} is the identity matrix, $\Delta\tau$ is the simulation time step (one hour for this study), and

$$\begin{aligned} \Phi &= e^{\hat{A}\Delta\tau} \\ e^{\hat{A}\Delta\tau} &= \hat{I} + \hat{A}\Delta\tau + \frac{\hat{A}^2(\Delta\tau)^2}{2!} + \frac{\hat{A}^3(\Delta\tau)^3}{3!} + \dots + \frac{\hat{A}^n(\Delta\tau)^n}{n!} + \dots \end{aligned} \quad (2.12)$$

Seem et al. (1989) presented an efficient algorithm for evaluating $e^{\hat{A}\Delta\tau}$ in equation 2.12 that is used within VSAT. The matrices \hat{R}_j used in the determination of \vec{S}_k and the e_j transfer function coefficients are determined recursively as

$$\begin{aligned}
\hat{R}_0 &= \hat{I} & e_1 &= -\frac{Tr(\Phi \hat{R}_0)}{1} \\
\hat{R}_1 &= \Phi \hat{R}_0 + e_1 \hat{I} & e_2 &= -\frac{Tr(\Phi \hat{R}_1)}{2} \\
\hat{R}_2 &= \Phi \hat{R}_1 + e_2 \hat{I} & e_3 &= -\frac{Tr(\Phi \hat{R}_2)}{3} \\
&\vdots & & \vdots \\
\hat{R}_{N_{state}-1} &= \Phi \hat{R}_{N_{state}-2} + e_{N_{state}-1} \hat{I} & e_{N_{state}} &= -\frac{Tr(\Phi \hat{R}_{N_{state}-1})}{N_{state}}
\end{aligned} \tag{2.13}$$

where $Tr()$ is the trace of the matrix (the sum of the diagonal elements).

The transfer function representation gives the wall conduction at the inside surface for any wall j . The heat transfer to the inside air due to wall j is then

$$\dot{Q}_{i,j} = \dot{Q}_{s,i,j} + A_j \dot{q}_{g,r} \tag{2.14}$$

2.1.2 Floor Slabs

Slab on grade floors are modeled using a similar formulation as for exterior walls. However, the exterior of the floor is exposed to the ground so that there is no convection, solar radiation, or long-wave radiation. Furthermore, the predominant mechanism for heat loss or gain is heat transfer at the perimeter of the slab. The transfer function of equation 2.9 is used to determine the conduction heat transfer at the inside surface for floors. However, the bottom side of the floor is assumed to be adiabatic (infinite resistance for heat transfer between the outside floor surface and the ground). The primary mode for heat transfer to and from the ambient is through the perimeter of the slab. Perimeter heat transfer is assumed to be quasi-steady state from the ambient to the inside air across a resistance that is based upon the slab perimeter heat loss factor (ASHRAE, 2001). The combined heat transfer to the inside air from the floor is then

$$\dot{Q}_i = \dot{Q}_{s,i} + A \dot{q}_{g,r} + F_p \cdot P \cdot (T_o - T_i) \tag{2.15}$$

where F_p is the slab perimeter heat loss factor and P is the perimeter of the slab.

2.1.3 Interior Walls

An interior wall differs from an exterior wall in that the inside boundary conditions are experienced on both sides of the wall. The transfer function of equation 2.9 is used to determine the conduction heat transfer at the inside surfaces for interior walls with both boundary conditions given by equation 2.6. Interior walls are assumed to be symmetric with identical boundary conditions, so that the total heat transfer to the air from both surfaces is

$$\dot{Q}_i = 2 \cdot (\dot{Q}_{s,i} + A \dot{q}_{g,r}) \tag{2.16}$$

where A is the surface area for one face and $\dot{Q}_{s,i}$ is the conduction heat transfer rate for one surface of the wall.

Interior walls/furnishings are represented with a single node (capacitance) having a total surface area equal to twice the total floor area, a mass of 25 lbm/ft², and an average specific heat of 0.2 Btu/lbm-F.

2.1.4 Windows

Figure 5 shows the relevant heat transfer rates for the k^{th} window. Windows are considered as quasi-steady-state elements that provide heat gains due to both solar transmission and conduction. Similar to walls, long-wave radiation is combined with convection using combined heat transfer coefficients at the inside and outside surfaces. Solar radiation passing through the window is partially absorbed and mostly transmitted. The overall absorptance and transmittance for solar radiation of the window are α and τ , respectively.

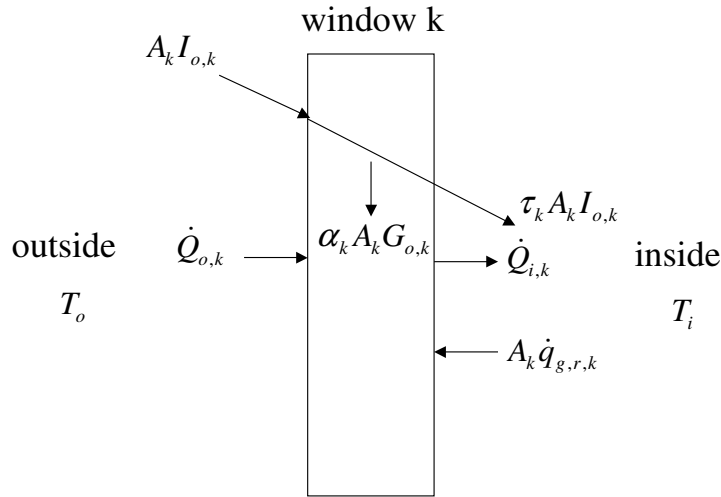


Figure 5. Heat transfer rates for a window

Assuming that the absorption of solar radiation occurs at the outside surface and absorption of internal radiative gains occurs at the inside surface, then the heat transfer rate by conduction through the glass is

$$\dot{Q}_{s,i,k} = U_k A_k (T_{eq,o,k} - T_{eq,i,k}) \quad (2.17)$$

where U is the overall unit conductance for the window. The equivalent inside and outside air temperatures ($T_{eq,i}$ and $T_{eq,o}$) are evaluated using equations 2.3 and 2.6, respectively. Then, the total heat gains through the window are

$$\dot{Q}_{win,k} = U_k A_k (T_{eq,o,k} - T_{eq,i,k}) + \tau_k \cdot A_k \cdot I_{o,k} + A_k \cdot \dot{q}_{g,r,k} \quad (2.18)$$

It is more common to have data for window shading coefficients than for window transmittances. The shading coefficient accounts for both solar transmission and solar absorption. In this formulation, the total heat gain to the air due to the window is given as

$$\dot{Q}_{win,k} = U_k A_k (T_o - T_{eq,i,k}) + SHGC_k \cdot A_k \cdot I_{o,k} + A_k \cdot \dot{q}_{g,r,k} \quad (2.19)$$

where $SHGC$ is the solar heat gain coefficient defined as

$$SHGC = \tau + \frac{U\alpha}{h_o} \quad (2.20)$$

where h_o is the outside heat transfer coefficient (combined convection and long-wave radiation). Equations 2.18 and 2.19 are equivalent.

The shading coefficient is defined as

$$SC = \frac{SHGC}{SHGC_{ref}} \quad (2.21)$$

where $SHGC_{ref}$ is the solar heat gain coefficient for a single pane of double strength glass, which has a value of 0.87. In general, the shading coefficient can account for multiple glazings, different types of glazing materials, and indoor shading devices.

Using the definition of shading coefficient, equation 2.19 can be rewritten as

$$\dot{Q}_{win,k} = U_k A_k (T_o - T_{eq,i,k}) + SC \cdot SHGC_{ref} \cdot A_k \cdot I_{o,k} + A_k \cdot \dot{q}_{g,r,k} \quad (2.22)$$

The concept of a shading coefficient was developed for building models where the heat gains due to solar radiation are added directly to the air. In reality, solar transmission through windows leads to solar absorptance on other interior surfaces, whereas solar absorption in windows leads to increased convection to the air by the window. Although it is not strictly correct, VSAT uses the total solar gains determined with a shading coefficient and distributes them to other internal surfaces. With this approach, the window solar transmission and convection to the air are determined as

$$\dot{Q}_{t,k} = SC \cdot SHGC_{ref} \cdot A_k \cdot I_{o,k} \quad (2.23)$$

$$\dot{Q}_{i,k} = U_k A_k (T_o - T_{eq,i,k}) + A_k \cdot \dot{q}_{g,r,k} \quad (2.24)$$

VSAT assumes constant values for the shading coefficient and overall window unit conductance. Solar transmission through windows is distributed solely to the floor with a uniform heat flux.

2.1.5 Infiltration

Infiltration is a relatively small effect for commercial buildings and is modeled with a constant flow rate that is based upon a specified volumetric flow rate per unit floor area. The

default value is 0.05 cfm/ft², but can be changed. For a building with 10-foot ceiling height, this infiltration rate corresponds to 0.3 air changes per hour.

The sensible and latent heat gains due to infiltration are determined as

$$\dot{Q}_{\text{inf},s} = \dot{m}_{\text{inf}} C_{pm} (T_o - T_i) \quad (2.25)$$

$$\dot{Q}_{\text{inf},L} = \dot{m}_{\text{inf}} h_{fg} (\omega_o - \omega_i) \quad (2.26)$$

where C_{pm} is the moist air specific heat, h_{fg} is the heat of vaporization of water, ω_o is the humidity ratio of the outside air, and ω_i is the humidity ratio of the inside air.

2.1.7 Internal Gains

Internal gains due to lights, equipment, and people vary according to an occupancy schedule that is specified. The specific values of the heat gains and the proportion of gains from people that influence latent loads vary according to building type (see Prototypical Building Descriptions). For people and lights, 50% of the heat gains are assumed to be radiative and 50% convective. All the gains from equipment (e.g, computers) are assumed to be convective. The radiative internal gains are distributed with an even heat flux to all internal surfaces (including windows).

2.1.8 Zone Loads

At any time, the sensible cooling (+) or heating (-) required to keep the zone temperature at a specified setpoint is determined as

$$\dot{Q}_z = \sum_{j=1}^{\text{walls}} \dot{Q}_{i,j} + \sum_{k=1}^{\text{windows}} \dot{Q}_{i,k} + \dot{Q}_{g,c} + \dot{Q}_{s,\text{inf}} \quad (2.27)$$

where $\dot{Q}_{g,c}$ is the total convective heat gain due to lights, people, and equipment.

Separate temperature setpoints are specified for heating and cooling and the temperature can float in between with no required cooling or heating. In order to evaluate whether heating or cooling is required for a given time step, it is necessary to determine the zone temperature where the sensible cooling requirement for the equipment is equal to zero. In the absence of ventilation (unoccupied mode) then equation 2.27 would be solved inversely for the floating inside air temperature with \dot{Q}_z set equal to zero. If the calculated zone temperature is less than the heating setpoint, then heating is required and equation 2.27 is evaluated using the heating setpoint. If the calculated zone temperature is greater than the cooling setpoint, then cooling is required and equation 2.27 is evaluated using the cooling setpoint. If the calculated temperature is between the setpoints, then the zone temperature is floating and the zone sensible cooling and heating requirement are zero. The case where the fans operate continuously with a ventilation load (unoccupied mode) is considered in section 4.

When there is a sensible cooling requirement, then the cooling equipment also provides latent cooling and it is necessary to know the latent loads for the zone. In this case, the zone latent gains are the sum of the latent gains due to people and due to infiltration.

2.1.9 Solar Radiation Processing

The weather data files used by VSAT contain hourly values of global horizontal radiation and direct normal radiation. The horizontal radiation is used for the roof, but it is necessary to calculate incident radiation on vertical surfaces for external walls. The total incident radiation for vertical surfaces is determined as

$$I_o = I_{DN} \sin(\theta_z) \cdot \cos(\gamma_s - \gamma) + \frac{I_D}{2} + \rho_g I_H \quad (2.28)$$

where I_{DN} is beam radiation that is measured normal to the line of sight to the sun, θ_z is the zenith angle, γ_s is the solar azimuth angle, γ is the surface azimuth angle, I_D is sky diffuse radiation, ρ_g is ground reflectance, and I_H is total radiation incident upon a horizontal surface. Zenith is the angle between the vertical and the line of site to the sun. Solar azimuth is the angle between the local meridian and the projection of the line of sight to the sun onto the horizontal plane. Zero solar azimuth is facing the equator, west is positive, while east is negative. The zenith and solar azimuth angle are calculated using relationships given in Duffie and Beckman (1980). The surface azimuth is the angle between the local meridian and the projection of the normal to the surface onto the horizontal plane (0 for south facing, -90 for east facing +90 for west facing, and +180 for north facing). The ground reflectance is assumed to have a constant value of 0.2, which is representative of summer conditions. The sky diffuse radiation is calculated from the

$$I_D = I_H - I_{DN} \cos(\theta_z) \quad (2.29)$$

2.2 Prototypical Building Descriptions

Seven different types of buildings are considered in VSAT: small office, school class wing, retail store, restaurant dining area, school gymnasium, school library, and school auditorium. Descriptions for these buildings were obtained from prototypical building descriptions of commercial building prototypes developed by Lawrence Berkeley National Laboratory (Huang, et al. 1990 & Huang, et al. 1995). These reports served as the primary sources for prototypical building data. However, additional information was obtained from DOE-2 input files used by the researchers for their studies.

Tables 1 - 7 contain information on the geometry, construction materials, and internal gains used in modeling the different buildings. Although not given in these tables, the walls, roofs and floors include inside air and outside air thermal resistances. The window R-value includes the effects of the window construction and inside and outside air resistances. Table 8 lists the properties of all construction materials and the air resistances. The geometry of each of the buildings is assumed to be rectangular with four sides and is specified with the following parameters: 1) floor area, 2) number of stories, 3) aspect ratio, 4) ratio of exterior perimeter to total perimeter, 5) wall height and 6) ratio of glass area to wall area. The aspect ratio is the ratio of the width to the length of the building. However, exterior perimeter and glass areas are assumed to be equally distributed on all sides of the building, giving equal exposure of exterior walls and windows to incident solar radiation. The four exterior walls face north, south, east, and west.

The user can specify occupancy schedules, but default values are based upon the original LBNL study. In the LBNL study, the occupancy was scaled relative to a daily average

maximum occupancy density (people per 1000 ft²). In VSAT, the user can specify a peak design occupancy density (people per 1000 ft²) that is used for determining fixed ventilation requirements (no DCV). This same design occupancy density is used as the scaling factor for the hourly occupancy schedules. As a result, the original LBNL occupancy schedules were rescaled using the default peak design occupancy densities.

The heat gains and CO₂ generation per person depend upon the type of building (and associated activity). Design internal gains for lights and equipment also depend upon the building and are scaled according to specified average daily minimum and maximum gain fractions. For all of the buildings, the lights and equipment are at their average maximum values whenever the building is occupied and are at their average minimum values at all other times.

Zone thermostat setpoints can be set for both occupied and unoccupied periods. The default occupied setpoints for cooling and heating are 75°F and 70°F, respectively. The default unoccupied setpoints for cooling (setup) and heating (setback) are 85°F and 60°F, respectively. The lights are assumed to come on one hour before people arrive and stay on one hour after they leave. The occupied and unoccupied setpoints follow this same schedule.

Table 1. Office Building Characteristics

Windows		
R-value, hr-ft ² -F/Btu	1.58	
Shading Coefficient	0.75	
Area ratio (window/wall)	0.15	
Exterior Wall Construction		
Layers	1" stone R-5.6 insulation R-0.89 airspace 5/8" gypsum	
Roof Construction		
Layers	Built-up roof (3/8") 4" lightweight concrete R-12.6 insulation R-0.92 airspace 1/2" acoustic tile	
Floor		
Layers	6" heavyweight concrete Carpet and pad	
Slab perimeter loss factor, Btu/h-ft-F	0.5	
General		
Floor area, ft ²	6600	
Wall height, ft	11	
Internal mass, lb/ft ²	25	
Number of stories	1	
Aspect Ratio	0.67	
Ratio of exterior perimeter to floor perimeter	1.0	
Design equipment gains, W/ft ²	0.5	
Design light gains, W/ft ²	1.7	
Ave. daily min. lights/equip. gain fraction	0.2	
Ave. daily max. lights/equip. gain fraction	0.9	
Sensible people gains, Btu/hr-person	250	
Latent people gains, Btu/hr-person	250	
CO ₂ people generation, L/min-person	0.33	
Design occupancy for vent., people/1000 ft ²	7	
Design ventilation, cfm/person	20	
Average weekday peak occupancy, ft ² /person	470	
Default average weekday occupancy schedule * Values given relative to average peak	Hours	Values
	1-7	0.0
	8	0.33
	9	0.66
	10-16	1.0
	17	0.5
Default average weekend occupancy schedule * Values given relative to average peak	Hours	Values
	1-8	0.0
	9	0.15
	10-12	0.2
	12-13	0.15
	13-24	0.0
Monthly occupancy scaling * relative to daily occupancy schedule	Month	Value
	1-12	1.0

Table 2. Restaurant Dining Area Characteristics

Windows		
R-value, hr-ft ² -F/Btu	1.53	
Shading Coefficient	0.8	
Area ratio (window/wall)	0.15	
Exterior Wall Construction		
Layers	3" face brick ½" plywood R-4.9 insulation 5/8" gypsum	
Roof Construction		
Layers	Built-up roof (3/8") ¾" plywood R-13.2 insulation R-0.92 airspace ½" acoustic tile	
Floor		
Layers	4" heavyweight concrete Carpet and pad	
Slab perimeter loss factor, Btu/h-ft-F	0.5	
General		
Floor area, ft ²	5250	
Wall height, ft	10	
Internal mass, lb/ft ²	25	
Number of stories	1	
Aspect Ratio	1.0	
Ratio of exterior perimeter to floor perimeter	0.75	
Design equipment gains, W/ft ²	0.0	
Design light gains, W/ft ²	2.0	
Ave. daily min. lights/equip. gain fraction	0.2	
Ave. daily max. lights/equip. gain fraction	1.0	
Sensible people gains, Btu/hr-person	250	
Latent people gains, Btu/hr-person	275	
CO ₂ people generation, L/min-person	0.35	
Design occupancy for vent., people/1000 ft ²	30	
Design ventilation, cfm/person	20	
Average weekday peak occupancy, ft ² /person	50	
Default average weekday occupancy schedule * Values given relative to average peak	Hours	Values
	1-6	0.0
	7-12	0.2,0.3,0.1,0.05,0.2,0.5
	13-24	0.5,0.4,0.2,0.05,0.1,0.4, 0.6,0.5,0.4,0.2,0.1,0.0
Default average weekend occupancy schedule * Values given relative to average peak	Hours	Values
	1-6	0.0
	7-12	0.3,0.4,0.5,0.2,0.2,0.3
	13-24	0.5,0.5,0.5,0.35,0.25, 0.5,0.8,0.8,0.7,0.4,0.2, 0.0
Monthly occupancy scaling * relative to daily occupancy schedule	Month	Value
	1-5	1.0
	6-8	0.5
	9-12	1.0

Table 3. Retail Store Characteristics

Windows		
R-value, hr-ft ² -F/Btu	1.5	
Shading Coefficient	0.76	
Area ratio (window/wall)	0.15	
Exterior Wall Construction		
Layers	8" lightweight concrete R-4.8 insulation R-0.89 airspace 5/8" gypsum	
Roof Construction		
Layers	Built-up roof (3/8") 1.25" lightweight concrete R-12 insulation R-0.92 airspace ½" acoustic tile	
Floor		
Layers	4" lightweight concrete Carpet and pad	
Slab perimeter loss factor, Btu/h-ft-F	0.5	
General		
Floor area, ft ²	80,000	
Wall height, ft	15	
Internal mass, lb/ft ²	25	
Number of stories	2	
Aspect Ratio	0.5	
Ratio of exterior perimeter to floor perimeter	1.0	
Design equipment gains, W/ft ²	0.4	
Design light gains, W/ft ²	1.6	
Ave. daily min. lights/equip. gain fraction	0.2	
Ave. daily max. lights/equip. gain fraction	0.9	
Sensible people gains, Btu/hr-person	250	
Latent people gains, Btu/hr-person	250	
CO ₂ people generation, L/min-person	0.33	
Design occupancy for vent., people/1000 ft ²	25	
Design ventilation, cfm/person	15	
Average weekday peak occupancy, ft ² /person	390	
Default average weekday occupancy schedule * Values given relative to average peak	Hours	Values
	1-7	0.0
	8	0.33
	9	0.66
	10-20	1.0
	21	0.5
Default average weekend occupancy schedule * Values given relative to average peak	Hours	Values
	1-7	0.0
	8	0.33
	9	0.66
	10-20	1.0
	21	0.5
Monthly occupancy scaling * relative to daily occupancy schedule	Month	Value
	1-12	1.0

Table 4. School Class Wing Characteristics

Windows		
R-value, hr-ft ² -F/Btu	1.7	
Shading Coefficient	0.73	
Area ratio (window/wall)	0.18	
Exterior Wall Construction		
Layers	8" concrete block R-5.7 insulation 5/8" gypsum	
Roof Construction		
Layers	Built-up roof (3/8") 3/4" plywood R-13.3 insulation R-0.92 airspace 1/2" acoustic tile	
Floor		
Layers	6" heavyweight concrete	
Slab perimeter loss factor, Btu/h-ft-F	0.5	
General		
Floor area, ft ²	9600	
Internal mass, lb/ft ²	25	
Wall height, ft	10	
Number of stories	2	
Aspect Ratio	0.5	
Ratio of exterior perimeter to floor perimeter	0.875	
Design equipment gains, W/ft ²	0.3	
Design light gains, W/ft ²	2.2	
Ave. daily min. lights/equip. gain fraction	0.1	
Ave. daily max. lights/equip. gain fraction	0.95	
Sensible people gains, Btu/hr-person	250	
Latent people gains, Btu/hr-person	200	
CO ₂ people generation, L/min-person	0.3	
Design occupancy for vent., people/1000 ft ²	25	
Design ventilation, cfm/person	15	
Average weekday peak occupancy, ft ² /person	50	
Default average weekday occupancy schedule * Values given relative to average peak	Hours	Values
	1-6	0.0
	7	0.1
	8-11	0.9
	12-15	0.8
	16	0.45
	17	0.15
	18	0.05
	19-21	0.33
	22-24	0.0
Default average weekend occupancy schedule * Values given relative to average peak	Hours	Value
	1-9	0.0
	10-13	0.1
	14-24	0.0
Monthly occupancy scaling * relative to daily occupancy schedule	Month	Value
	1-5	1.0
	6-8	0.5
	9-12	1.0

Table 5. School Gymnasium Characteristics

Windows		
R-value, hr-ft ² -F/Btu	1.7	
Shading Coefficient	0.73	
Area ratio (window/wall)	0.18	
Exterior Wall Construction		
Layers	8" concrete block R-5.7 insulation 5/8" gypsum	
Roof Construction		
Layers	Built-up roof (3/8") 3/4" plywood R-13.3 insulation R-0.92 airspace 1/2" acoustic tile	
Floor		
Layers	6" heavyweight concrete	
Slab perimeter loss factor, Btu/h-ft-F	0.5	
General		
Floor area, ft ²	7500	
Internal mass, lb/ft ²	25	
Wall height, ft	32	
Number of stories	1	
Aspect Ratio	0.86	
Ratio of exterior perimeter to floor perimeter	0.86	
Design equipment gains, W/ft ²	0.2	
Design light gains, W/ft ²	0.65	
Ave. daily min. lights/equip. gain fraction	0.0	
Ave. daily max. lights/equip. gain fraction	0.9	
Sensible people gains, Btu/hr-person	250	
Latent people gains, Btu/hr-person	550	
CO ₂ people generation, L/min-person	0.55	
Design occupancy for vent., people/1000 ft ²	30	
Design ventilation, cfm/person	20	
Average weekday peak occupancy, ft ² /person	180	
Default average weekday occupancy schedule * Values given relative to average peak	Hours	Value
	1-7	0.0
	8-15	1.0
	16-24	0.0
Default average weekend occupancy schedule * Values given relative to average peak	Hours	Value
	1-24	0.0
Monthly occupancy scaling * relative to daily occupancy schedule	Month	Value
	1-5	1.0
	6-8	0.1
	9-12	1.0

Table 6. School Library Characteristics

Windows		
R-value, hr-ft ² -F/Btu	1.7	
Shading Coefficient	0.73	
Area ratio (window/wall)	0.18	
Exterior Wall Construction		
Layers	8" concrete block R-5.7 insulation 5/8" gypsum	
Roof Construction		
Layers	Built-up roof (3/8") 3/4" plywood R-13.3 insulation R-0.92 airspace 1/2" acoustic tile	
Floor		
Layers	6" heavyweight concrete	
Slab perimeter loss factor, Btu/h-ft-F	0.5	
General		
Floor area, ft ²	1500	
Internal mass, lb/ft ²	25	
Wall height, ft	10	
Number of stories	1	
Aspect Ratio	0.2	
Ratio of exterior perimeter to floor perimeter	0.75	
Design equipment gains, W/ft ²	0.4	
Design light gains, W/ft ²	1.5	
Ave. daily min. lights/equip. gain fraction	0.1	
Ave. daily max. lights/equip. gain fraction	0.95	
Sensible people gains, Btu/hr-person	250	
Latent people gains, Btu/hr-person	250	
CO ₂ people generation, L/min-person	0.33	
Design occupancy for vent., people/1000 ft ²	20	
Design ventilation, cfm/person	15	
Average weekday peak occupancy, ft ² /person	100	
Default average weekday occupancy schedule * Values given relative to average peak	Hours	Value
	1-6	0.0
	7	0.1
	8-11	0.9
	12-15	0.8
	16	0.45
	17	0.15
	18	0.05
	19-21	0.33
	22-24	0.0
Default average weekend occupancy schedule * Values given relative to average peak	Hours	Value
	1-9	0.0
	10-13	0.1
	14-24	0.0
Monthly occupancy scaling * relative to daily occupancy schedule	Month	Value
	1-5	1.0
	6-8	0.5
	9-12	1.0

Table 7. School Auditorium Characteristics

Windows		
R-value, hr-ft ² -F/Btu	1.7	
Shading Coefficient	0.73	
Area ratio (window/wall)	0.18	
Exterior Wall Construction		
Layers	8" concrete block R-5.7 insulation 5/8" gypsum	
Roof Construction		
Layers	Built-up roof (3/8") 3/4" plywood R-13.3 insulation R-0.92 airspace 1/2" acoustic tile	
Floor		
Layers	6" heavyweight concrete	
Slab perimeter loss factor, Btu/h-ft-F	0.5	
General		
Floor area, ft ²	6000	
Internal mass, lb/ft ²	25	
Wall height, ft	32	
Number of stories	1	
Aspect Ratio	0.64	
Ratio of exterior perimeter to floor perimeter	0.85	
Design equipment gains, W/ft ²	0.2	
Design light gains, W/ft ²	0.8	
Ave. daily min. lights/equip. gain fraction	0.0	
Ave. daily max. lights/equip. gain fraction	0.9	
Sensible people gains, Btu/hr-person	250	
Latent people gains, Btu/hr-person	200	
CO ₂ people generation, L/min-person	0.3	
Design occupancy for vent., people/1000 ft ²	150	
Design ventilation, cfm/person	15	
Average weekday peak occupancy, ft ² /person	100	
Default average weekday occupancy schedule * Values given relative to average peak	Hours	Values
	1-9	0.0
	10-11	0.75
	12	0.2
	13-14	0.75
	15-24	0.0
Default average weekend occupancy schedule * Values given relative to average peak	Hours	Value
	1-24	0.0
Monthly occupancy scaling * relative to daily occupancy schedule	Month	Value
	1-5	1.0
	6-8	0.1
	9-12	1.0

Table 8. Construction Material Properties

	Conductivity (Btu/h*ft*F)	Density (lb/ft ³)	Specific Heat (Btu/lb*F)
stone	1.0416	140	0.20
light concrete	0.2083	80	0.20
heavy concrete	1.0417	140	0.20
built-up roof	0.0939	70	0.35
face brick	0.7576	130	0.22
acoustic tile	0.033	18	0.32
gypsum	0.0926	50	0.20
	Resistance (h*ft ² *F/Btu)		
3/4" plywood	0.93703		
1/2" plywood	0.62469		
carpet and pad	2.08		
inside air	0.67		
outside air	0.33		

2.3 Model Validation

The prototypical buildings were chosen to give representative building loads in order to determine if particular building types will benefit more or less from the ventilation strategies under examination. Absolute model predictions are not the goal but rather the impact of ventilation strategies on savings compared to a baseline. Even so, it is very important that the building load predictions have representative dynamics and absolute load levels. In order to validate predictions of VSAT, results have been compared with predictions of the TYPE 56 building model within TRNSYS (2000). This model has been validated with detailed measurements and through comparison with other accepted building load calculation programs.

The TYPE 56 is a very detailed model that is built up from individual descriptions of wall layers, windows, internal gains, schedules, etc. The user enters all pertinent information into a “front-end” program called *PRE-BID*. This program assimilates all the information into four different files that are used by the TYPE 56 component for generating the specific building loads and ultimately the total building load.

Two building prototypes were chosen as case studies to validate the building loads portion of VSAT. Identical construction properties, schedules, internal gains and weather data for each case study were entered into the TYPE 56 and VSAT models for comparison.

2.3.1 TYPE 56 and VSAT Building Model Assumptions

The TYPE 56 building type predicts the thermal behavior of a building having multiple zones. To determine zone heating and cooling requirements, an “energy rate” method is employed. The user specifies the zone setpoints for heating and cooling with any added setup

or setback control schedules. If the floating zone temperature is less than the heating setpoint, then heating is required or if the calculated zone temperature is greater than the cooling setpoint, then cooling is required. Otherwise, the zone temperature is floating and the zone sensible cooling and heating requirement are zero. Unlimited equipment capacity was assumed in the TYPE 56 for purposes of validating the building model in the VSAT.

Walls are modeled in the TYPE 56 using a transfer function method that is equivalent to the approach used in VSAT with a large number of resistors and capacitors. The primary differences between the building model in VSAT and the TYPE 56 are related to the way that solar and long-wave radiation are handled. The solar transmittance for windows is calculated as a function of window properties and solar incidence angle as opposed to the use of a constant shading coefficient employed within VSAT. The solar radiation that is transmitted through windows is distributed to all surfaces in the zone according to the following relation

$$f_j = \frac{\alpha_j \cdot A_j}{\sum_{j=1}^{surfaces} \alpha_j * A_j} \quad (2.30)$$

where f_j is the fraction of transmitted radiation that is absorbed on surface j , A_j is the area of surface j , α_j is the solar absorptance of surface j . In contrast, VSAT distributes all of the transmitted solar radiation to the floor with an even heat flux. It's difficult to say which approach is best, since both are simplifications and the actual solar distribution depends upon the specific geometry of the room and time.

Long-wave radiation exchange between surfaces within the zone is handled in the TYPE 56 using an effective zone surface temperature termed the star temperature. The zone air is coupled to the surface temperatures and star temperature through convective resistances. In contrast, VSAT uses a combined convective and radiative heat transfer coefficient that couples the surface temperatures to the zone air temperature. In both models, surfaces are assumed to be black with respect to long-wave radiation.

Long-wave radiation exchange between outside surfaces and the atmosphere is considered explicitly in the TYPE 56. Radiation occurs between the surface temperatures and an effective temperature that depends upon the surface orientation. The effective temperature is determined as

$$T_{r,o} = (1 - f_{sky}) * T_o + f_{sky} * T_{sky} \quad (2.31)$$

where f_{sky} is the view factor between the surface and the sky, T_o is the outside air temperature, and T_{sky} is a sky temperature that depends upon the air temperature and cloud cover. In contrast, VSAT uses a combined convective and radiative heat transfer coefficient, which is equivalent to assuming that the effective temperature for long-wave radiation is equal to the outside air temperature. In both models, surfaces are assumed to be black with respect to long-wave radiation.

2.3.2 Case Study Description

Two case study descriptions were simulated and compared in VSAT and TRNSYS. The

prototypical office and restaurant (see Tables 1 and 2) were both modeled in Madison, WI and San Diego, CA. Only sensible zone loads were considered, not including ventilation.

In VSAT, combined convective and radiation coefficients were utilized for the inside and outside air of 1.5 Btu/hr-ft²-F and 3.0 Btu/hr-ft²-F, respectively. Since long-wave radiation is handled explicitly in the TYPE 56, convective heat transfer coefficients need to be specified for the inside and outside air. Convective heat transfer coefficients that result in approximately the combined coefficients used in VSAT were found to be 1.25 Btu/hr-ft²-F and 2.75 Btu/hr-ft²-F and were used within the TYPE 56.

The TYPE 56 estimates U-Values for windows based upon the glass properties. For a single pane glass, the U-Value is about 1.0 Btu/hr-ft²-F. In order to realize the specified overall R-values for the windows used in VSAT, the outside and inside convective heat transfer coefficients were set to 2.3 Btu/hr-ft²-F and 6.8 Btu/hr-ft²-F for windows within the TYPE 56.

In order to distribute transmitted solar radiation to the floor only, the solar absorptances of all inside walls were set to zero in the TYPE 56 and the floor solar absorptance was set equal to unity. Finally, the sky temperature used by the TYPE 56 was set equal to the ambient temperature.

2.3.3 Results for Constant Temperature Setpoints

As a first step, cooling and heating loads were evaluated for a constant temperature setpoint of 70°F (21.11°C). This eliminates any transients due to return from night setup and setback. Figure 6 shows hourly heating load comparisons for the office and restaurant over two days in January. VSAT predicts the correct transients and peak load. The relative differences are largest when the loads are smallest at night. Similar results are shown for two days of cooling load predictions in Figure 7.

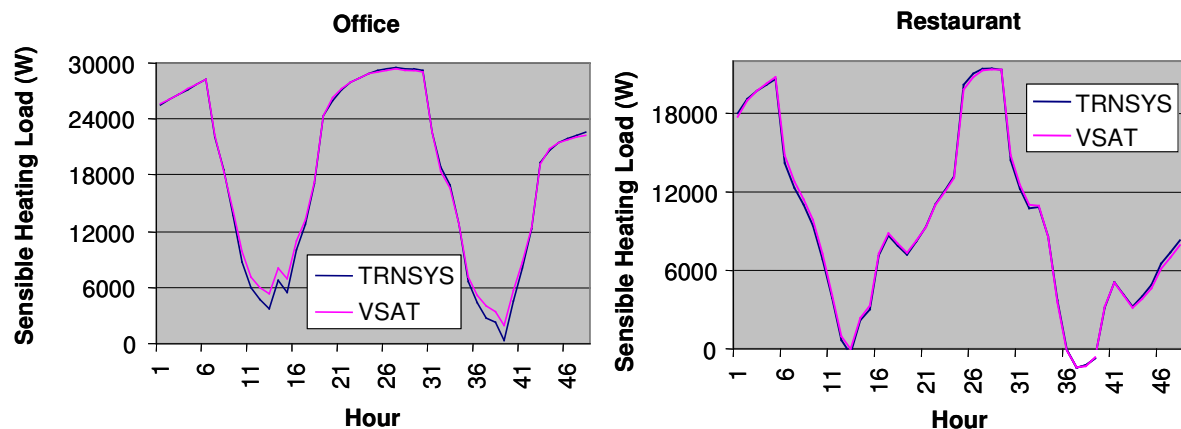


Figure 6. Hourly zone heating loads for constant setpoints (Jan. 9 – 10, Madison, WI)

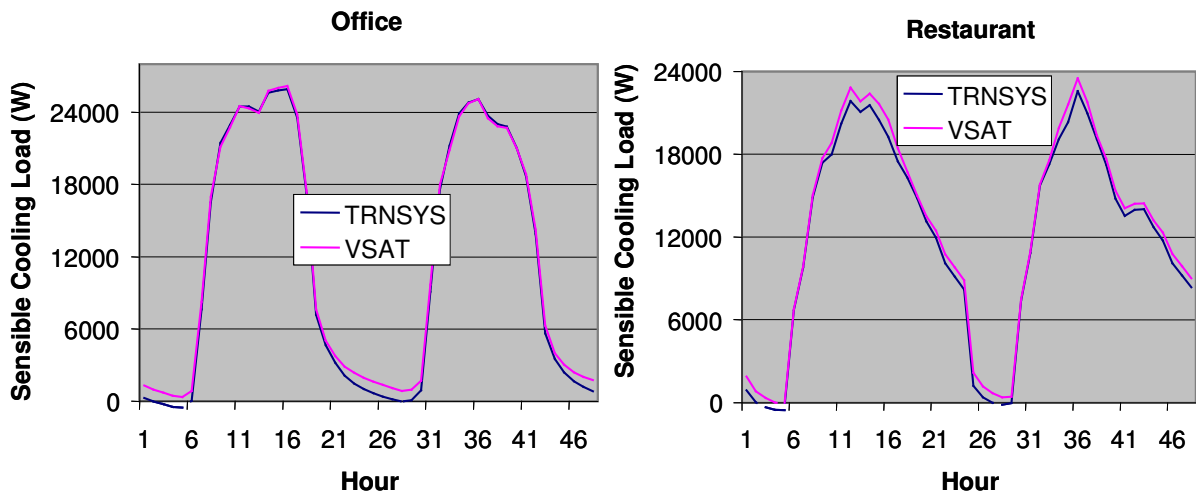


Figure 7. Hourly zone sensible cooling loads for constant setpoints (June 9– 10, San Diego, CA)

Figure 8 and Figure 9 give monthly comparisons for sensible heating and cooling loads. In general, VSAT tends to slightly underpredict heating loads and overpredict cooling loads. This may be due to differences in the manner in which solar radiation transmitted through windows is handle. Overall, the monthly loads are within 5%.

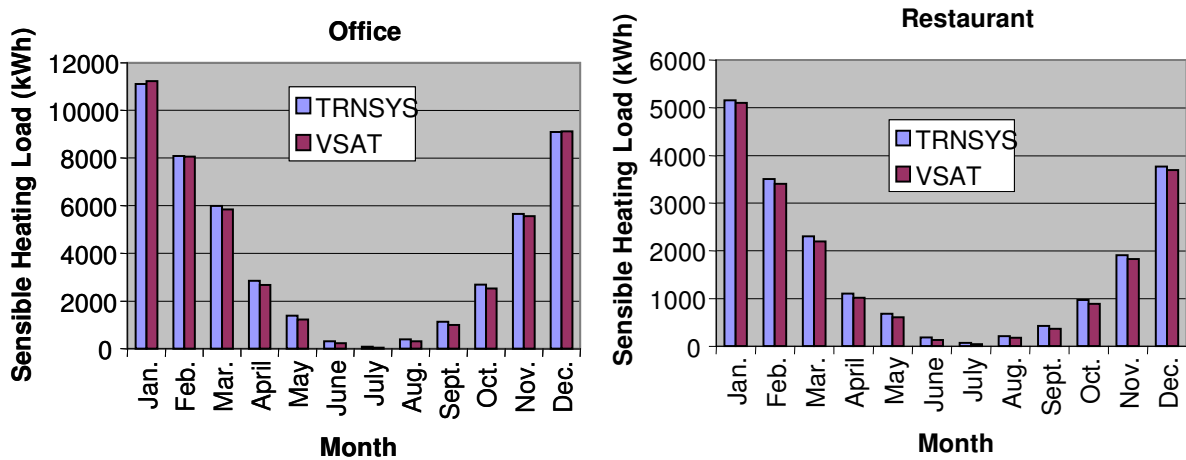


Figure 8. Monthly zone heating loads for constant setpoints (Madison, WI)

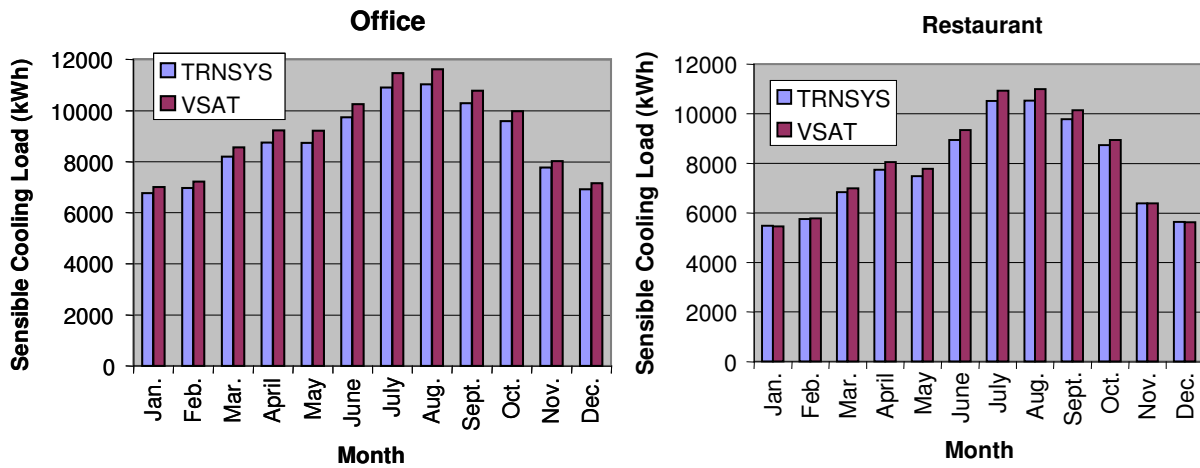


Figure 9. Monthly zone sensible cooling loads for constant setpoints (San Diego, CA)

2.3.4 Results for Night Setback/ Setup Control

The use of a night setback/setup thermostat results in significant dynamics at the start of the occupied period that are not encountered with constant setpoints. Results were generated using both the TYPE 56 and VSAT with night setup for cooling and night setback for heating. For cooling, the occupied period setpoint temperature was 75°F (23.89°C) and the unoccupied setpoint (night setup) temperature was 85°F (29.44°C). For heating, the occupied setpoint was 70°F (21.11°C) and the unoccupied setpoint (night setback) temperature was 60°F (15.56°C). Figure 10 shows sample hourly heat requirements and hourly average zone temperatures for the office in Madison. For both models, there is a large “spike” in the heating requirements when the setpoint returns to the occupied value at 7 am (one hour prior to occupancy). However, the spike is much larger for VSAT than for TRNSYS. This difference is due to differences in the way that zone temperature setpoint adjustments are handled in the two models. VSAT models a true step change in the setpoint at 7 am, whereas TRNSYS assumes a linear variation in setpoint over the course of the hour from 7 am to 8 am. This difference is apparent in the zone temperature results in Figure 10. Similar results were obtained for the restaurant.

Figure 11 shows similar results for cooling in Madison. Once again, VSAT exaggerates the effect of return from night setup on the cooling loads because it assumes a pure step change in the temperature. Figure 11 also shows that both TRNSYS and VSAT predict similar floating temperatures during the setup (nighttime) period.

Figure 12 shows monthly heating and sensible cooling loads for the office in Madison with night setback/setup control. VSAT tends to overpredict the integrated loads by about 5%. This is partly due to the overprediction of loads at the onset of the return from night setback/setup.

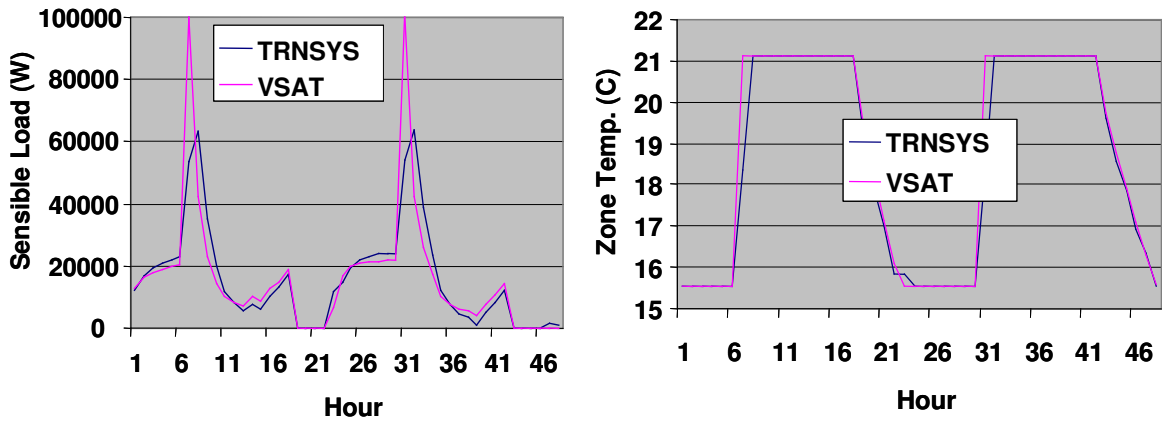


Figure 10. Hourly zone heating loads for the office with night setback (Jan. 9 – 10, Madison, WI)

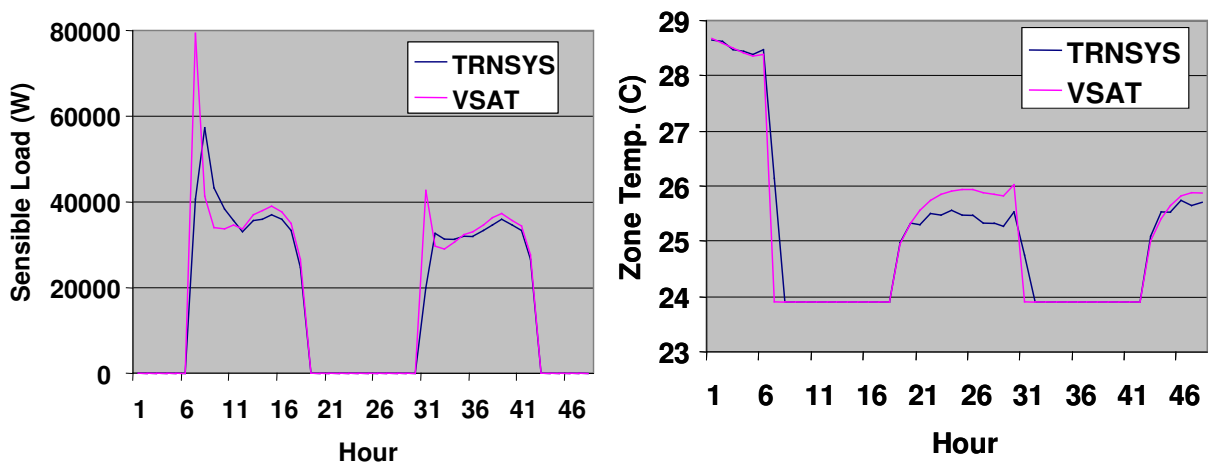


Figure 11. Hourly zone cooling loads for the office with night setup (June 9 – 10, Madison, WI)

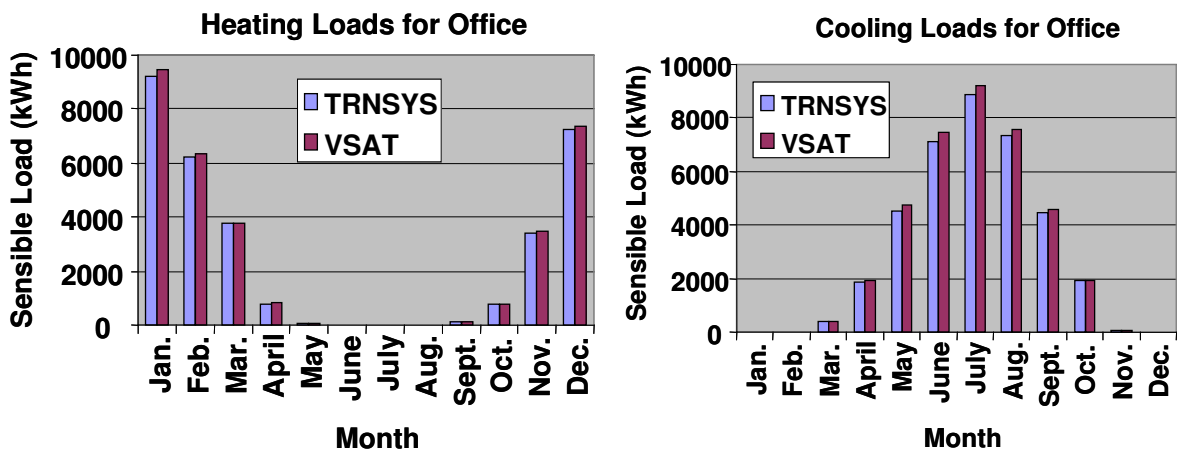


Figure 12. Monthly zone heating and sensible cooling loads for the office with night setup/setup (Madison, WI)

2.3.5 Conclusions

The TYPE 56 building component in TRNSYS is more detailed and accurate in predicting building loads than VSAT. However, for the purposes of comparing different ventilation techniques, this level of detail is not required. Except for return from night setback or setup, VSAT predicts very reasonable transients and overall load levels. Furthermore, VSAT is computationally much more efficient than the TYPE 56, which will facilitate large parametric studies involving many locations and system parameters. The issue of large peak loads at return from night setback or setup will be investigated and VSAT will be modified to predict more reasonable load requirements.

SECTION 3: HEATING AND COOLING EQUIPMENT MODELS

The primary cooling and heating are provided by unitary equipment incorporating a vapor compression air conditioner, a gas or electric heater, and a supply fan. In addition, rotary air-to-air enthalpy exchangers or heat pump heat recovery units can be used to reduce ventilation loads for the primary equipment. Figure 13 depicts a rooftop unit in combination with a heat pump heat recovery unit operating in cooling mode. Ventilation air is cooled and dehumidified by the heat recovery unit prior to mixing with return air from the zone. The mixed air is further cooled and dehumidified (when necessary) by the primary evaporator of the rooftop unit. Heat is rejected to the building exhaust air from the condenser of the recovery unit. The heat pump contains an exhaust fan. In addition, an optional supply fan is used if necessary to provide the proper ventilation air.

In heating mode, refrigerant flow within the heat pump is changed so that the exhaust air stream is cooled (the condenser becomes an evaporator) and heat is rejected to the ventilation air (the evaporator becomes a condenser). The preheated air is then mixed with return air. Although not shown in Figure 13, a gas or electric heater is located after the evaporator to provide additional heating of the supply air when necessary.

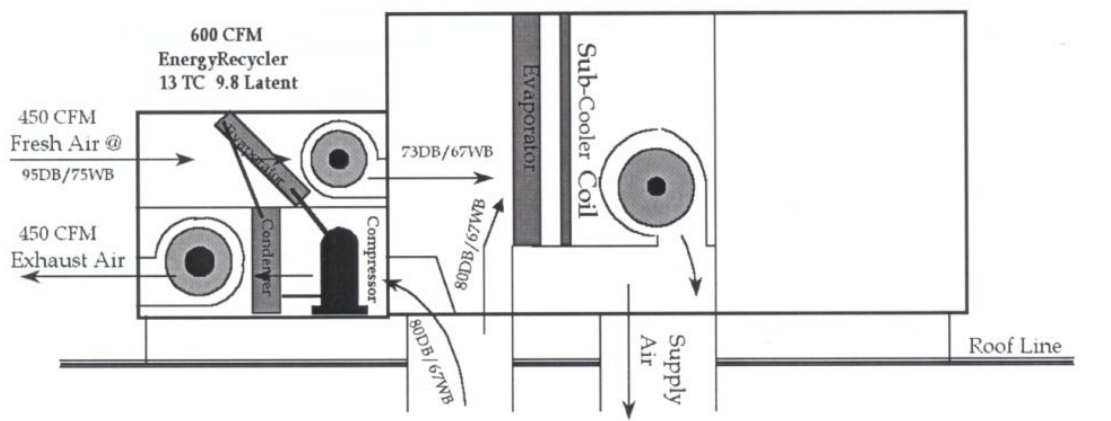


Figure 13. Rooftop air conditioner with heat pump heat recovery unit (cooling mode)

An alternative to heat pump heat recovery is an enthalpy exchanger. Figure 14 depicts a rotary air-to-air enthalpy exchanger considered in VSAT. The device consists of a revolving cylinder filled with an air-permeable medium having a large internal surface area that incorporates a desiccant material. Adjacent supply and exhaust air streams each flow through the exchanger in a counter-flow direction. Sensible heat is transferred as the wheel acquires heat from the hot air stream and releases it to the cold air stream. Moisture is adsorbed from the high humidity air stream to the desiccant material and desorbed into the low humidity air stream. In cooling mode, warm and moist ventilation air is cooled and dehumidified and exhaust air is warmed and humidified. In heating mode, cool and dry air is heated and humidified and exhaust air is cooled and dehumidified.

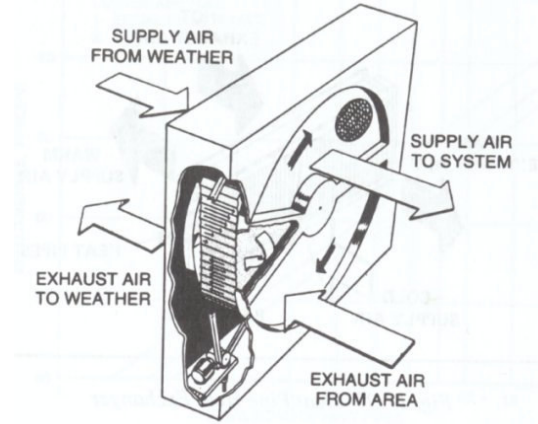


Figure 14. Rotary air-to-air enthalpy exchanger

This section describes the models used for the primary cooling, heating, and heat recovery equipment. Different efficiency equipment can be specified, since this may affect the economics of alternative ventilation strategies. Control strategies for this equipment, along with the description of ventilation control strategies are given in Section 4.

3.1 Vapor Compression System Modeling

Both the primary air conditioning and heat pump heat recovery units utilize a basic vapor compression cycle consisting of a compressor, evaporator coil, expansion valve and condenser coil. Both of these devices are modeled using an approach similar to that incorporated in ASHRAE's *HVAC Toolkit* (Brandemuehl et al., 1993). The model for the primary air conditioner utilizes prototypical performance characteristics, which are scaled according to the capacity requirements and efficiency at design conditions. The characteristics of the heat pump heat recovery unit are based upon measurements obtained from the manufacturer and from tests conducted at the Herrick Labs, which are also scaled for different applications.

3.1.1 Mathematical Description

Steady-State Capacity and COP

The total capacity (cooling or heating), \dot{Q}_{cap} , and coefficient of performance, COP, are calculated by applying correction factors to values specified at rating conditions. The correction factors include the effects of air temperature entering the condenser ($T_{c,i}$), evaporator entering wet bulb temperature ($T_{e,wb,i}$) or dry bulb temperature ($T_{e,i}$) and air flow rate (\dot{m}). For the case where moisture is removed from the air flowing over the evaporator, the capacity and COP are calculated using the following relations

$$\dot{Q}_{cap} = \dot{Q}_{cap,rat} \cdot f_{cap,t}(T_{e,wb,i}, T_{c,i}) \cdot f_{cap,m}(\dot{m} / \dot{m}_{rat}) \quad (3.1)$$

$$\frac{1}{COP_{cap}} = \frac{1}{COP_{rat}} \cdot f_{COP,t}(T_{e,wb,i}, T_{c,i}) \cdot f_{COP,m}(\dot{m} / \dot{m}_{rat}) \quad (3.2)$$

where \dot{Q}_{cap} and COP_{cap} are the capacity and COP for the unit in steady state with the current operating conditions, $\dot{Q}_{cap,rat}$ and COP_{rat} are the capacity and COP at specified rating conditions, $f_{cap,t}$ is the capacity correction factor based on temperature, $f_{cap,m}$ is the capacity correction factor based on air mass flowrate, $f_{COP,t}$ is the COP correction factor based on temperature, and $f_{COP,m}$ is the COP correction factor based on air mass flowrate. The COP is defined as the ratio of the cooling or heating capacity to the power input. For the primary cooling equipment, the power includes both the compressor and condenser fan, but not the evaporator fan. For the heat pump heat recovery unit, the power includes only the compressor. For either type of equipment, the capacity (cooling or heating) does not include the effect of the supply air fan.

For the primary cooling equipment, the inlet wet bulb temperature to the evaporator is associated with the mixed air condition (mixture of outside and return air) and the inlet condenser temperature is the dry bulb ambient temperature (T_a). The air mass flow rate used within the correlations is the flow rate over the evaporator coil. The air flow rate for the condenser is assumed to be the value at the rating condition.

For the heat pump heat recovery unit, the air flow rate used within the correlations is the ventilation flow rate, which is assumed to be equal for the evaporator and condenser (ventilation and exhaust streams considered to have equal flow rates). For the heat pump recovery unit operating in a cooling mode, the inlet wet bulb to the evaporator is the ambient wet bulb temperature (T_{wb}) and the inlet condenser temperature is the return air temperature from the zone (T_z). During heating mode for the heat pump heat recovery unit, the inlet condenser air temperature is the ambient dry bulb temperature and the inlet condition to the evaporator is the state of air returning from the zone. Since the room air is relatively cool and dry, moisture is not generally condensed as the exhaust air flows over the heat pump evaporator. Therefore, the return air dry bulb temperature (T_z) is used in place of the wet bulb temperature for this case.

The correction factors are based upon correlations of the following form.

$$f_{cap,t}(T_{e,wb,i}, T_{c,i}) = a_1 + b_1 \cdot T_{e,wb,i} + c_1 \cdot T_{e,wb,i}^2 + d_1 \cdot T_{c,i} + e_1 \cdot T_{c,i}^2 + f_1 \cdot T_{e,wb,i} \cdot T_{c,i} \quad (3.3)$$

$$f_{COP,t}(T_{e,wb,i}, T_{c,i}) = a_2 + b_2 \cdot T_{e,wb,i} + c_2 \cdot T_{e,wb,i}^2 + d_2 \cdot T_{c,i} + e_2 \cdot T_{c,i}^2 + f_2 \cdot T_{e,wb,i} \cdot T_{c,i} \quad (3.4)$$

$$f_{cap,m}(\dot{m} / \dot{m}_{rat}) = a_3 + (\dot{m} / \dot{m}_{rat}) \cdot (b_3 + (\dot{m} / \dot{m}_{rat}) \cdot (c_3 + d_3 (\dot{m} / \dot{m}_{rat}))) \quad (3.5)$$

$$f_{COP,m}(\dot{m} / \dot{m}_{rat}) = a_4 + (\dot{m} / \dot{m}_{rat}) \cdot (b_4 + (\dot{m} / \dot{m}_{rat}) \cdot (c_4 + d_4 (\dot{m} / \dot{m}_{rat}))) \quad (3.6)$$

Different coefficients are used in equations 3.3 – 3.6 for three different cases: 1) primary cooling unit, 2) heat pump heat recovery operating in a cooling mode, and 3) heat pump heat recovery operating in heating mode. For the primary cooling, the coefficients are from the DOE 2.1E building simulation program. For the heat pump heat recovery unit, the coefficients were determined using performance data as described in a later section.

For cooling, the evaporator inlet air is not always humid enough to result in moisture condensation. In this case, unit performance depends upon inlet evaporator dry bulb rather than wet bulb temperature. However, the correlations developed in terms of wet bulb should

provide accurate predictions as long as the correct inlet dry bulb is used and the inlet humidity is set to a value where condensation just begins. This point represents the end of the range where the correlations apply (i.e., the correlation should apply at the point dehumidification begins to occur). Performance is independent of humidity for lower values. Therefore, if the moisture condensation is found not to occur (see section on sensible heat ratio), then the inlet humidity ratio is adjusted until the point where moisture condensation just begins (sensible heat ratio of one). The air inlet wet bulb temperature associated with the actual dry bulb temperature and this fictitious humidity is then used as the evaporator inlet condition for the capacity and COP correlations.

Sensible Heat Ratio

The model for cooling capacity allows determination of the leaving enthalpy using an energy balance, but not the leaving temperature or humidity. A model for moisture removal is utilized that incorporates the concept of a bypass factor (BF). The bypass factor approach considers two different air streams flowing across the evaporator. One air stream is in close proximity to the coil surface and exits the evaporator as saturated air at the effective temperature of the coil surface and the other air stream is away from the coil and assumed to remain at the entering air condition. Since the air close to the coil is allowed to come into equilibrium with the effective surface temperature at a saturated condition, then the effective surface temperature must be the dewpoint of inlet air. As a result, it is termed the apparatus dewpoint temperature, T_{adp} .

Mass and energy balances on both air streams give the following

$$\dot{m} = \dot{m}_{app} + \dot{m}_{byp} \quad (3.7)$$

$$\dot{m}\omega_{e,o} = \dot{m}_{app}\omega_{adp} + \dot{m}_{byp}\omega_{e,i} \quad (3.8)$$

$$\dot{m}h_{e,o} = \dot{m}_{app}h_{adp} + \dot{m}_{byp}h_{e,i} \quad (3.9)$$

where \dot{m} is the total air mass flow rate, \dot{m}_{app} is the air mass flow rate near the coil, \dot{m}_{byp} is the air mass flow rate away from the coil (bypass), $h_{e,i}$ and $h_{e,o}$ are the evaporator inlet and outlet air enthalpy, and $\omega_{e,i}$ and $\omega_{e,o}$ are the evaporator inlet and outlet humidity ratio.

The bypass factor is defined as the ratio of the bypass flow to the total flow. With this definition and equations 3.7 – 3.9, the bypass factor can be related to the operating conditions according to

$$BF = \frac{\dot{m}_{byp}}{\dot{m}} = \frac{h_{e,o} - h_{adp}}{h_{e,i} - h_{adp}} = \frac{\omega_{e,o} - \omega_{adp}}{\omega_{e,i} - \omega_{adp}} \quad (3.10)$$

For a given bypass factor (BF), equation 3.10 indicates that on a psychrometric chart the outlet air state ($h_{e,o}, \omega_{e,o}$) is on a straight line that connects the inlet state with the apparatus dewpoint. This is depicted in Figure 15. The larger the bypass factor the closer the outlet state is to the inlet state.

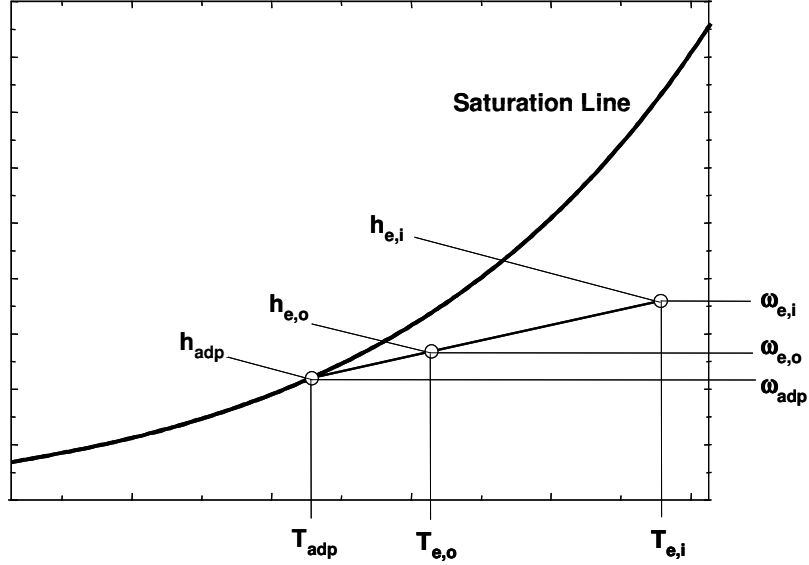


Figure 15. Psychrometric depiction of evaporator air process

The bypass factor can be determined from the heat transfer characteristics of a specific evaporator coil. The bypass factor is estimated from

$$BF = e^{-NTU} \quad (3.11)$$

$$NTU = \frac{UA}{\dot{m} \cdot C_{pm}} \approx \frac{NTU_{rated}}{(\dot{m}/\dot{m}_{rated})} \quad (3.12)$$

and where NTU is the number of transfer units, UA is the air-side conductance of the evaporator coil, C_{pm} is the specific heat of moist air, and NTU_{rated} is the value of NTU at the rated flow rate. The right-hand form of equation 3.12 employs the assumption that the conductance does not change with air flow rate. NTU_{rated} can be determined from rated performance since the bypass factor can be determined from entering and leaving conditions. Then, the bypass factor is estimated as a function of air flow using equations 3.11 and 3.12.

The outlet air enthalpy for the evaporator operating at steady state is first determined using an energy balance with the known entering enthalpy and the cooling capacity determined as described in the previous section. For a given bypass factor and inlet and outlet enthalpy, the saturated air enthalpy corresponding to the apparatus dewpoint is determined from equation 3.10 as

$$h_{adp} = h_{e,i} - \frac{h_{e,i} - h_{e,o}}{1 - BF} \quad (3.13)$$

The apparatus dewpoint temperature and saturated humidity ratio are determined using psychrometric relationships for a relative humidity of 100% and an air enthalpy of h_{adp} . Then,

the outlet air humidity ratio is determined from equation 3.10 as

$$\omega_{e,o} = BF \cdot \omega_{e,i} + (1 - BF) \cdot \omega_{adp} \quad (3.14)$$

Since the outlet state lies on the locus of point connecting the inlet and apparatus dewpoint conditions (see Figure 15), the sensible heat ratio (SHR) can be determined as

$$SHR = \frac{h(T_{e,i}, \omega_{adp}) - h_{adp}}{h_{e,i} - h_{adp}} \quad (3.15)$$

where SHR is the ratio of the sensible cooling capacity to the total cooling capacity.

If the calculated value of SHR is greater than unity, then moisture condensation does not occur and SHR is unity. In this case, the inlet humidity ratio is adjusted until the point where $SHR = 1$. The air inlet wet bulb temperature associated with the actual dry bulb temperature and this fictitious humidity is then used as the evaporator inlet condition for the capacity and COP correlations given in the previous section.

Compressor Power Consumption

When there is a cooling requirement for the primary equipment, the compressor(s) and condenser fan(s) cycle on and off to maintain the zone temperature at the cooling setpoint. VSAT utilizes one-hour timesteps and yet the equipment must generally cycle on and off at smaller time intervals. The fraction of the hour that the equipment must operate in order to meet the load is assumed to be equal to the part-load ratio (PLR), which is the ratio of the average hourly equipment cooling requirement (\dot{Q}_c) to the steady-state capacity (\dot{Q}_{cap}) of the equipment or

$$PLR = \frac{\dot{Q}_c}{\dot{Q}_{cap}} \quad (3.16)$$

There are energy losses associated with cycling primarily due to the loss of the pressure differential between the condenser and evaporator when the unit shuts down. The compressor must re-establish the steady-state evaporator and condenser pressures to achieve the steady-state capacity whenever the unit turns on. These pressures equilibrate very quickly after the unit is shut down. The effect of cycling on power consumption is considered through the use of a part-load factor (PLF). For any given hour, the average power consumption of the compressor and condenser fan are calculated as

$$\dot{W}_c = PLF \cdot \frac{\dot{Q}_{cap}}{COP_{cap}} \quad (3.17)$$

where PLF is ratio of the average power to the full-load power consumption. PLF is determined in terms of PLR using the following correlation from DOE 2.1E.

$$PLF = a_5 + PLR \cdot (b_5 + PLR \cdot (c_5 + d_5 \cdot PLR)) \quad (3.18)$$

For the heat pump heat recycler, both the ventilation (optional) and exhaust fans operate continuously during the occupied period and do not cycle with the compressor. As a result, the correlations presented for COP_{cap} only include the compressor. For this equipment, the compressor power is determined with equation 3.17.

3.1.2 Prototypical Rooftop Air Conditioner Characteristics

The correlations for the primary rooftop cooling equipment were taken from DOE 2.1E. In VSAT, the rated cooling capacity in equation 3.1 is determined based upon the peak cooling requirements associated with the building, ventilation system, and location (see sizing section). The rated flow rate is 450 cfm/ton. The user can choose between three different rated COPs corresponding to EERs of 8, 10, 12. The default is an EER of 12. The actual evaporator air flow rate when the unit is operating can be set by the user, but the default is 350 cfm/ton.

Figure 16 shows the variation in the temperature-dependent capacity and COP correction factors as a function of condenser air inlet temperature and evaporator air inlet wet bulb temperature for the prototypical rooftop air conditioner. The values were determined with equations 3.3 and 3.4 using the coefficients given in Table 9. The cooling capacity and COP vary by about a factor of two over the range of interest. The maximum capacity and COP (minimum $f_{COP,t}$) occur at a low condenser inlet temperature and high evaporator inlet wet bulb temperature.

Figure 17 shows the mass flow rate-dependent capacity and COP correction factors as a function of the ratio of the supply air flow rate to the rated flow rate. The values were determined with equations 3.5 and 3.6 using the coefficients given in Table 10. Over the range of interest, the impact of supply air flow on COP is relatively small. The COP decreases by only about 5% when the flow is 50% of the design flow. The sensitivity of cooling capacity to changes in flow rate is greater than for COP and the effect becomes more important at low flow rates.

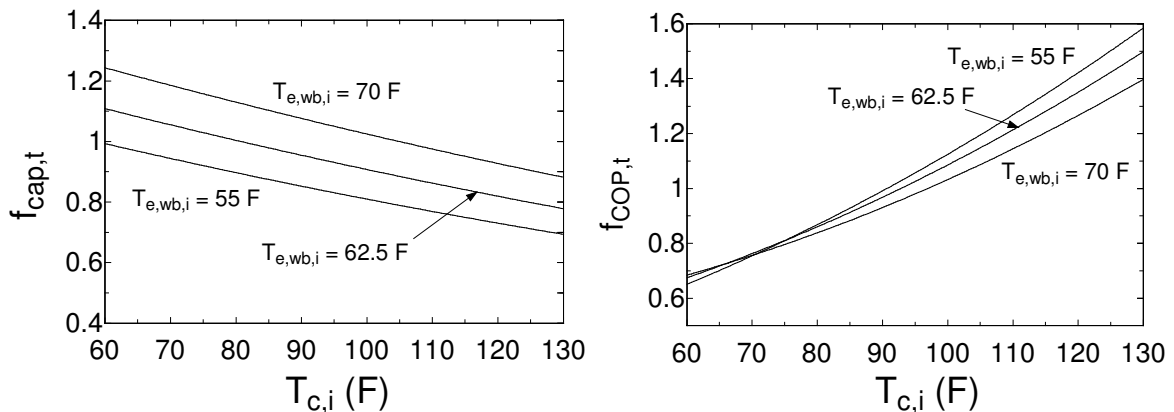


Figure 16. Temperature-dependent capacity and COP correction factors for prototypical rooftop air conditioner

Table 9: Coefficients of temperature-dependent capacity and COP correction factor correlations for the prototypical rooftop air conditioner

Coefficient	Value	Units
a_1	0.8740302	-
b_1	-0.0011416	F ⁻¹
c_1	0.0001711	F ⁻²
d_1	-0.0029570	F ⁻¹
e_1	0.0000102	F ⁻²
f_1	-0.0000592	F ⁻²
a_2	-1.0639310	-
b_2	0.0306584	F ⁻¹
c_2	-0.0001269	F ⁻²
d_2	0.0154213	F ⁻¹
e_2	0.0000497	F ⁻²
f_2	-0.0002096	F ⁻²

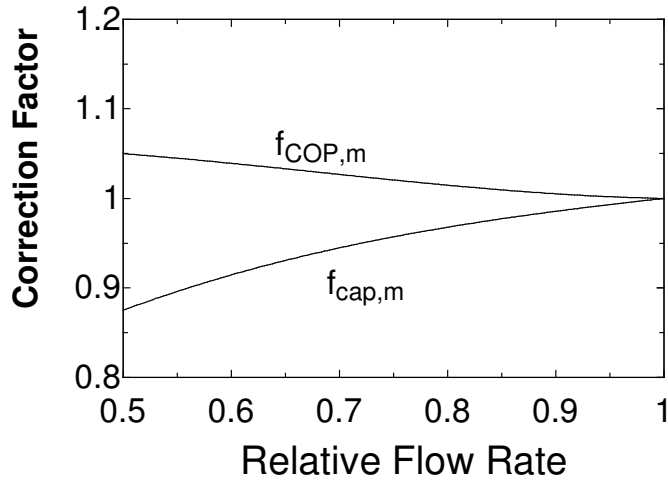


Figure 17. Flow rate-dependent capacity and COP correction factors for prototypical rooftop air conditioner

Table 10: Coefficients of mass flow rate-dependent capacity and COP correction factor correlations for the prototypical rooftop air conditioner

Coefficient	Value
a_3	0.4727859
b_3	1.2433414
c_3	-1.0387055
d_3	0.3225781
a_4	1.0079484
b_4	0.3454413
c_4	-0.6922891
d_4	0.3388994

Figure 18 shows PLF as a function of PLR determined using the correlation of equation

3.18 with coefficients given in Table 11. Also shown in this plot is a line for constant COP ($PLF = PLR$). The impact of cycling on power consumption is relatively small for part-load ratios greater than about 30%. The deviation from constant COP becomes very significant below a PLR of 0.2.

Table 11: Coefficients of part-load factor correlations

Coefficient	Value
a_5	0.2012301
b_5	-0.0312175
c_5	1.9504979
d_5	-1.1205105

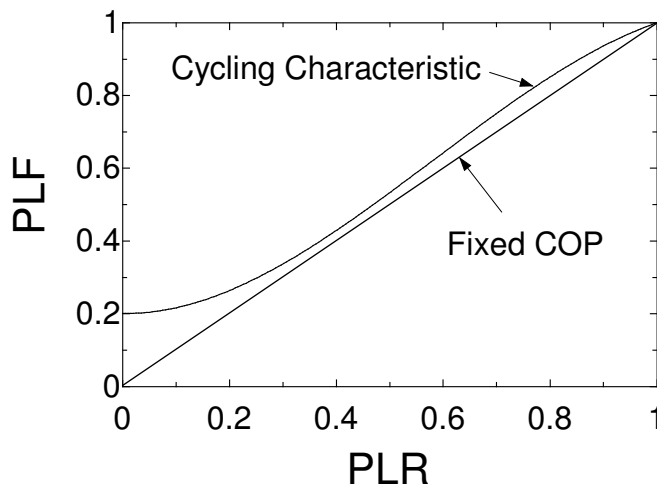


Figure 18. Part-load factor correlation

The user can specify a sensible heat ratio (SHR) at the rating condition. This value is used along with the rated flow rate per unit cooling capacity (cfm/ton) and the rated operating conditions to determine the rated bypass factor (BF) and NTU . The bypass factor is then corrected for the actual flow rate using equations 3.11 and 3.12. Standard ARI rating conditions are assumed: condenser inlet temperature of 95 F, evaporator inlet temperature of 80 F, and evaporator inlet wet bulb temperature of 67 F. The default value for the rated SHR is 0.75. For the prototypical unit with these specifications, the rated bypass factor is 0.261 and the rated NTU is 1.35.

3.1.3 Heat Pump Heat Recovery Unit (Energy Recycler[®])

The heat pump heat recovery unit is modeled using a very similar approach as for the primary air conditioner except that equation 3.2 is replaced with

$$COP_{cap} = COP_{rat} \cdot f_{COP,t}(T_{e,wb,i}, T_{c,i}) \cdot f_{COP,m}(\dot{m} / \dot{m}_{rat}) \quad (3.19)$$

This form resulted in better correlation of data. Coefficients of equations 3.3 - 3.6 were determined using manufacturer's data and tests conducted at the Herrick Labs. The laboratory tests provided data beyond the range available from the manufacturer. The rating conditions for the heat pump were taken from suggested rating points given in the manufacturer's data for both cooling and heating modes (Carrier, 1999).

Cooling Mode

For the unit considered, the rated air supply flow rate for cooling mode is 533 cfm/ton (1000 cfm rated supply air divided by 22.5 MBtu/hr gross cooling capacity). Rated air conditions are 75°F condenser air inlet dry bulb temperature, 95°F evaporator air inlet dry bulb temperature and 75°F evaporator air inlet wet bulb temperature. For the unit tested at this rating point, the total capacity is 22.5 MBtu/hr, COP is 4.515 and SHR is 0.902. The Energy Recycler is not available at different EERs, thus only one performance characteristic is available for analysis. The coil heat transfer units (NTUs) parameter at the rated condition is 1.08 and the rated bypass factor is 0.34.

Figure 19 shows the variation of temperature dependent correction factors for total cooling capacity and COP as a function of condenser air inlet temperature and evaporator air inlet wet bulb temperature. The correction factors were determined from equations 3.3 and 3.4 using the coefficients in Table 12.

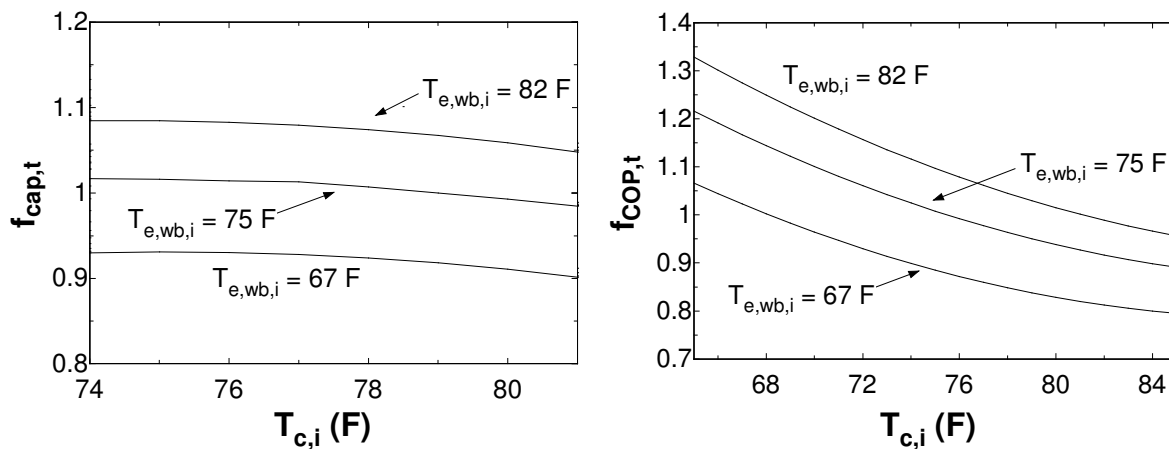


Figure 19. Temperature-dependent capacity and COP correction factors for heat pump heat recovery unit – cooling mode

Table 12: Coefficients of temperature-dependent capacity and COP correction factor correlations for the heat pump heat recovery unit – cooling mode

Coefficient	Value	Units
a_1	-6.758	-
b_1	0.0946	F ⁻¹
c_1	-0.000223	F ⁻²
d_1	0.09721	F ⁻¹
e_1	-0.0003967	F ⁻²
f_1	-0.0005549	F ⁻²
a_2	0.8402	-
b_2	0.06599	F ⁻¹
c_2	-0.0001786	F ⁻²
d_2	-0.0592	F ⁻¹
e_2	0.0004547	F ⁻²
f_2	-0.0003368	F ⁻²

Figure 20 shows the variation of mass dependent correction factors for total cooling capacity and COP as a function of the flow rate relative to the rated flow rate. The correction factors were determined from equations 3.5 and 3.6 using the coefficients in Table 13. The impact of flow rate on performance is much more significant than for the primary air conditioner because both condenser and evaporator flow rate change (not just evaporator flow rate).

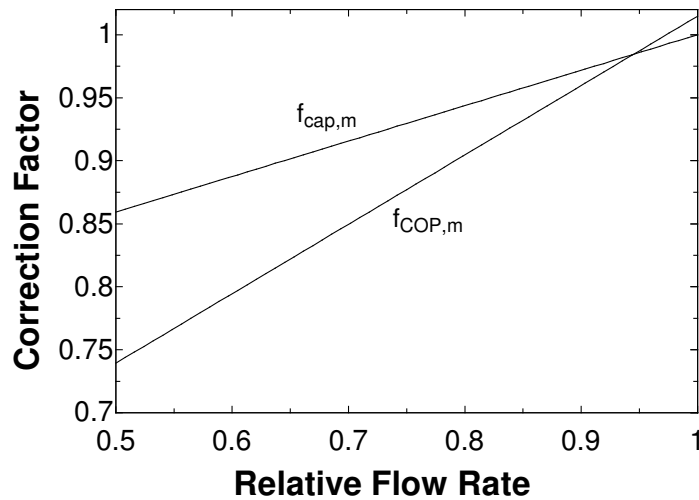


Figure 20. Flow rate-dependent capacity and COP correction factors for heat pump heat recovery unit – cooling mode

Table 13: Coefficients of mass flow rate-dependent capacity and COP correction factor correlations for heat pump heat recovery unit – cooling mode

Coefficient	Value
a_3	0.7187
b_3	0.2813
c_3	0.0
d_3	0.0
a_4	0.4639
b_4	0.5509
c_4	0.0
d_4	0.0

Heating Mode

For the unit considered, the rated air supply flow rate for heating mode is 540 cfm/ton (1000 cfm rated supply air divided by 22.2 MBtu/hr gross heating capacity). Rated air conditions are 70°F evaporator air inlet temperature and 33°F condenser air inlet temperature. The total capacity is 22.2 MBtu/hr and COP is 7.425 at this rating point.

Figure 21 shows the variation of the temperature dependent correction factors for total heating capacity and COP as a function of evaporator (return) air inlet temperature and condenser air inlet temperature. The correction factors were determined from equations 3.3 and 3.4 using the coefficients in Table 14. Total heating capacity and COP increase as the evaporator inlet temperature increases and condenser inlet temperature decreases. The maximum capacity for heating is thus experienced at higher air evaporating temperatures and lower condenser inlet temperatures.

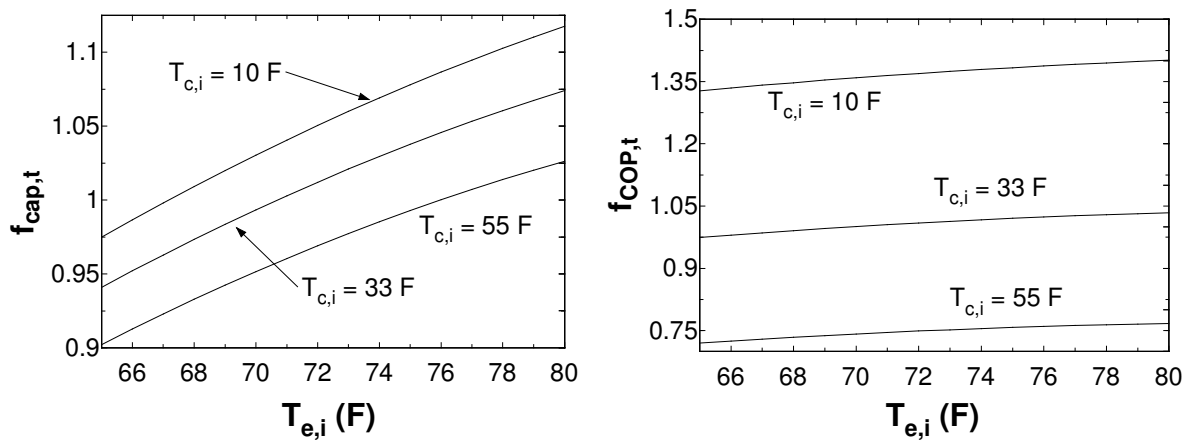


Figure 21. Temperature-dependent capacity and COP correction factors for heat pump heat recovery unit – heating mode

Table 14: Coefficients of temperature-dependent capacity and COP correction factor correlations for the heat pump heat recovery unit – heating mode

Coefficient	Value	Units
a_1	-0.4831	-
b_1	0.0006157	F ⁻¹
c_1	-0.000006376	F ⁻²
d_1	0.03305	F ⁻¹
e_1	-0.0001604	F ⁻²
f_1	-0.0000279	F ⁻²
a_2	0.4873	-
b_2	-0.01648	F ⁻¹
c_2	0.00008504	F ⁻²
d_2	0.02423	F ⁻¹
e_2	-0.0001307	F ⁻²
f_2	-0.00003938	F ⁻²

Figure 22 shows the variation of mass dependent correction factors for total heating capacity and COP as a function of the relative flow rate. The correction factors were determined from equations 3.5 and 3.6 using the Energy Recycler coefficients in Table 15.

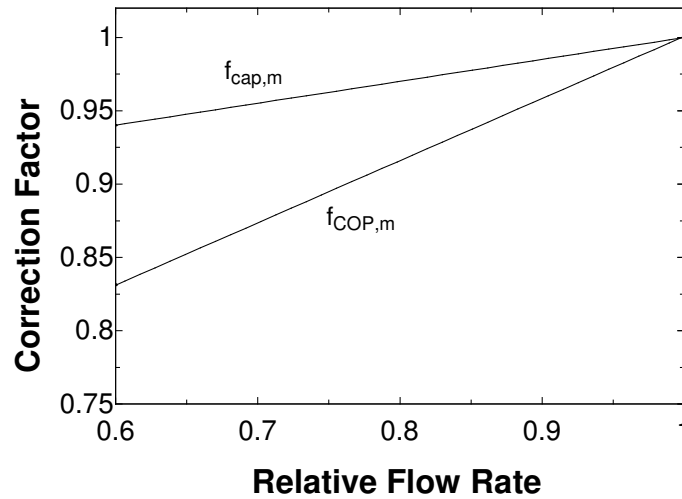


Figure 22. Flow rate-dependent capacity and COP correction factors for heat pump heat recovery unit – heating mode

Table 15: Coefficients of mass flow rate-dependent capacity and COP correction factor correlations for heat pump heat recovery unit – heating mode

Coefficient	Value
a_3	0.8505
b_3	.1495
c_3	0.0
d_3	0.0
a_4	0.5768
b_4	0.424
c_4	0.0
d_4	0.0

3.2 Primary Heater

The primary heater incorporated within the rooftop unit can be either gas or electric. For electric heat, the power consumption at any time is assumed to be equal to the heating requirement for any hour. For a gas heater, gas costs are based upon the primary fuel energy consumption integrated over the billing period (therms). For any time, the rate of primary fuel energy consumption is calculated as

$$\dot{Q}_F = \frac{\dot{Q}_h}{\eta_F} \quad (3.20)$$

where \dot{Q}_h is the heating requirement for the heating and η_f is the heater efficiency. The efficiency is assumed to be constant. The user can choose between three different efficiencies of 0.65, 0.80, and 0.95. The default efficiency is 0.95

3.3 Enthalpy Exchanger

3.3.1 Mathematical Description

The model for enthalpy exchangers that is incorporated within VSAT was developed by Stiesch et al. (1995) and Klein et al. (1990). Both of these studies incorporate the use of temperature, humidity, and enthalpy effectiveness defined as

$$\varepsilon_T = \frac{T_v - T_a}{T_z - T_a} \quad (3.21)$$

$$\varepsilon_\omega = \frac{\omega_v - \omega_a}{\omega_z - \omega_a} \quad (3.22)$$

$$\varepsilon_h = \frac{h_v - h_a}{h_z - h_a} \quad (3.23)$$

where ε is effectiveness, T is temperature, ω is humidity ratio, h is enthalpy, and the subscripts a, v, and z refer to conditions associated with the ambient air, ventilation air leaving the enthalpy exchanger, and return air from the zone, respectively.

For known values of effectiveness, equations 3.21 – 3.23 are used to estimate ventilation stream conditions in terms of ambient and zone air conditions. As the effectiveness values go to one, the ventilation temperature, humidity, and enthalpy approach the conditions of the return air. In general, the effectiveness increases as the speed of the wheel increases for given air flow rates.

Klein et al. (1990) used detailed numerical studies and found that for balanced flow rates, a Lewis number of one, and at high rotation speeds, the temperature, humidity, and enthalpy effectiveness for enthalpy exchangers are equal and can be estimated in terms of the number of transfer units as

$$\varepsilon_T = \varepsilon_\omega = \varepsilon_h = \frac{NTU}{NTU + 2} \quad (3.24)$$

where NTU is defined as

$$NTU = \frac{hA_s}{\dot{m}_{vent} C_{pm}} \quad (3.25)$$

and h is the heat transfer coefficient and A_s is the total surface area of the exchanger.

Stiesch et al. (1995) correlated temperature and enthalpy effectiveness as a function of rotation speeds, where the results were generated from detailed simulations. The correlations are of the form

$$\varepsilon_T = \frac{NTU}{NTU + 2} \cdot (1 - \exp[a_T \cdot \Gamma^2 + b_T \cdot \Gamma]) \quad (3.26)$$

$$\varepsilon_h = \frac{NTU}{NTU + 2} \cdot (1 - \exp[a_h \cdot \Gamma^3 + b_h \cdot \Gamma^2 + c_h \cdot \Gamma]) \quad (3.27)$$

where the a , b , and c coefficients are empirical factors that depend upon ambient temperature and Γ is a dimensionless rotation speed defined as

$$\Gamma = \frac{M_m / \dot{m}_{vent}}{t_r} \quad (3.28)$$

and where t_r is the time required for one exchanger rotation, M_m is the mass of the dry matrix, and \dot{m}_{vent} is the ventilation flow rate.

Equations 3.26 and 3.27 tend to approach the limiting case result of equation 3.24 for dimensionless rotation speeds greater than about 3. Well-designed enthalpy exchangers would tend to operate at higher speeds. However, it may be necessary to operate at lower

speeds to maintain a fixed ventilation supply air temperature under feedback control conditions.

Feedback control of the wheel speed is initiated under two situations: 1) the ambient air temperature is below 55 F and the ventilation stream outlet air temperature rises above 55 F or 2) the exhaust stream outlet air temperature falls below a freeze setpoint. The control logic incorporated in VSAT is based upon typical practice (Semco, 2002).

If the ambient temperature is below 55 F and the ventilation stream outlet air temperature falls would rise above 55 F (at full speed), then the wheel speed is modulated below the maximum speed to maintain an outlet temperature of 55 F. This limits preheating of the ventilation stream under conditions where cooling may be required. The temperature effectiveness necessary to achieve this condition is calculated as

$$\mathcal{E}_{T,vent,sp} = \frac{T_{vent,sp} - T_a}{T_z - T_a} \quad (3.29)$$

where $T_{vent,sp}$ is the setpoint temperature (55 F) for the ventilation supply air. Under low ambient conditions, the ventilation temperature is below 55 F and the wheel operates at full speed.

At low ambient temperatures, water vapor removed from the exhaust stream may condense and freeze. Reducing the speed reduces the effectiveness of the enthalpy exchanger and increases the matrix temperature within the exhaust speed. Freeze protection is initiated in VSAT when the exhaust temperature falls below a specified freeze protection limit. In this case, the exhaust temperature is set equal to the freeze protection limit and the temperature effectiveness necessary to achieve this condition is calculated as

$$\mathcal{E}_{T,freeze} = \frac{T_z - T_{freeze}}{T_z - T_a} \quad (3.30)$$

where T_{freeze} is the freeze protection limit for the exhaust temperature.

For either feedback control case, the dimensionless rotation speed necessary to achieve the required effectiveness given by equation 3.29 or 3.30 is determined from equation 3.26 using the required temperature effectiveness. Then, the ventilation stream enthalpy is evaluated using equations 3.27 and 3.23.

A frost set point is specified based on winter ambient and zone design conditions as discussed by Semco (2002) and Stiesch (1995). Figure 23 depicts the process on a psychrometric chart. Point A1 represents a low ambient temperature condition, whereas points Z1 and Z2 represent zone conditions with high and low humidities, respectively. For an enthalpy exchanger operating at full speed, the ventilation and exhaust air streams follow processes that are approximately on these lines. For process line Z2-A1, the exhaust air process line never crosses the saturation line and therefore moisture would not condense. However, for process line Z1-A1, moisture condenses at point Z1a for a wheel operating at full speed. In this case, the frost setpoint should be set a temperature greater than the temperature at Z1a.

The frost set point is determined by first estimating the point where the enthalpy exchanger process line (e.g., one Z1-A1) crosses the saturation line (e.g., point Z1a) assuming 1) an

ambient condition of 90% relative humidity at the lowest temperature occurring during the year and 2) a zone condition of 35% relative humidity at the heating setpoint. The crossing point is determined numerically and then a 2 C safety factor is added to the result

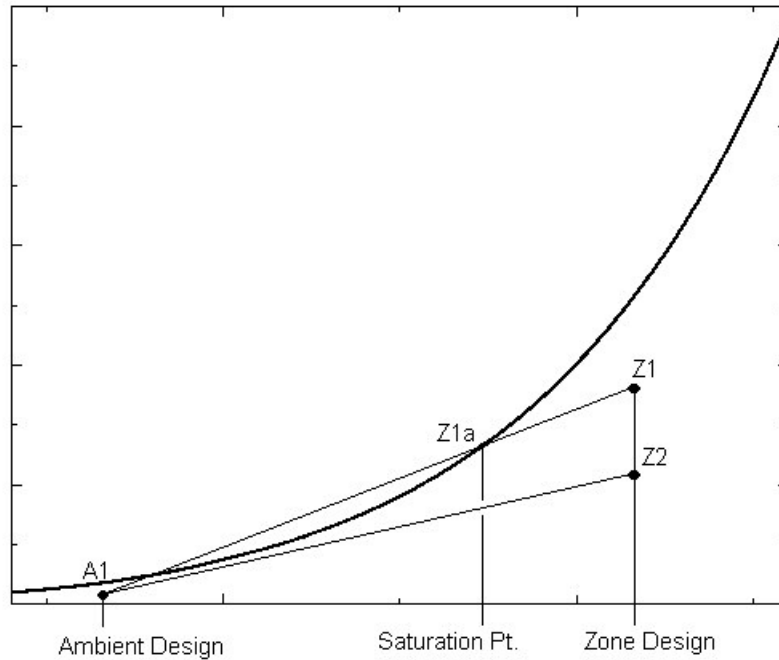


Figure 23. Frost set point determination

3.3.2 Prototypical Exchanger Descriptions

The specific correlations developed by Stiesch et al. (1995) were obtained using data from a commercial enthalpy exchanger (Carnes 1989) having a medium constructed of aluminum foil of thickness 0.025 mm coated with a thin, uniform layer of polymer desiccant. The medium has a counter-flow design and is constructed by coiling smooth and corrugated aluminum sheets to produce small triangular air passages. The equivalent hydraulic diameter of the triangular air passages is approximately 1.7 mm and the medium has a length in the direction of flow of 0.2 m. The diameter of the wheel is 1.23 m and the idealized rotational speed is approximately 15 rpm.

The manufacturer gives effectiveness as a function of air face velocity for their designs. At a face velocity of 650 fpm, the effectiveness for heat and mass transfer is about 0.75. From equation 3.24, this results in an NTU of about 6. These values are assumed for the prototypical enthalpy exchanger.

The effectiveness is constant unless the feedback control is initiated as described in the previous subsection. If this occurs, then the empirical factors determined by Stiesch et al. (1995) are used in equations 3.26 and 3.27. These are:

$$a_T = a_{T_1} + \frac{a_{T_2}}{NTU a_{T_3}} \quad (3.31)$$

$$b_T = b_{T_1} + \frac{b_{T_2}}{NTU} b_{T_3} \quad (3.32)$$

$$a_h = a_{h_1} + a_{h_2} \cdot NTU + a_{h_3} \cdot NTU^2 \quad (3.33)$$

$$b_h = b_{h_1} + b_{h_2} \cdot NTU + b_{h_3} \cdot NTU^2 \quad (3.34)$$

$$c_h = c_{h_1} + \frac{c_{h_2}}{NTU^{0.8}} \quad (3.35)$$

where

$$a_{T_1} = 0.002259 - 1.376 \times 10^{-3} \cdot T_a - 6.91 \times 10^{-6} \cdot T_a^2$$

$$a_{T_2} = 0.09084 - 3.263 \times 10^{-4} \cdot T_a + 7.4 \times 10^{-6} \cdot T_a^2$$

$$a_{T_3} = 0.7388 - 0.01994 \cdot T_a - 3.829 \times 10^{-4} \cdot T_a^2$$

$$b_{T_1} = -1.007 + 0.0093 \cdot T_a + 2.778 \times 10^{-4} \cdot T_a^2$$

$$b_{T_2} = -1.533 + 0.02287 \cdot T_a - 2.356 \times 10^{-4} \cdot T_a^2$$

$$b_{T_3} = 1.111 - 2.667 \times 10^{-3} \cdot T_a - 1.378 \times 10^{-4} \cdot T_a^2$$

$$a_{h_1} = 3.381 \times 10^{-3} - 9.679 \times 10^{-4} \cdot T_a \quad \text{for } T_a \leq 0^\circ\text{C}$$

$$a_{h_1} = 3.381 \times 10^{-3} - 4.127 \times 10^{-5} \cdot T_a \quad \text{for } T_a > 0^\circ\text{C}$$

$$a_{h_2} = 5.088 \times 10^{-4} + 4.89 \times 10^{-6} \cdot T_a$$

$$a_{h_3} = 5.298 \times 10^{-6} - 7.652 \times 10^{-7} \cdot T_a$$

$$b_{h_1} = 6.237 \times 10^{-3} + 8.827 \times 10^{-3} \cdot T_a - 6.042 \times 10^{-4} \cdot T_a^2$$

$$b_{h_2} = -0.02133 + 1.323 \times 10^{-4} \cdot T_a$$

$$b_{h_3} = 4.908 \times 10^{-4} + 6.46 \times 10^{-6} \cdot T_a$$

$$c_{h_1} = -0.4087 + 0.00253 \cdot T_a + 3.34 \times 10^{-4} \cdot T_a^2$$

$$c_{h_2} = -1.449 + 0.02337 \cdot T_a - 5.578 \times 10^{-4} \cdot T_a^2$$

SECTION 4: AIR DISTRIBUTION SYSTEM AND CONTROLS

The air distribution system includes ducts, fans, dampers, and controls. A supply fan integrated with the primary cooling/heating equipment provides the flow rate to the zone. A return fan is not considered. The ventilation heat pump heat recovery unit utilizes an exhaust fan and an optional ventilation fan. The ventilation fan is only necessary if the required ventilation flow rate cannot be provided using the primary supply fan. During the occupied period, the fan(s) operate(s) continuously and provide a constant flow rate of air to the zone, while the equipment cycles on and off as necessary to maintain the zone temperature setpoint. During the unoccupied period, the fan(s) cycle(s) on and off with the equipment, but the airflow rate is constant when the system is on.

There are separate heating and cooling setpoints for the zone. If the zone temperature falls between these setpoints, then the temperature is “floating” and no heating or cooling is required. If the zone temperature falls below the heating setpoint, then the heating required to maintain the zone at this temperature is calculated as the zone heating load. The total equipment heating load includes an additional load associated with ventilation. If the zone temperature rises above the cooling setpoint, then the cooling required to maintain the zone at this temperature is calculated as the sensible zone cooling load. The total equipment cooling load includes additional loads associated with ventilation and latent gains within the zone.

When installed, the ventilation heat pump heat recovery unit is only enabled during occupied hours. During unoccupied hours, the primary air conditioner and heater must meet the cooling and heating requirements. In addition, the heat pump will only operate in cooling mode when the ambient temperature is above 68 F.

The enthalpy exchanger operates when the primary fan is on and the ambient temperature is less than 55 F or greater than the return air temperature. When the ambient temperature is between 55 F and the return air temperature, it is assumed that a cooling requirement exists and it is better to bring in cooler ambient air. When the ambient temperature is below 55 F, then a feedback controller adjusts the speed to maintain a ventilation supply air temperature of 55 F. When the ambient temperature is above the return air temperature, then wheel operates at maximum speed.

There are four ventilation control strategies considered in VSAT: fixed ventilation, demand-controlled ventilation, economizer, and night ventilation precooling. When a heat recovery heat exchanger or heat pump is employed within the ventilation stream, then fixed ventilation is assumed. Demand-controlled ventilation is considered both with and without an economizer. Night ventilation is considered with and without an economizer and with and without demand-controlled ventilation.

This section describes modeling of the air distribution components and controls and calculation of the equipment heating and cooling loads.

4.1 Ventilation Flow

4.1.1 Fixed Ventilation

In the absence of demand-controlled ventilation and during occupied mode, the minimum ventilation flow rate is a fixed value and is determined using ASHRAE Standard 62-1999 based upon the design occupancy. Table 1 - Table 7 include ventilation requirements and design occupancies for the prototypical buildings considered in VSAT. Note that in many

cases, the average occupancy levels are much lower than the design occupancies used to determine minimum ventilation flow requirements. During unoccupied mode, the minimum ventilation flow is zero and the damper is closed.

4.1.2 Demand-Controlled Ventilation

When demand-controlled ventilation is enabled, a minimum flow rate of ventilation air is determined that will keep the CO₂ concentration in the zone at or below a specified level. The minimum flow rate is calculated assuming a quasi-steady state mass balance on the air within the zone and the ducts, fully-mixed zone air, and a constant ventilation effectiveness that accounts for short-circuiting of ventilation air within the supply to the return duct. With these assumptions, the minimum ventilation flow rate is

$$\dot{m}_{vent,min} = \min\left(\frac{\dot{C}_{CO_2,gen}}{\eta_v \cdot (C_{CO_2,set} - C_{CO_2,amb})}, \dot{m}_{sup}\right) \quad (4.1)$$

where $\dot{C}_{CO_2,gen}$ is the rate of CO₂ generation within the zone, $C_{CO_2,set}$ is the setpoint for CO₂ concentration in the zone, $C_{CO_2,amb}$ is the ambient CO₂ concentration, and η_v is the ventilation efficiency. The ventilation efficiency is a measure of how effectively the ventilation air removes pollutants from the zone. The default value is 0.85. The user can set values for the zone setpoint and ambient CO₂ concentrations. The default values are 1000 ppm and 350 ppm, respectively.

The CO₂ generation rate is the product of the generation rate per person and the number of occupants at any given time. Table 1 - Table 7 include generation rates per person and default occupancy information for the prototypical buildings considered in VSAT.

4.1.3 Economizer

At any given time, the ventilation flow can be greater than the minimum due to economizer operation. VSAT considers a differential enthalpy economizer. The differential enthalpy economizer is engaged whenever the enthalpy of the ambient air is less than the enthalpy of the air in the return duct and the zone requires cooling.

In economizer mode, the ventilation flow rate is modulated between the minimum and maximum (wide open) values to maintain a specified setpoint for the mixed air temperature supplied to the primary equipment. The default mixed air setpoint is 55 F. During the occupied mode, the economizer will cycle on and off as necessary to maintain the zone temperature setpoint. However, during unoccupied mode, both the economizer and the fan cycle on and off together to maintain the zone temperature. In either case, the average hourly ventilation flow rate when the economizer is enabled is determined as

$$\dot{m}_{vent} = \min(\max(\dot{m}_{vent,min}, \dot{m}_{vent,mix}), \dot{m}_{vent,z}, \dot{m}_{sup}) \quad (4.2)$$

where $\dot{m}_{vent,mix}$ is the ventilation flow rate necessary to give a mixed air temperature equal to its setpoint and $\dot{m}_{vent,z}$ is the ventilation flow rate that keeps the zone temperature at its setpoint. This logic simulates a perfect economizer controller that requires a call for 1st stage

cooling to enable the economizer (and fan during unoccupied mode) and uses damper modulation to maintain a mixed air temperature setpoint.

With the economizer enabled, the ventilation flow rate necessary to maintain the zone temperature at its setpoint is

$$\dot{m}_{vent,z} = \frac{\dot{Q}_{z,c} + \dot{W}_{fan,s}}{C_{pm}(T_{z,c} - T_a)} \quad (4.3)$$

where $\dot{Q}_{z,c}$ is the zone sensible cooling load, $T_{z,c}$ is the zone temperature setpoint for cooling, and $\dot{W}_{fan,s}$ is the power associated with the primary supply fan.

4.1.4 Night Ventilation Precooling

Whenever the ambient temperature drops below the zone temperature, the ambient air can be used to precool the zone and reduce cooling loads during the next day. However, the next day savings associated with operating the ventilation system at night should be sufficient to offset the cost of operating the fan. In addition, the ambient humidity should be low enough to avoid increased latent loads during the next day and the ambient temperature should be high enough so as to avoid additional heating requirements after occupancy. With these issues in mind, the rules in Table 16 are employed to enable precooling.

Table 16. Rules for Enabling Ventilation Precooling

Rule	Description
$(T_z - T_a) > \Delta T_{on}$	The ambient temperature (T_a) must be less than the zone temperature (T_z) by a threshold (ΔT_{on}) chosen to balance fan operating costs with next day savings.
$T_a > 50^\circ\text{F}$	The ambient temperature must be greater than 50 °F to avoid conditions where heating might be required the next day.
$T_{a,dp} < 55^\circ\text{F}$	The ambient dew point ($T_{a,dp}$) must be less than 55 °F to avoid conditions where the latent load might increase the next day.
$\Delta t_{occ} < 6$ hours	The time to occupancy (Δt_{occ}) must be less than 6 hours to achieve good storage efficiency.
$N_{heat} > 24$ hours	The number of hours (N_{heat}) since the last call for heating should be greater than 24 hours to lock out precooling in the heating season

When night ventilation precooling is enabled, mechanical cooling is disabled and the ventilation system operates with 100% outside air to precool the zone with a setpoint of 67 °F. Once the zone temperature reaches 67 °F, the fan cycles to maintain this setpoint. Just prior to the occupied period, the setpoint for ventilation precooling is raised to 69 °F. Once the occupied period begins, there are separate setpoints associated cooling provided by the economizer (1st stage cooling) and the packaged air conditioner (2nd stage cooling). The 1st and 2nd stage setpoints are 69 °F and 75 °F, respectively. Once the occupied period ends, the zone temperature setpoint is raised to 80 °F.

The threshold for the zone/ambient temperature difference is determined based upon trading off nighttime fan energy and daytime compressor energy saved. When ventilation precooling is enabled, mechanical cooling is disabled and the zone temperature setpoint is set at 67 F. The damper is fully open and the ventilation flow rate is equal to the primary supply air flow rate. The fan cycles, as necessary, to maintain the zone setpoint. At this point, the temperature difference required to achieve savings is estimated from equation 2.7 as

$$\Delta T_{on} = \frac{\dot{W}_{fan}}{\rho_a c_{pa} \dot{V}_{fan}} \cdot \left(\frac{COP_{nv,occ}}{\eta_s} \cdot \frac{\bar{R}_{unocc}}{\bar{R}_{occ}} + 1 \right) \quad (4.4)$$

Figure 24 shows the breakeven temperature difference as a function of the ratio of unoccupied to occupied energy rates and the ratio of fan power to volumetric flow rate for a storage efficiency of 0.8 and an occupied period COP of 3. For typical values, the threshold varies between about 1 F and 10 F. The breakeven point increases with fan power (i.e., pressure drop) for a given flow rate since the cost of providing a given quantity of precooling increases. The fan power typically varies between about 0.4 and 0.7 W/cfm. The threshold also increases as the ratio between occupied and unoccupied energy rates decreases. Lower occupied period energy costs reduce the savings associated with precooling leading to a larger threshold. For similar reasons, the threshold increases with increasing occupied period COP. For packaged air conditioning equipment, the COP varies between about 2 and 4. Finally, the threshold increases with decreasing storage efficiency as less of the precooling results in cooling load reductions during the occupied period. Storage efficiencies vary between about 0.5 and 0.9.

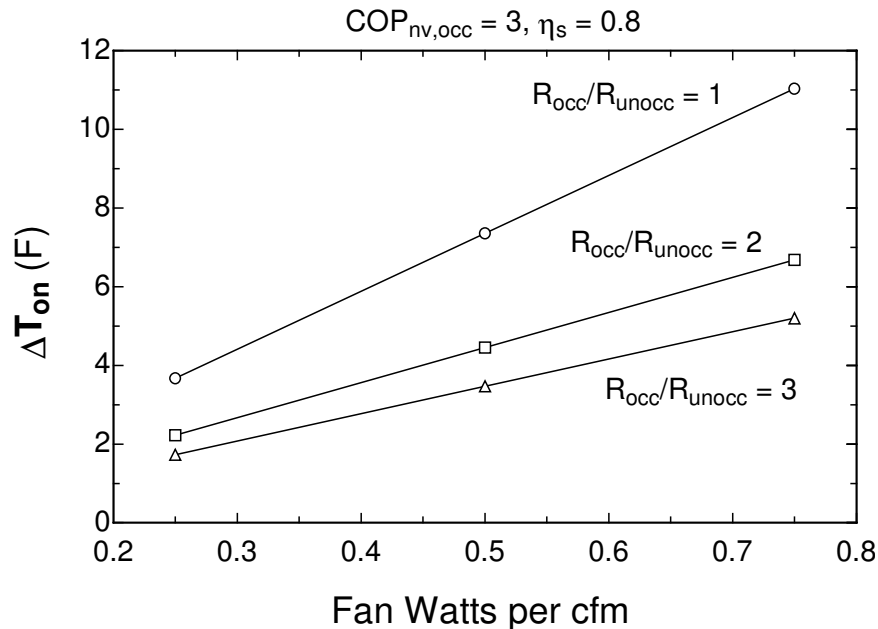


Figure 24. Night Ventilation Breakeven Threshold

4.2 Mixed Air Conditions

The mixed air conditions entering the primary air conditioner and heater are determined from mass and energy balances for adiabatic mixing according to

$$\omega_{mix} = \frac{\dot{m}_{vent}}{\dot{m}_{sup}} \omega_v + \left(1 - \frac{\dot{m}_{vent}}{\dot{m}_{sup}}\right) \omega_z \quad (4.4)$$

$$h_{mix} = \frac{\dot{m}_{vent}}{\dot{m}_{sup}} h_v + \left(1 - \frac{\dot{m}_{vent}}{\dot{m}_{sup}}\right) h_z \quad (4.5)$$

where ω is humidity ratio, h is air enthalpy, and the subscripts z and v refer to zone return and ventilation air conditions, respectively. For a system with a heat recovery heat exchanger or heat pump, ω_v and h_v are the conditions exiting the device within the ventilation stream. Otherwise, these properties are evaluated at ambient humidity conditions. The mixed air temperature is evaluated with psychrometric property routines in terms of the mixed air humidity and enthalpy or

$$T_{mix} = T(h_{mix}, \omega_{mix}) \quad (4.6)$$

4.3 Equipment Heating Requirements

If the zone requires heating to maintain the temperature at the heating setpoint, then the furnace and/or heat pump heat recovery unit must operate to meet the zone requirements and any additional load associated with ventilation. The furnace and heat pump provide only sensible heating (no humidification). If a heat pump heat recovery unit is employed, then it has the first priority for heating (i.e., 1st stage heating) during occupied mode. During unoccupied mode, the heat pump unit does not operate.

4.3.1 Heat Pump Heat Recovery Unit

From an energy balance on the air within the zone and distribution system, the heating load for the heat pump during occupied mode is

$$\dot{Q}_{hphr,h} = \min(\dot{Q}_{z,h} + \dot{m}_{vent} C_{pm} (T_{z,h} - T_a) - \dot{W}_{fan,s} - \dot{W}_{fan,v}, \dot{Q}_{hphr,h,cap}) \quad (4.7)$$

where $\dot{Q}_{z,h}$ is the zone heating load, \dot{m}_{vent} is the ventilation flow rate, $T_{z,h}$ is the zone heating temperature setpoint, $\dot{W}_{fan,s}$ is the power associated with the primary supply fan, $\dot{W}_{fan,v}$ is the power associated with the optional ventilation fan for the heat pump, and $\dot{Q}_{hphr,h,cap}$ is the heating capacity associated with the heat pump.

4.3.2 Primary Heater

The heating requirement for the primary heater is

$$\dot{Q}_h = \dot{Q}_{z,h} + \dot{m}_{vent} C_{pm} (T_{z,h} - T_v) - \dot{W}_{fan,s} \quad (4.8)$$

where T_v is the temperature of the ventilation air that is mixed with return air. For a system with a heat recovery heat exchanger or heat pump, T_v is the temperature exiting the device within the ventilation stream. Otherwise, T_v is equal to the ambient temperature.

4.4 Equipment Cooling Requirements

The first priority for cooling (1st stage cooling) is the economizer if it is installed and enabled. If the economizer can meet the sensible zone cooling requirement, then the primary air conditioner does not operate. If a heat pump heat recovery unit is installed, then an economizer is not employed and the heat pump is the first priority for cooling during occupied mode. During unoccupied mode, the heat pump unit does not operate.

4.4.1 Heat Pump Heat Recovery Unit

The sensible cooling requirement for the heat pump is

$$\dot{Q}_{hphr,s,c} = \min(\dot{Q}_{s,T}, SHR \cdot \dot{Q}_{hphr,c,cap}) \quad (4.9)$$

where $\dot{Q}_{hphr,c,cap}$ is the cooling capacity of the heat pump, SHR is the heat pump sensible heat ratio, and $\dot{Q}_{s,T}$ is the total sensible load determined as

$$\dot{Q}_{s,T} = \dot{Q}_{z,c} + \dot{m}_{vent} C_{pm} (T_a - T_{z,c}) + \dot{W}_{fan,s} + \dot{W}_{fan,v} \quad (4.10)$$

where $\dot{Q}_{z,c}$ is the zone sensible cooling load. The cooling capacity and SHR are evaluated using the ambient and zone return air conditions as inlet conditions for the evaporator and condenser.

The total cooling requirement for the heat pump is

$$\dot{Q}_{hphr,c} = \frac{\dot{Q}_{hphr,s,c}}{SHR} \quad (4.11)$$

4.4.2 Primary Air Conditioner

The sensible cooling requirement for the primary air conditioner is

$$\dot{Q}_{ac,s,c} = \min(\dot{Q}_{s,T}, SHR \cdot \dot{Q}_{ac,c,cap}) \quad (4.12)$$

where $\dot{Q}_{ac,c,cap}$ is the cooling capacity of the air conditioner, SHR is the air conditioner sensible heat ratio, and $\dot{Q}_{s,T}$ is the total sensible load determined as

$$\dot{Q}_{s,T} = \dot{Q}_{z,c} + \dot{m}_{vent} C_{pm} (T_v - T_{z,c}) + \dot{W}_{fan,s} \quad (4.13)$$

where T_v is the temperature of the ventilation air that is mixed with return air. For a system with a heat recovery heat exchanger or heat pump, T_v is the temperature exiting the device within the ventilation stream. Otherwise, T_v is equal to the ambient temperature.

The cooling capacity and *SHR* are evaluated using the mixed air conditions as described in Section 3. When an economizer is not enabled, the mixed air condition depends on both ventilation and zone return air conditions according to equations 4.4 and 4.5. However, the return air humidity depends on the exit humidity from the air conditioner, which in turn depends on the mixed air condition. A quasi-steady state mass balance for humidity within the air distribution system is used along with an iterative solution to determine the zone and mixed air states and equipment performance. The zone return air humidity ratio must satisfy equations 4.4, 4.5, 4.12, 4.13 and the following equations.

$$(1 - SHR) \cdot \dot{Q}_{ac,c} = \dot{Q}_{p,L} + \dot{m}_{inf} (\omega_a - \omega_z) h_{fg} + \dot{m}_{vent} (\omega_v - \omega_z) h_{fg} \quad (4.14)$$

$$\dot{Q}_{ac,c} = \frac{\dot{Q}_{ac,s,c}}{SHR} \quad (4.15)$$

where $\dot{Q}_{ac,c}$ is the total equipment cooling requirement, $\dot{Q}_{p,L}$ is the latent load associated with people in the zone, \dot{m}_{inf} is the infiltration flow rate, ω_a is the ambient humidity ratio, and h_{fg} is the heat of vaporization of water.

4.5 Supply, Ventilation, and Exhaust Fans

Only single-speed air distribution fans are considered in VSAT. For systems without a heat pump heat recovery unit or enthalpy exchanger, only a single supply fan is used for each primary air conditioner. The heat pump heat recovery unit incorporates a fan for the exhaust stream and has an optional fan for the ventilation stream. Enthalpy exchangers typically employ both ventilation and exhaust stream fans to ensure effective purging. For each fan, the fan power is scaled with the volumetric flow according to

$$\dot{W}_{fan,on} = w_f \cdot \dot{V}_{on} \quad (4.16)$$

where $\dot{W}_{fan,on}$ is fan power at steady state, w_f is fan power per unit of volume flow and \dot{V}_{on} is the volumetric flow rate when the fan is operating. The user can specify values for w_f . For the primary supply fans, the default value for w_f is 0.5 W/cfm. For the ventilation and exhaust fans, the default value for w_f is 0.25 W/cfm.

During occupied mode, any of the air distribution fans operate continuously. However, during unoccupied mode, the fans cycle with the heater or primary air conditioner and/or economizer. In this case, the average hourly fan power is calculated as

$$\dot{W}_{fan} = PLR \cdot \dot{W}_{fan,on} \quad (4.17)$$

where *PLR* is the ratio of the average hourly heating or cooling requirement to the heat or cooling capacity. When heating or mechanical cooling is required, then the *PLR* is determined as outlined in Section 3. When cooling is required and the economizer can meet the cooling requirements, then *PLR* is determined as

$$PLR = \frac{\dot{Q}_{z,c}}{\dot{m}_{sup} C_{pm} (T_{z,c} - T_{mix,econ})} \quad (4.18)$$

where $T_{mix,econ}$ is the mixed air setpoint temperature for the economizer.

4.6 Zone Controls – Call for Heating or Cooling

The first step in evaluating whether heating or cooling is required is to determine the zone temperature if the equipment were off. During unoccupied mode, the supply air fan is off when there is no heating and cooling requirement. In this case, the floating zone temperature is determined by setting \dot{Q}_z to zero in equation 2.27 and solving for the zone temperature. During occupied mode, the fan(s) operate(s) continuously so that ventilation loads and fan energy influence the floating zone temperature. In this case, the zone temperature is determined that satisfies the following equation.

$$\dot{Q}_z + \dot{W}_{fan,s} + \dot{W}_{fan,v} + \dot{m}_{vent} C_{pm} (T_a - T_z) = 0 \quad (4.19)$$

SECTION 5: WEATHER DATA, SIZING, AND COSTS

5.1 Weather Data

VSAT contains typical meteorological year (TMY2) weather data for 239 US locations and California Climate Zone data for 16 representative zones within California. The data include hourly values of ambient temperature, horizontal radiation, and direct normal radiation. In addition, the user can specify the ambient CO₂ level. The default value is 350 ppm.

The California Climate Zones are shown in Figure 25 and the representative cities for each climate zone (CZ) are given in Table 17. The climate zones are based on energy use, temperature, weather and other factors. They are basically a geographic area that has similar climatic characteristics. The California Energy Commission originally developed weather data for each climate zone by using unmodified (but error-screened) data for a representative city and weather year (representative months from various years). The Energy Commission analyzed weather data from weather stations selected for (1) reliability of data, (2) currency of data, (3) proximity to population centers, and (4) non-duplication of stations within a climate zone.

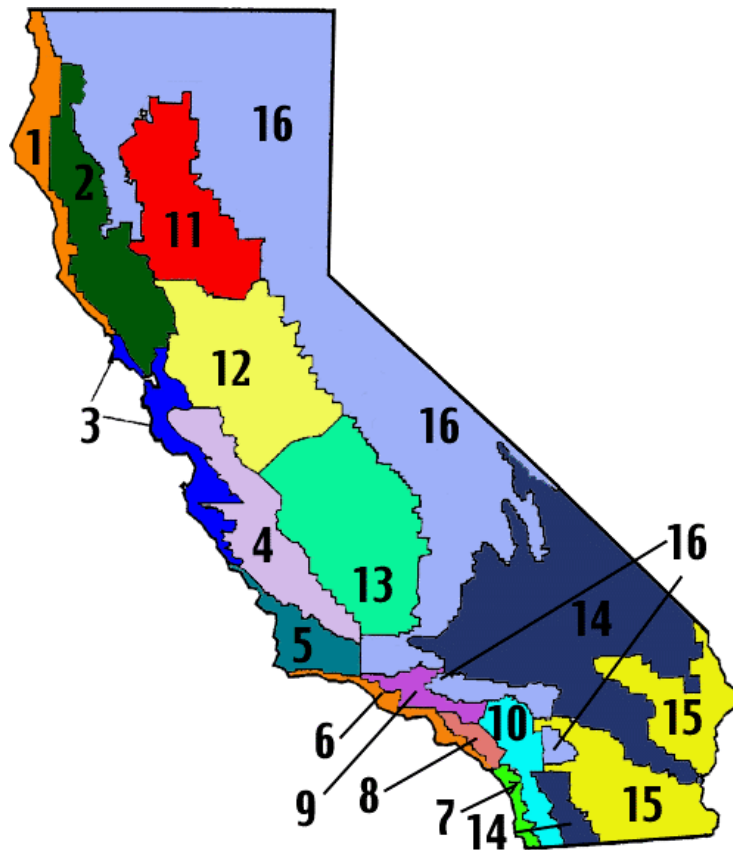


Figure 25. California Climate Zones

Table 17. Cities associated with California Climate Zones

CZ 1: Arcata	CZ 5: Santa Maria	CZ 9: Pasadena	CZ13: Fresno
CZ 2: Santa Rosa	CZ 6: Los Angeles	CZ10: Riverside	CZ14: China Lake
CZ 3: Oakland	CZ 7: San Diego	CZ11: Red Bluff	CZ15: El Centro
CZ 4: Sunnyvale	CZ 8: El Toro	CZ12: Sacramento	CZ16: Mount Shasta

There are two sets of Climate Zone data included in VSAT, the original and a massaged set. In the message data, the dry bulb temp has been modified in an effort to give the file a better "average" across the entire zone. Because only dry bulb was adjusted, the humidity conditions are affected and therefore the massaged files are not preferred.

5.2 Equipment Sizing

The heating and cooling equipment are automatically sized for a given building and location. The primary heating and cooling equipment are sized assuming no ventilation heat recovery (enthalpy exchanger or heat pump), no economizer, fixed ventilation, and constant zone temperature setpoints (no night setup or setback). The peak sensible heating and cooling requirements are first determined by calculating the hourly zone and ventilation loads throughout the heating and cooling seasons. The heating capacity is set at 1.4 times the peak sensible heating load.

For cooling, the required equipment cooling capacity depends upon the latent load, which depends on ambient and zone humidities and the zone internal latent gains. The required capacity is determined iteratively using the ambient conditions and zone latent gains associated with the peak sensible cooling requirement along with the equipment and air distribution models. The cooling equipment is then oversized by 10%.

The supply air flow rate is determined based upon a specified flow per unit cooling capacity with a default of 350 cfm/ton. The supply fan power is based upon a specified fan power per unit flow rate with a default of 0.5 W/cfm.

The number of rooftop units employed for a given application will influence the economics of the different ventilation strategies. Individual rooftop units require separate enthalpy exchangers, heat pump heat recovery units, economizers, or controllers (demand-controlled ventilation or night ventilation precooling). It will be assumed that rooftop units are available in sizes of 3.5, 5, 7.5, 10, 15, and 20 ton cooling capacities. For a given application and location, the number of individual rooftop units will be based upon the using fewest possible number of units necessary to realize a cooling capacity that is greater than, but within 10% of the target equipment cooling capacity.

The diameter of individual enthalpy exchangers will be scaled so as to achieve a flow velocity of 650 fpm. At this velocity, the exchanger has a constant effectiveness for heat and mass transfer of 0.75 when operated at normal speed.

The heat pump heat recovery unit cooling capacity will be scaled to achieve a flow per unit cooling capacity of 533 cfm/ton based upon the rated cooling capacity and the ventilation flow requirements.

5.3 Costs

VSAT is set up to calculate the simple payback period associated with different ventilation strategies. The alternatives are compared with a base case that has fixed ventilation with no

economizer or other ventilation strategy. For any alternative k, the simple payback period is calculated as

$$N_{pb} = \frac{C_k}{S_k} \quad (5.1)$$

where S_k is the annual savings in utility costs associated with the ventilation strategy as compared with the base case and C_k is the installed cost associated with implementing the ventilation strategy.

The annual utility costs associated with operating the HVAC system are calculated according to

$$C_{HVAC} = \sum_{m=1}^{m=12} \left\{ r_{d,on,m} \cdot \dot{W}_{peak,on,m} + r_{d,mid,m} \cdot \dot{W}_{peak,mid,m} + r_{d,off,m} \cdot \dot{W}_{peak,off,m} + \sum_{i=1}^{N_m} (r_{e,i,m} \cdot W_{i,m} + r_{g,i,m} \cdot G_{i,m}) \right\} \quad (5.2)$$

where m is the month, i is the hour, N_m is the number of hours in month m , and for each month m : $r_{d,on,m}$, $r_{d,mid,m}$ and $r_{d,off,m}$ are the utility rates for electricity demand during the on-peak, mid-peak and off-peak periods (\$/kW) and $\dot{W}_{peak,on,m}$, $\dot{W}_{peak,mid,m}$ and $\dot{W}_{peak,off,m}$ are the peak power consumption for the HVAC equipment during the on-peak, mid-peak and off-peak periods; and for each hour i of month m : r_e is the utility rate for electricity usage (\$/kWh), W is the electricity usage (kWh), r_g is the utility rate for natural gas usage (\$/therm), G is the gas usage (therm).

The electricity costs include both energy (\$/kWh) and demand charges (\$/kW) for on-peak, off-peak, and mid-peak periods. Gas energy usage does not vary with time of the day. However, the user can enter different electric and gas rates for summer and winter periods.

The default rates and periods incorporated in VSAT are given in Table 18, Table 19, and Table 20. The default electric utility rates incorporated in VSAT are based upon Pacific, Gas and Electric Company (PG&E) Schedule E-19. The default natural gas rates are based on PG&E Schedule G-NR1.

Table 18. Default time periods for utility rates

PG&E			
Summer:	May 1 - Oct. 31	Winter:	Nov. 1 - April 30
On-Peak	12:00 - 6:00, M - F	On-Peak	N/A
Mid-Peak	8:30 AM - 12:00 & 6:00 PM - 9:30 PM, M - F	Mid-Peak	8:30 AM - 9:30 PM, M - F
Off-Peak	9:30 PM - 8:30 AM, all week	Off-Peak	9:30 PM - 8:30 AM, all week

Table 19. Default natural gas rates in VSAT

PG&E Schedule G-NR1, CA Climate Zones 1, 2, 3, 4, 11, 12, 13, 1	
Summer Season	\$0.67355
Winter Season	\$0.74220

Table 20: Default electric rates in VSAT

PG&E Schedule E-19, CA Climate Zones 1, 2, 3, 4, 5, 11, 12, 13		
<i>Energy Charge - \$/kWh</i>		
Summer Season	On-Peak	\$0.08773
	Mid-Peak	\$0.05810
	Off-Peak	\$0.05059

Winter Season	On-Peak	N/A
	Mid-Peak	\$0.06392
	Off-Peak	\$0.05038
<i>Time Related Demand Charge - \$/kW</i>		
Summer Season	On-Peak	\$13.35
	Mid-Peak	\$3.70
	Off-Peak	\$2.55

Winter Season	On-Peak	N/A
	Mid-Peak	\$3.65
	Off-Peak	\$2.55

SECTION 6: SAMPLE RESULTS AND COMPARISONS WITH ENERGY-10

6.1 Sample Results

Figure 26 shows sample hourly results for the Base Case (night setup with no economizer) and with Night Ventilation Precooling for the school class wing within early summer in Climate Zone 10 obtained using the default VSAT utility rates (PG&E E-19 and GNR-1). Night ventilation precooling is enabled during the unoccupied mode when the ambient temperature is sufficiently cooler than the zone temperature. For this example, this occurs during the hour from 11-12:00 pm and continues until the occupied mode begins at 5 am. Prior to occupancy the zone temperature is cooled to around 20°C. At occupancy, the economizer keeps the zone temperature at a lower economizer setpoint until 8 am when the temperature begins to rise. The temperature reaches the setpoint for mechanical cooling at 11:00 am.

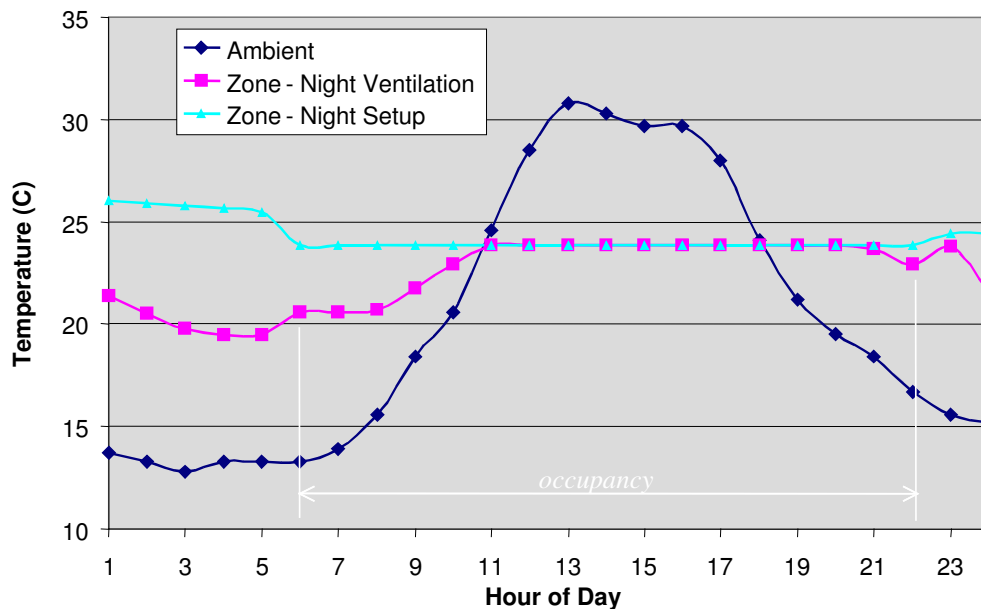


Figure 26. Sample hourly results night ventilation precooling and the base case (class school wing during early summer in Rialto, California).

Figure 27 shows hourly fan and compressor power comparisons for the situation considered for Figure 26. Additional fan energy is utilized during the early morning hours with night ventilation precooling, but this leads to a reduction in compressor energy over much of the day. Part of the savings is due to the low zone setpoint for the economizer, which acts to maintain a cool building thermal mass during the morning hours. For the night ventilation control, mechanical cooling is not needed until 11 am. Clearly, the night ventilation control requires significantly less compressor energy and has slightly lower peak electrical demand at the expense of additional fan energy.

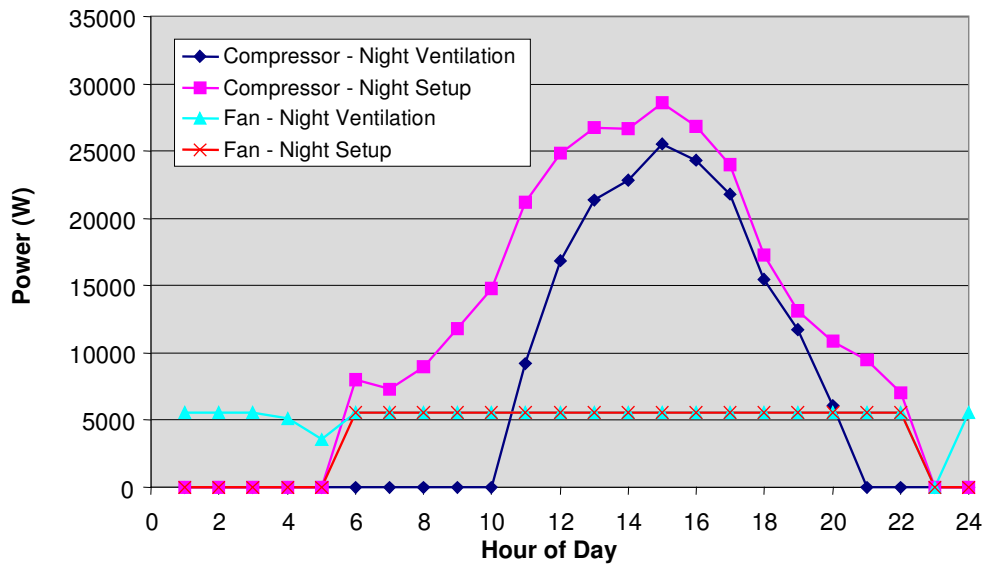


Figure 27: Simulated hourly power for night ventilation precooling and the base case (class school wing during early summer in California Climate Zone 10).

Figure 28 gives annual electrical energy usage for the class school wing in California Climate Zone 10 for three ventilation strategies: 1) a base case with a night setup thermostat, 2) case 1 with the addition of a differential enthalpy-based economizer, and 3) case 2 with the addition of the night ventilation precooling algorithm. Compared to the base case, the economizer results in a savings in compressor energy of 17.4%. The combined compressor and fan savings are about 11.1%. Compared to the economizer, the addition of the night ventilation algorithm leads to an additional savings of about 14.0% in compressor energy. However, the fan energy increases by about 14.2%, and because the compressor energy is the major consumption, the energy saved in compressor is more than the additional consumption by fan, the combined savings about 2.6% is achieved compared to the economizer only.

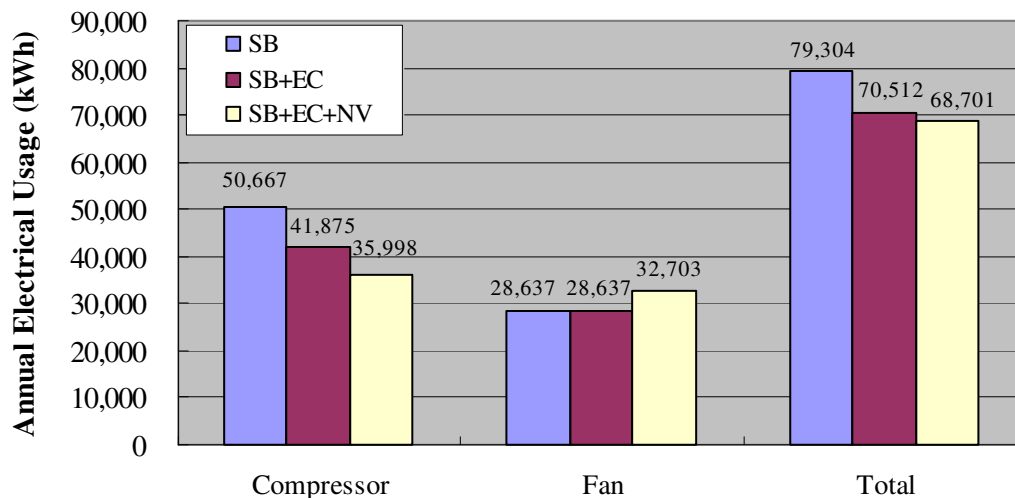


Figure 28: Simulated electrical energy usage for different ventilation strategies (class school wing in California Climate Zone 10).

6.2 Comparisons with Energy-10

Energy-10 is a conceptual design tool for low-energy buildings developed under sponsorship of the U.S. Department of Energy (DOE). The program performs transient, hour-by-hour load calculations for small commercial and residential buildings and allows comparisons of different energy savings strategies. The underlying methods used in Energy-10 are very similar to those used in VSAT. However, VSAT focuses on energy savings due to different ventilation strategies, whereas Energy-10 considers more conventional design changes such as day-lighting, air leakage control, glazing, shading, economizer, thermal mass, passive solar heating and high efficiency equipment. More information on Energy-10 can be found at www.sbicouncil.org or from the user manual.

Since Energy-10 is an accepted tool for analysis of small commercial building, it was chosen for benchmarking predictions of VSAT for a base case system with a night setup/setback thermostat and no economizer. The office-building prototype was chosen for this case study and comparisons of monthly equipment loads and energy consumptions were performed in two locations, Madison, WI, and Atlanta, GA.

There are some basic differences in the modeling approaches in Energy-10 and VSAT that had to be considered. VSAT neglects the effects of cycling on furnace efficiency, whereas Energy-10 includes a significant penalty for cycling. For the purposes of comparison, the part-load effects of furnace cycling were not included in the Energy-10 results. However, part-load effects for the air conditioning equipment were included for both models.

A window in Energy-10 is characterized with a rough-frame opening dimension (the hole left by the framers), a glazing type, and a frame type. The U-value is calculated from the dimensions and the U-values of the glass and frame. In VSAT, the window U-value is simply a given value in the building description and no frame is assumed. Solar transmittances and shading coefficients are also inputs in VSAT, whereas these values are calculated from a windows library in Energy-10. For comparison purposes, a window assembly was built in Energy-10 that had an effective U-value and transmittance very similar to that in VSAT.

Energy-10 weather files are constructed using the 1994 and 1995 updated TMY2 weather

files. This update is based on 30 years of data, rather than 20 years, and incorporates new and improved solar radiation information from the 1992 National Solar Radiation Data Base. The weather data in VSAT used for comparison purposes is TMY data.

The prototypical office was modeled in both Madison and Atlanta. The air-conditioner and furnace equipment models assumed a rated EER of 11 and efficiency of 85%, respectively. In VSAT, the supply fan power was assumed to be 0.5 W/cfm. This value corresponds to a fan efficiency of 11.78% and 0.5 inches H₂O system static pressure as entered in Energy-10. Infiltration was neglected for both models. The occupied zone set point for cooling was 23.89°C with a night setup to 29.44°C. The occupied zone set point for heating was 21.11°C with a night setback to 15.56°C.

Table 21 gives equipment sizing determined by VSAT for Madison and Atlanta. These equipment sizes were specified in Energy-10.

Table 21: Equipment Sizing Results from VSAT

	Office - Madison, WI	Office - Atlanta, GA
AC Rated Total Cap., Btu/h	210180	210260
AC Rated Sens. Cap., Btu/h	153064	162822
Furnace Rated Cap., Btu/h	252924	148583
Total Air Flow, cfm	6130	6133
Ventilation Air Flow, cfm	924	924
Office Floor Area, ft ²	6600	6600

Figures 29 – 31 give monthly electricity for the condensing units (compressors and condenser fans), furnace gas input, and supply fan power for both VSAT and Energy-10 in Atlanta, GA. Figures 32 – 34 give similar results for Madison, WI. The trends and absolute magnitudes are very similar for predictions obtained with VSAT and Energy-10. In general, VSAT tends to give slightly higher condensing unit energy and lower gas input energy than Energy-10. Tables 22 and 23 gives tabulated results along with percentage differences between Energy-10 and VSAT for Atlanta and Madison.

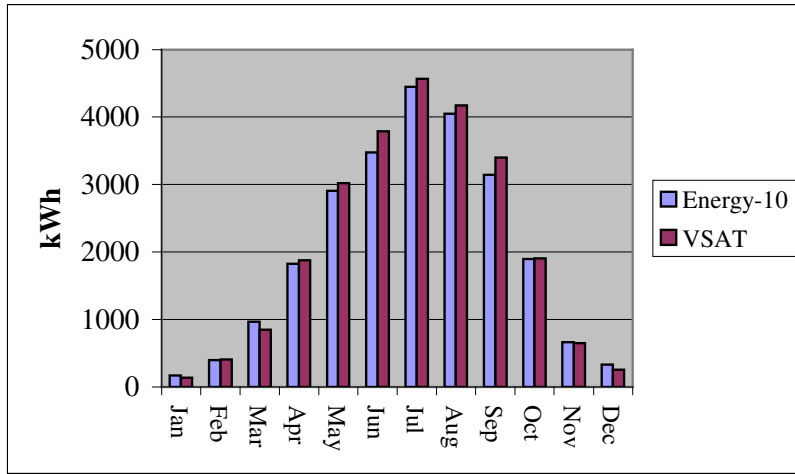


Figure 29. Monthly Electrical Consumption for Cooling – Atlanta, GA

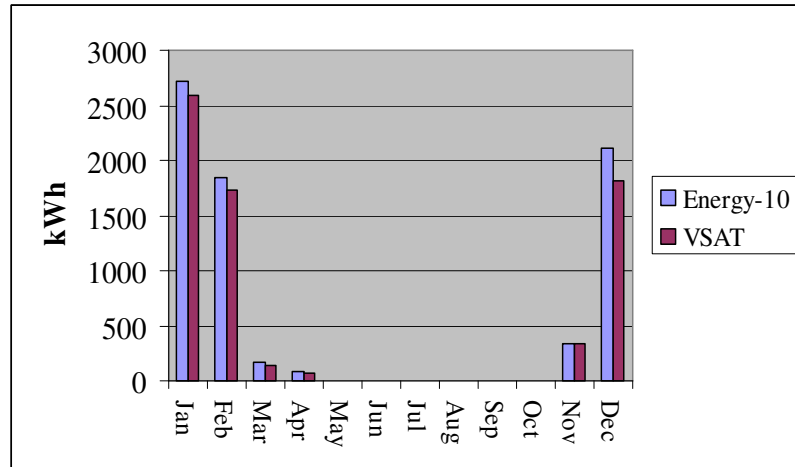


Figure 30. Monthly Furnace Gas Input – Atlanta, GA

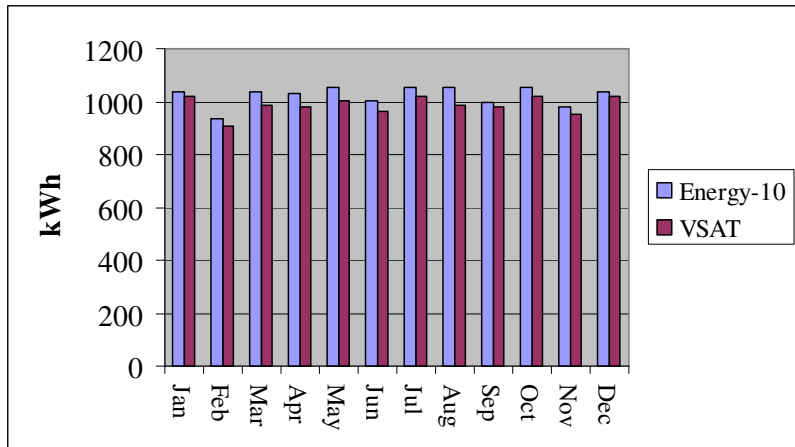


Figure 31. Monthly Supply Fan Power Consumption – Atlanta, GA

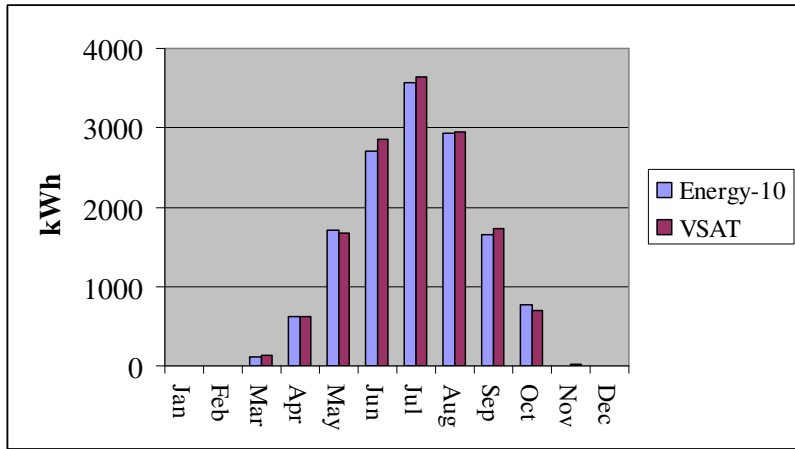


Figure 32. Monthly Electrical Consumption for Cooling –Madison, WI

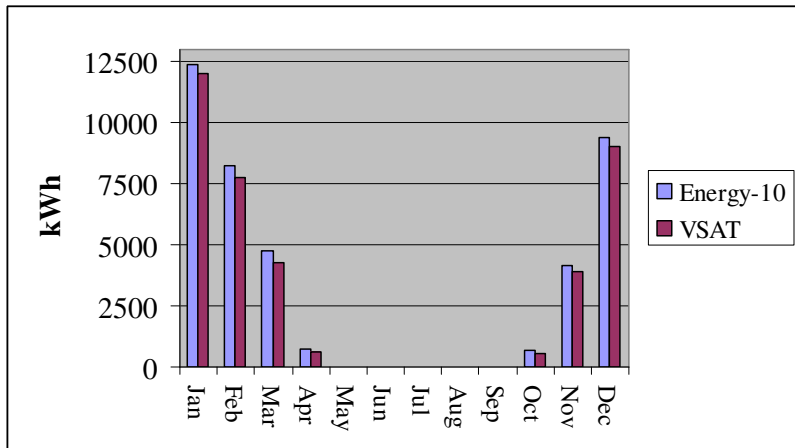


Figure 33. Monthly Furnace Gas Input – Madison, WI

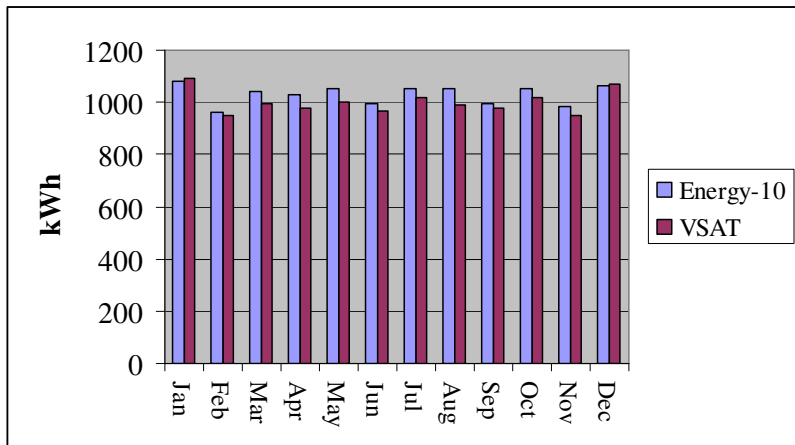


Figure 34. Monthly Supply Fan Power Consumption – Madison, WI

Table 22: VSAT and Energy-10 Results – Atlanta, GA

Month	AC kWhr		Furnace kWhr		Fan kWhr	
	Energy-10	VSAT	Energy-10	VSAT	Energy-10	VSAT
Jan	168	139	2712	2589	1038	1020
Feb	397	407	1851	1738	937	909
Mar	968	849	171	142	1037	987
Apr	1828	1878	78	74	1031	981
May	2905	3021	0	0	1053	1003
Jun	3474	3790	0	0	1000	966
Jul	4448	4570	0	0	1054	1018
Aug	4050	4173	0	0	1054	987
Sep	3144	3398	0	0	999	981
Oct	1898	1905	0	0	1053	1018
Nov	662	650	332	345	982	951
Dec	330	258	2118	1815	1037	1018
Yr	24272	25038	7262	6703	12275	11839
	AC error	3.06%	Furnace error	-8.35%	Fan error	-3.68%

Table 23: VSAT and Energy-10 Results – Madison, WI

Month	AC kWhr		Furnace kWhr		Fan kWhr	
	Energy-10	VSAT	Energy-10	VSAT	Energy-10	VSAT
Jan	0	0	12378	12018	1082	1092
Feb	5	0	8247	7779	960	948
Mar	110	128	4779	4264	1039	994
Apr	622	618	711	622	1030	981
May	1716	1664	11	12	1053	1002
Jun	2705	2852	0	0	998	966
Jul	3561	3636	0	0	1054	1018
Aug	2934	2943	0	0	1053	987
Sep	1650	1728	0	18	998	981
Oct	766	687	694	523	1053	1018
Nov	2	20	4178	3927	982	951
Dec	0	0	9414	9023	1065	1070
Yr	14070	14276	40412	38186	12367	12008
	AC error	1.44%	Furnace error	-5.83%	Fan error	-2.99%

SECTION 7: REFERENCES

- ASHRAE. 2000. *ASHRAE Handbook: HVAC Systems and Equipment*, Atlanta: American Society of Heating, Refrigerating and Air-Conditioning Engineers, Inc.
- ASHRAE. 1999. “ANSI/ASHRAE Standard 62-1999, “Ventilation for Acceptable Indoor Air Quality”, Atlanta: American Society of Heating, Refrigerating and Air-Conditioning Engineers, Inc.
- ASHRAE. 1993. *ASHRAE Handbook: Fundamentals*, Atlanta: American Society of Heating, Refrigerating and Air-Conditioning Engineers, Inc.
- Brandemuehl, M.J. and Braun, J.E., “The Impact of Demand-Controlled and Economizer Ventilation Strategies on Energy Use in Buildings, ASHRAE Transactions, Vol. 105, Pt. 2, pp. 39-50, 1999.
- Brandemuehl, M.J., Gabel, S., and Andresen, I. 1993. *HVAC2 Toolkit: Algorithms and Subroutines for Secondary HVAC System Energy Calculations*. American Society of Heating, Refrigerating, and Air Conditioning Engineers, Inc., Atlanta, GA.
- Braun, J.E. and Brandemuehl, M.J. 2002. *Savings Estimator Technical Reference Manual*.
- Carrier Corporation. 1999. “Product Data: 62AQ Energy\$Recycler Energy Recovery Accessory For 3 to 12.5 Ton Rooftops”, Form 62AQ-1PD. Syracuse, New York.
- Carnes Company. 1989. “Energy Recovery Wheel Design Manual,” Verona, WI.
- Chaturvedi, N. and Braun, J.E. “An Inverse Gray-Box Model for Transient Building Load Prediction,” *International Journal of Heating, Ventilating, Air-Conditioning and Refrigeration Research*, Vol. 8, No. 1, pp. 73-100, 2002.
- Duffie, J.A. and Beckman, W.A., *Solar Engineering of Thermal Processes*, Wiley—Interscience, 1980.
- DOE-2. 1982. *Engineer’s Manual, Version 2.1A*. Lawrence Berkeley Laboratory and Los Alamos National Laboratory.
- Huang, Y.J., Akbari, H., Rainer, L., and Ritschard, R.L. 1990. *481 Prototypical Commercial Buildings for Twenty Urban Market Areas (Technical documentation of building loads data base developed for the GRI Cogeneration Market Assessment Model)*. LBL Report 29798, Lawrence Berkley National Laboratory, Berkley CA.
- Huang, Y.J., and E. Franconi. 1995. *Commercial Heating and Cooling Loads Component Analysis*. LBNL Report 38970, Lawrence Berkeley National Laboratory, Berkeley, CA.

- Kays, W.M., and M.E. Crawford. 1980. *Convective Heat and Mass Transfer*. New York: McGraw-Hill.
- Klein, H., Klein, S.A., and Mitchell, J.W., 1990, "Analysis of regenerative enthalpy exchangers," *International Journal of Heat and Mass Transfer*, Vol. 33, No.4, pp. 735-744.
- Maclaine-cross, I.L. 1974. *A Theory of Combined Heat and Mass Transfer in Regenerators*. Ph.D. Thesis in Mechanical Engineering, Monash University, Australia.
- Seem, J.E., Klein, S.A., Beckman, W.A., and Mitchell, J.W., 1989, "Transfer functions for efficient calculations of multi dimensional heat transfer," *Journal of Heat Transfer-Transactions of the ASME*, Vol. 111, No.1, pp. 5-12.
- Stiesch, G., S.A. Klein, J.W. Mitchell. 1995. *Performance of Rotary Heat and Mass Exchangers*. HVAC&R Research 1(4): 308-324.
- TRNSYS. 2000. *TRNSYS Users Guide: A Transient Simulation Program*. Solar Energy Laboratory, University of Wisconsin-Madison.

DEVELOPMENT AND EVALUATION OF A NIGHT VENTILATION PRECOOLING ALGORITHM

Submitted to

California Energy Commission

Final Report as Deliverable 3.2.4

Prepared by

**James E. Braun and Zhipeng Zhong
Purdue University**

August 2003

ACKNOWLEDGEMENTS

The research that resulted in this document was part of the “Energy Efficient and Affordable Small Commercial and Residential Buildings Research Program”, which was a Public Interest Energy Research Program (PIER) sponsored by the California Energy Commission (CEC). We are extremely grateful for the funding from the CEC through PIER. Several organizations and people were involved in the project described in this final report and deserve our many thanks. Chris Scruton of the CEC was very enthusiastic throughout this project and provided valuable insight and encouragement. Vern Smith and Erin Coats of Architectural Energy Corporation (AEC) provided excellent overall project management for the numerous projects within this large program. Todd Rossi and Doug Dietrich of Field Diagnostic Services, Inc. (FDSI) and Lanny Ross of Newport Design Consultants (NDS) were essential in setting up and maintaining the field sites. Martin Nankin of FDSI provided monitoring equipment at cost for this project. Bob Sundberg of Honeywell, Inc. arranged the donation of Honeywell equipment and was an enthusiastic supporter of the research. Adrienne Thomle and Bill Bray at Honeywell, Inc. made sure that equipment was delivered to the field sites and provided replacement equipment and troubleshooting when necessary. We also had excellent support from the organizations that own and/or operate buildings at the field sites. Individual contributors include Jim Landberg for the Woodland schools, Tadashi Nakadegawa for the Oakland schools, Tony Spata and Mike Godlove for McDonalds, and Mike Sheldon, Paul Hamann, Gordon Pellegrinetti, and Tim Schmid for Walgreens.

EXECUTIVE SUMMARY

The goal of this project was to develop a simple, low-cost algorithm for night ventilation precooling that can be integrated within a controller for packaged air conditioners that employ economizers, such as rooftop units. In addition to reducing operating costs, the algorithm needs to ensure that indoor comfort is maintained.

The basic night ventilation precooling algorithm was developed based upon a simple optimization and heuristics derived from simulation results. The cost savings potential of the algorithm was evaluated using simulations for a range of buildings and locations throughout California. The simulations were performed using a tool, termed the Ventilation Strategy Assessment Tool (VSAT), that was developed as part of this project (see Braun and Mercer, 2003). The buildings considered within VSAT include a small office building, a sit-down restaurant, a retail store, a school class wing, a school auditorium, a school gymnasium, and a school library.

All of these buildings are considered to be single zone with a slab on grade (no basement or crawl space). VSAT considers only packaged HVAC equipment, such as rooftop air conditioners with integrated cooling equipment, heating equipment, supply fan, and ventilation.

The slab floor and walls act as the primary thermal storage for load shifting. VSAT models transients in walls and floors using one-dimensional transfer function representations. Heat transfer in the soil underneath and near the slab floor can also have an impact on the thermal storage and overall performance. As part of this project, a simplified floor/soil model was developed and compared with a detailed two-dimensional analysis. The simplified model combines a one-dimensional transient conduction analysis in the floor and ground with a quasi-steady-state model for edge heat transfer. Figure A shows hourly heat transfer results for a day obtained with the simplified model with and without edge effects as compared with predictions from a detailed 2-dimensional finite element program (FEHT). The results agree very well with the detailed predictions and the inclusion of edge effects provide an improvement.

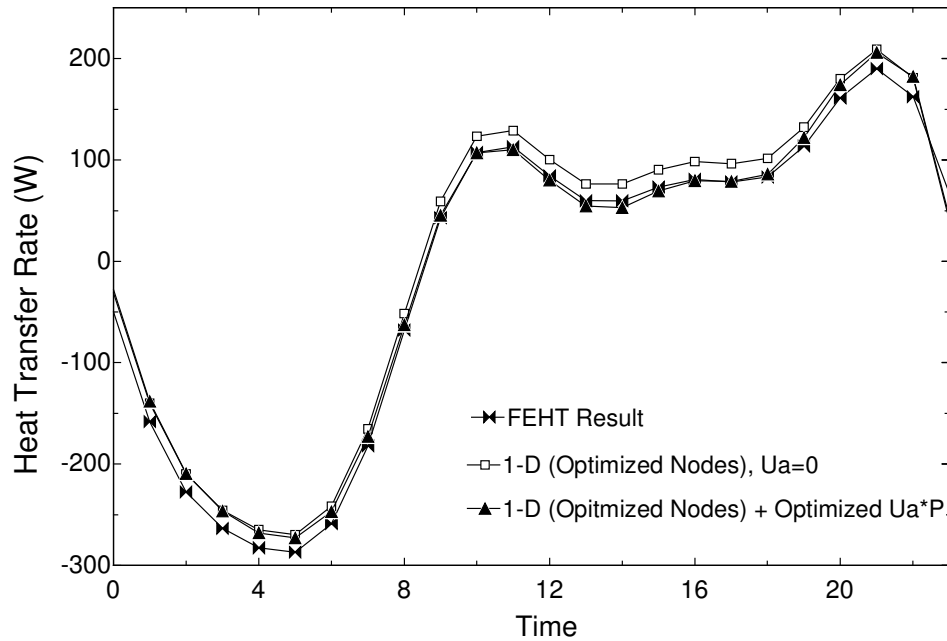


Fig. A: Optimizing the peripheral heat loss factor U_a

The night ventilation precooling algorithm utilizes a set of rules given in Table A to enable precooling. Whenever the ambient temperature drops below the zone temperature, the ambient air can be used to precool the zone and reduce cooling loads during the next day. However, the next day savings associated with operating the ventilation system at night should be sufficient to offset the cost of operating the fan. In addition, the ambient humidity should be low enough to avoid increased latent loads during the next day and the ambient temperature should be high enough so as to avoid additional heating requirements after occupancy.

When night ventilation precooling is enabled, mechanical cooling is disabled and the ventilation system operates with 100% outside air to precool the zone with a setpoint of 67°F. Once the zone temperature reaches 67°F, the fan cycles to maintain this setpoint. Just prior to the occupied period, the setpoint for ventilation precooling is raised to 69°F. Once the occupied period begins, there are separate setpoints associated cooling provided by the economizer (1st stage cooling) and the packaged air conditioner (2nd stage cooling). The 1st and 2nd stage setpoints are 69°F and 75°F, respectively. Once the occupied period ends, the zone temperature setpoint is raised to 80°F.

Table A: Rules for Enabling Ventilation Precooling

Rule	Description
$(T_z - T_a) > \Delta T_{on}$	The ambient temperature (T_a) must be less than the zone temperature (T_z) by a threshold (ΔT_{on}) chosen to balance fan operating costs with next day savings.
$T_a > 50^\circ\text{F}$	The ambient temperature must be greater than 50 °F to avoid conditions where heating might be required the next day.
$T_{a,dp} < 55^\circ\text{F}$	The ambient dew point ($T_{a,dp}$) must be less than 55 °F to avoid conditions where the latent load might increase the next day.
$\Delta t_{occ} < 6$ hours	The time to occupancy (Δt_{occ}) must be less than 6 hours to achieve good storage efficiency.
$N_{heat} > 24$ hours	The number of hours (N_{heat}) since the last call for heating should be greater than 24 hours to lock out precooling in the heating season

A threshold for the temperature difference between the zone and ambient was derived by considering tradeoffs between operating costs during the precooling and occupied periods. The threshold that achieves positive savings is estimated according to

$$\Delta T_{on} = \frac{\dot{W}_{fan}}{\rho_a c_{pa} \dot{V}_{fan}} \cdot \left(\frac{COP_{nv,occ}}{\eta_s} \cdot \frac{\bar{R}_{unocc}}{\bar{R}_{occ}} + 1 \right) \quad (\text{A})$$

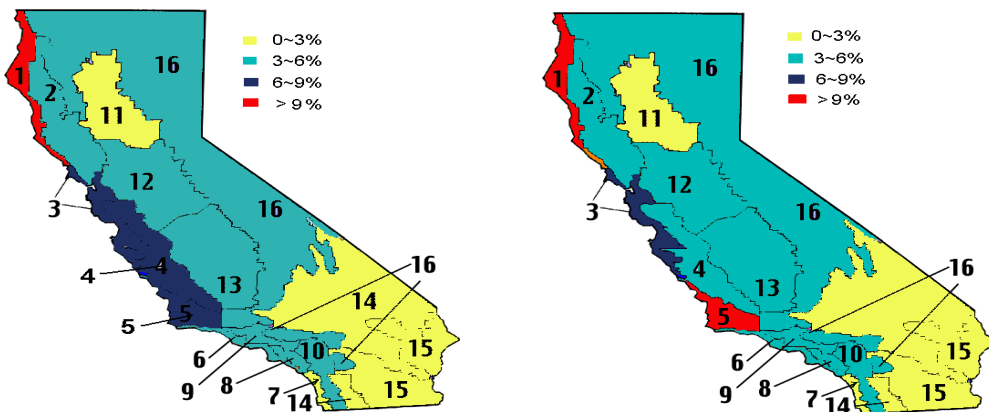
where \dot{V}_{fan} is the fan volumetric flow rate, \dot{W}_{fan} is the fan power, ρ_a is the air density, c_{pa} is the air specific heat, \bar{R} is the average utility energy charge (\$/kWh), COP is an average system coefficient of performance, η_s is a storage efficiency. The subscripts “*occ*” and “*unocc*” refer to the occupied and unoccupied periods. In this case, COP is defined as the ratio of the zone cooling to the required electrical energy usage. The storage efficiency is defined as the reduction in occupied period load divided by the precooling energy.

For typical parameter values, the threshold varies between about 2 F and 12 F. The breakeven point given in equation A increases with fan power (i.e., pressure drop) for a given flow rate since the cost of providing a given quantity of precooling increases. The threshold also increases as the ratio between occupied and unoccupied energy rates decreases. Lower occupied period energy costs reduce the savings associated with precooling leading to a larger threshold. For similar reasons, the threshold increases with

increasing occupied period COP. Finally, the threshold increases with decreasing storage efficiency as less of the precooling results in cooling load reductions during the occupied period.

The simulation tool was used to evaluate savings associated with the night ventilation precooling algorithm applied throughout California for different building types. For the default building and system parameters, the savings in compressor energy ranged from about 0 to 53% depending on the location and building type. However, the savings in total air conditioning electrical energy usage are much smaller than the compressor savings due to an increase in fan energy. The electrical energy savings varied between about 0 and 8%. However, the ventilation algorithm is based upon reducing total energy costs, including the effects of differences between on-peak and off-peak electrical rates. In addition, there are demand cost reductions. The electrical demand cost savings associated with night ventilation varied between about 0 and 28%, whereas the total electrical cost savings ranged from about 0 to 17%.

Approximate percentage savings in electrical costs for the default parameters are shown on a map of California in Figure B for four featured buildings. The savings are all relative to a base case that includes a night setup thermostat with a differential enthalpy economizer. Generally, the greatest percentage compressor and total cost savings occur in coastal climates with relatively mild ambient temperatures. However, the savings are also significant in hot inland climates having larger total loads. The savings are considerably smaller for the restaurant than for the other buildings. Compared to the other buildings, the restaurant has less thermal mass, smaller internal gains, a longer occupancy schedule, and greater ventilation requirements.



a. Office

b. Retail Store

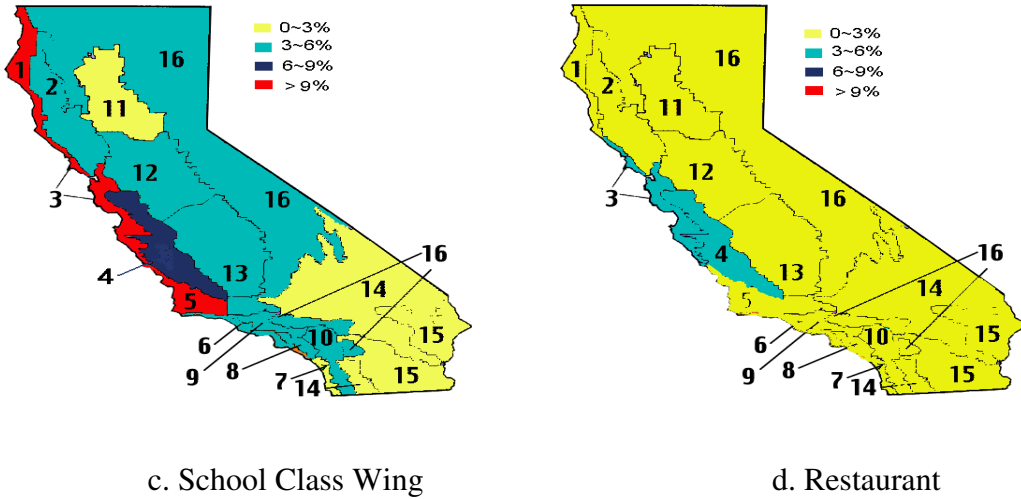


Figure B: Cost savings in California for different buildings

Fan and fan motor efficiencies have a very significant effect on the savings potential for night ventilation. Typically, fans that are employed within packaged equipment have very poor overall efficiencies (e.g., 15% for combined fan and motor). In many cases, the cost savings can nearly double if the fan/motor efficiency is doubled. Thus, it is important to utilize efficient fans and fan motors in combination with night ventilation precooling. Even greater savings would be possible if efficient, variable-speed fan motors were employed.

The savings are also very sensitive to the utility rates. Greater savings are possible with higher ratios of on-peak to off-peak charges and on-peak periods that start earlier in the day. In addition, higher occupied period cooling setpoints, higher levels of internal thermal mass and the elimination of carpets increase savings significantly.

The night ventilation precooling strategy can be implemented using the same sensors and control hardware employed within a economizer controller. Therefore, it should be cost effective to integrate night ventilation control with economizers for packaged equipment used in small commercial buildings.

A simplified version of the control algorithm was implemented within two field sites. The first field site, located at the Field Diagnostic Services, Inc. (FDSI) headquarters near Philadelphia, PA, was used primarily for initial debugging of the implementation. Correct operation of the basic algorithm embedded in the controller was demonstrated using data from this site. The second field site is a Walgreens located in Rialto, CA. The Walgreens site employs five rooftop units (RTUs) each with a controller that provides ventilation

precooling under the appropriate conditions. The algorithm was shown to work properly, but there were difficulties in demonstrating energy savings at the site due to several problems, including: 1) unfavorable weather conditions for night ventilation this past spring, 2) lack of a return air damper limited the amount of ventilation precooling that is possible, 3) uncontrolled changes in occupied period setpoints, 4) service problems with the RTUs.

Currently, the site is being used to explore the potential for use of mechanical precooling with demand-limiting during the on-peak period.

Table of Contents

<u>ACKNOWLEDGEMENTS</u>	i
<u>EXECUTIVE SUMMARY</u>	ii
<u>1. Introduction</u>	1
<u>1.1 Literature review</u>	1
<u>1.2 Objective</u>	4
<u>1.3 Approach</u>	4
<u>2. Night Ventilation Precooling Algorithm</u>	6
<u>2.1 Threshold for ventilation precooling</u>	7
<u>3. Simulation Description</u>	10
<u>3.1 General Modeling Approach</u>	10
<u>3.2 Slab and Ground Modeling</u>	11
<u>3.3 Modeling Parameters</u>	22
<u>3.3 Weather Data</u>	22
<u>3.4 Operating Costs</u>	24
<u>4. Simulated Savings</u>	28
<u>4.1 Sample Hourly Results</u>	28
<u>4.2 Annual Cost Savings</u>	30
<u>4.3 Impact of Fan Efficiency</u>	37
<u>4.4 Impact of Utility Rates</u>	41
<u>4.5 Impact of Occupied Period Cooling Setpoint</u>	43
<u>4.6 Impact of Internal Thermal Mass Level</u>	45
<u>4.7 Impact of Ground Coupling and Carpeting</u>	47
<u>5. Prototype Development and Implementation</u>	49
<u>5.1 General description</u>	49
<u>5.2 Description of the main control variables</u>	51
<u>5.3 Description of control algorithm</u>	53
<u>5.4 Logic simulation tests</u>	54
<u>6. Field test results</u>	61
<u>6.1 Overview of the field sites</u>	61
<u>6.2 Web-Based Interface</u>	64

<u>6.3 Results for the FDSI site</u>	64
<u>6.4 Results from the Walgreen's</u>	67
<u>7. Summary</u>	79
<u>8. References</u>	81
<u>APPENDIX A – PROTOTYPICAL BUILDING DESCRIPTIONS</u>	83

1. Introduction

1.1 Literature review

ASHRAE Standard 62.2-1999 (1999) requires that the ventilation system provide fresh air of at least 7.5 liter per person in office buildings. However, there are circumstances under which greater ventilation rates lead to lower energy usage. The most obvious example is an economizer, where the goal is maximize the amount of ventilation air when the ambient enthalpy is less than the zone return air enthalpy and there is a call for cooling. Another opportunity is associated with night ventilation for precooling.

Figure 1.1 depicts the concept for night ventilation precooling in commercial buildings. At the end of the occupied period, the zone temperature setpoint is raised, the equipment turns off and the zone temperature floats above the daytime setpoint. At some point during the nighttime, the ambient temperature is cooler than the zone temperature by a sufficient amount that it is worthwhile to open the ventilation damper and turn on the fan. If possible, the zone temperature is cooled to a lower (precooling) setpoint and then the fan cycles to maintain this setpoint. The nighttime ventilation leads to lower building surface temperatures, which tends to reduce the heat gains to the air during the daytime and the associated energy and peak power consumption for the mechanical cooling equipment.

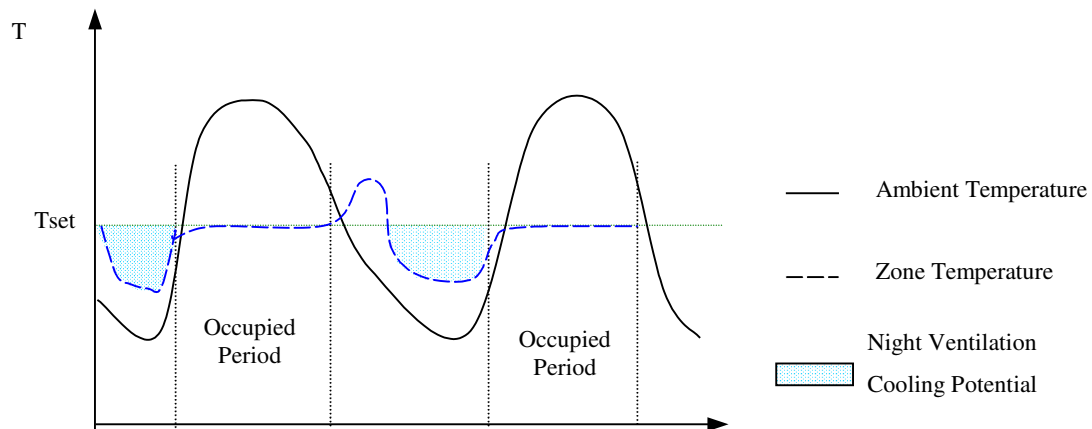


Figure 1.1: Night ventilation precooling concept

Significant potential for use of building thermal mass for load shifting and peak load reduction has been demonstrated through simulation, laboratory testing, and field testing (see Braun (1990), Synder and Newell (1990), Rabl and Norford (1991), Andresen and Brandemuehl (1992), Andrews et al. (1993), Morris et al. (1994), Keeney and Braun

(1997), and Braun et al. (2001, 2002)). For the most part, these studies focused on the use of precooling using the primary air conditioning equipment. Braun (1990) did find that as a percentage of daily costs, the savings associated with precooling are greatest at low ambient temperatures where the greatest "free" cooling opportunities exist. For conditions where night ventilation could be applied, the daily energy cost savings ranged between about 10% and 50% depending upon the type of building and equipment and utility rates.

Keeney and Braun (1995) developed a simplified ventilation precooling algorithm for application in large commercial buildings with VAV air distribution systems. The algorithm is expressed in terms of a zone temperature setpoint for night cooling and a set of rules for occupant comfort during the occupied period. The algorithm for estimating the nighttime setpoint was derived from a simple cost function that includes important system parameters such as utility rates, cooling plant and fan performances, and building storage efficiency. Simulations were conducted over the entire cooling season in five geographic locations. The ventilation precooling algorithm provided seasonal cost savings for cooling of up to 32% when compared to cooling costs under night setup control. The highest savings were found to occur in dry climates with relatively mild summer temperatures, but savings of up to 10% were possible even in hot humid areas. The savings in hot humid climates were found to be primarily due to the comfort-based rules. Lightweight buildings which were well coupled to the environment were found to have limited savings potential under ventilation precooling. Utility rates with large differentials between on-peak and off-peak rates provided the best opportunities for application of the ventilation precooling algorithm, however significant savings were also found for electric utility rates which did not change over the course of the day. Demand costs were not considered in this study.

Geros (1999) performed night ventilation precooling experiments in a building operating under both free-floating and thermostatically controlled conditions. The building has multiple zones, heavyweight construction, and is located in Athens, Greece. For the free-floating tests, the temperature was not controlled and was heavily ventilated at night using from 10 to 30 air changes per hour (ACH). Compared to no night ventilation, the average reduction of the temperature varied between 1.8 and 3°C for the different zones and the mean reduction for the entire building was about 2.6°C. The peak temperature was reduced by about 6.2°C. For thermostatic control, the energy savings due to night ventilation was about 50% for a daytime zone temperature setpoint of 25°C.

Night ventilation doesn't always save energy because of increased fan power consumption. Kolokotroni and Aronis (1999) performed a simulation study of air-conditioned office buildings in England to investigate the potential for applying night ventilation and found several situations where night ventilation precooling was economic. However, greater savings potential was demonstrated for buildings with high exposed thermal mass, tighter construction, lower internal and solar gains, and use of natural ventilation.

Shaviv (2001) studied the influence of thermal mass and night ventilation on the maximum indoor temperature for buildings that are not air conditioned. A reduction of 3–6°C was shown for a heavy constructed building in the hot humid climate of Israel. Givoni (1998) did night ventilation experiments on different buildings in southern California in the absence of air conditioning. Night ventilation had only a very small effect on the maximum indoor temperature for a low-mass building, but was very effective in lowering the indoor maximum temperatures for a high-mass building. Even on an extremely hot day with a maximum ambient temperature of 38°C, the indoor maximum temperature of the high-mass building was only 24.5°C.

The thermal mass of a building can be increased by employed phase change materials (PCM) within the building structure. Zhong (2001) simulated the use of PCM incorporated within the wallboard (melting temperature of 26.5-27.5°C, 1 inch gypsum wallboard in depth and 20% PCM by weight, placed on the inner surface of wall) for buildings that are not air conditioned.

Since commercial buildings such as offices, restaurants, and retail stores are not occupied at night, they are better candidates for use of night ventilation as compared to residential buildings, which are occupied at night. Furthermore, there is also a greater opportunity for savings in large commercial buildings than smaller ones because of a smaller ratio of external area to thermal mass, the use of heavier weight materials, and the availability of more favorable electrical rate structures. However, it is much easier to develop a general night ventilation controller for small commercial buildings because they typically use packaged air conditioners with a single thermostat controlling a single unit for individual zones. In large commercial buildings, the systems tend to be centralized and complex, serving many zones with specialized control software.

1.2 Objective

The goal of this project was to develop a simple, low-cost algorithm for night ventilation precooling that can be integrated within a controller for packaged air conditioners that employ economizers. In addition to reducing operating costs, the algorithm needs to ensure that indoor comfort conditions (temperature and humidity) are maintained during occupied periods.

1.3 Approach

The basic night ventilation precooling algorithm was developed based upon a simple optimization and heuristics derived from simulation results. The cost savings potential of the algorithm was evaluated using simulations for a range of buildings and locations throughout California. The simulations were performed using a tool, termed the Ventilation Strategy Assessment Tool (VSAT), that was developed as part of this project (see Braun and Mercer, 2003). The buildings considered within VSAT include a small office building, a sit-down restaurant, a retail store, a school class wing, a school auditorium, a school gymnasium, and a school library.

All of these buildings are considered to be single zone with a slab on grade (no basement or crawl space). VSAT considers only packaged HVAC equipment, such as rooftop air conditioners with integrated cooling equipment, heating equipment, supply fan, and ventilation.

The slab floor and walls act as the primary thermal storage for load shifting. VSAT models transients in walls and floors using one-dimensional transfer function representations. Heat transfer in the soil underneath and near the slab floor can also have an impact on the thermal storage and overall performance. As part of this project, a simplified floor/soil model was developed and compared with a detailed two-dimensional analysis.

A simplified version of the algorithm was implemented in a prototype controller and installed at two field sites. The first site is the headquarters for Field Diagnostic Services, Inc. (FDSI) and is located outside of Philadelphia, PA. This site was used primarily to debug the implementation, since it is relatively easy to monitor and update the algorithm. The second site is a Walgreens drug store located in Rialto, CA. The primary goal for testing was to verify proper implementation of the algorithm and to demonstrate load shifting associated with night ventilation precooling.

2. Night Ventilation Precooling Algorithm

This section describes the night ventilation precooling algorithm that was evaluated through simulation. The algorithm implemented in the field sites was slightly simpler and is described in a later section.

Whenever the ambient temperature drops below the zone temperature, the ambient air can be used to precool the zone and reduce cooling loads during the next day. However, the next day savings associated with operating the ventilation system at night should be sufficient to offset the cost of operating the fan. In addition, the ambient humidity should be low enough to avoid increased latent loads during the next day and the ambient temperature should be high enough so as to avoid additional heating requirements after occupancy. With these issues in mind, the rules in Table 2.1 are employed to enable precooling.

Table 2.1: Rules for Enabling Ventilation Precooling

Rule	Description
$(T_z - T_a) > \Delta T_{on}$	The ambient temperature (T_a) must be less than the zone temperature (T_z) by a threshold (ΔT_{on}) chosen to balance fan operating costs with next day savings.
$T_a > 50^\circ\text{F}$	The ambient temperature must be greater than 50 °F to avoid conditions where heating might be required the next day.
$T_{a,dp} < 55^\circ\text{F}$	The ambient dew point ($T_{a,dp}$) must be less than 55 °F to avoid conditions where the latent load might increase the next day.
$\Delta t_{occ} < 6 \text{ hours}$	The time to occupancy (Δt_{occ}) must be less than 6 hours to achieve good storage efficiency.
$N_{heat} > 24 \text{ hours}$	The number of hours (N_{heat}) since the last call for heating should be greater than 24 hours to lock out precooling in the heating season

When night ventilation precooling is enabled, mechanical cooling is disabled and the ventilation system operates with 100% outside air to precool the zone with a setpoint of 67°F. Once the zone temperature reaches 67°F, the fan cycles to maintain this setpoint. Just prior to the occupied period, the setpoint for ventilation precooling is raised to 69°F. Once the occupied period begins, there are separate setpoints associated cooling provided by the economizer (1st stage cooling) and the packaged air conditioner (2nd stage cooling). The 1st and 2nd stage setpoints are 69°F and 75°F, respectively. Once the occupied period ends, the zone temperature setpoint is raised to 80°F.

2.1 Threshold for ventilation precooling

A threshold for the temperature difference between the zone and ambient is derived by considering tradeoffs between operating costs during the precooling and occupied periods. The daily savings associated with ventilation precooling can be expressed in a simplified manner as

$$S = \frac{Q_{z,ns} \cdot \bar{R}_{ns}}{COP_{ns}} - \left(\frac{Q_{z,nv,occ} \cdot \bar{R}_{occ}}{COP_{nv,occ}} + \frac{Q_{z,nv,unocc} \cdot \bar{R}_{unocc}}{COP_{nv,unocc}} \right) \quad (2.1)$$

where Q_z is the zone cooling load (kWh), \bar{R} is the average utility energy charge (\$/kWh), and COP is an average system coefficient of performance defined as the ratio of the zone cooling to the required electrical energy usage. The subscripts “*ns*” and “*nv*” refer to the night setup and night ventilation control strategies. The subscripts “*occ*” and “*unocc*” refer to the occupied and unoccupied periods. The first term on the right-hand side of the equation 2.1 is the daily cost associated with conventional night setup control. The second and third terms are the daily cost associated with the night ventilation control strategy.

The quantity $Q_{z,ns}$ in equation 2.1 can be eliminated through the use of a storage efficiency. The storage efficiency is defined as the reduction in occupied period load divided by the precooling energy or

$$\eta_s = \frac{Q_{z,ns} - Q_{z,nv,occ}}{Q_{z,nv,unocc}} \quad (2.2)$$

Assuming that $\bar{R}_{ns} = \bar{R}_{occ}$ and $COP_{ns} = COP_{nv,occ}$, then

$$S = \frac{\eta_s \cdot Q_{z,nv,unocc} \cdot \bar{R}_{occ}}{COP_{nv,occ}} - \frac{Q_{z,nv,unocc} \cdot \bar{R}_{unocc}}{COP_{nv,unocc}} \quad (2.3)$$

The COP for night ventilation precooling is

$$COP_{nv,unocc} = \frac{Q_{z,nv,unocc}}{W_{f,nv,unocc}} \quad (2.4)$$

where $W_{f,nv,unocc}$ is the fan energy usage during the precooling period. The ventilation cooling and fan energy during the precooling period are

$$Q_{z,nv,unocc} = \rho_a \cdot \dot{V}_{fan} \cdot c_{pa} \cdot \sum_{k=1}^{N_{pre}} \{ (T_{z,k} - T_{a,k}) - \dot{W}_{fan} \} \cdot \Delta t \quad (2.5)$$

$$W_{f,nv,unocc} = \sum_{k=1}^{N_{pre}} \dot{W}_{fan} \cdot \Delta t \quad (2.6)$$

where \dot{V}_{fan} is the fan volumetric flow rate, \dot{W}_{fan} is the fan power, ρ_a is the air density, c_{pa} is the air specific heat, T_z is zone temperature, T_a is ambient temperature, Δt is a timestep (e.g., 1 hour), N_{pre} is the number steps in the precooling period, and the subscript “ k ” represents the k^{th} timestep of the precooling period.

Substituting equations 2.4, 2.5, and 2.6 into equation 2.3 yields

$$S = \sum_{k=1}^{N_{pre}} \left(\frac{\eta_s \cdot (\rho_a \cdot \dot{V}_{fan} \cdot c_{pa} \cdot (T_{z,k} - T_{a,k}) - \dot{W}_{fan}) \cdot \bar{R}_{occ}}{COP_{nv,occ}} - \dot{W}_{fan} \cdot \bar{R}_{unocc} \right) \cdot \Delta t \quad (2.7)$$

The quantity within the brackets of equation 2.7 should be positive in order for operation of the fan to be worthwhile. The breakeven point occurs when this quantity is zero. At this point, the temperature difference required to achieve savings is estimated from equation 2.7 as

$$\Delta T_{on} = \frac{\dot{W}_{fan}}{\rho_a c_{pa} \dot{V}_{fan}} \cdot \left(\frac{COP_{nv,occ}}{\eta_s} \cdot \frac{\bar{R}_{unocc}}{\bar{R}_{occ}} + 1 \right) \quad (2.8)$$

Figure 2.1 shows the breakeven temperature difference as a function of the ratio of unoccupied to occupied energy rates and the ratio of fan power to volumetric flow rate for a storage efficiency of 0.8 and an occupied period COP of 3. For typical values, the threshold varies between about 2 F and 12 F. The breakeven point increases with fan power (i.e., pressure drop) for a given flow rate since the cost of providing a given quantity of precooling increases. The fan power typically varies between about 0.3 and 0.7 W/cfm. The threshold also increases as the ratio between occupied and unoccupied energy rates decreases. Lower occupied period energy costs reduce the savings associated with precooling leading to a larger threshold. For similar reasons, the threshold increases with increasing occupied period COP. For packaged air conditioning equipment, the COP varies between about 2 and 4. Finally, the threshold increases with decreasing storage efficiency as less of the precooling results in cooling load reductions during the occupied period. Storage efficiencies vary between about 0.5 and 0.9.

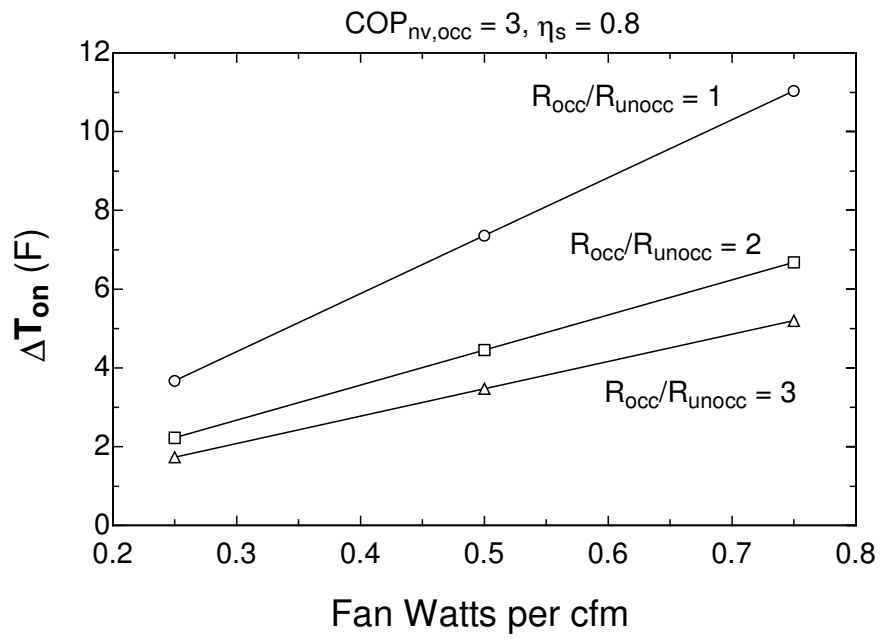


Figure 2.1: Night Ventilation Breakeven Threshold

3. Simulation Description

The Ventilation Strategy and Assessment Tool (Braun and Mercer, 2003) was used to simulate the performance of the night ventilation precooling algorithm. VSAT was designed to perform calculations for small commercial and public buildings with packaged air conditioning equipment. Seven different types of buildings are considered in VSAT: a small office, a school class wing, a retail store, a restaurant dining area, a school gymnasium, a school library, and a school auditorium.

The primary objectives of the simulation work were to: 1) evaluate different night ventilation algorithms during the development process, 2) evaluate the overall savings potential associated with the resulting algorithm, and 3) understand the importance of buildings and locations on the savings.

The building type and associated HVAC equipment are important because of several factors, including the energy storage density, thermal mass coupling to zone air and ambient, occupancy schedule, internal gains, and the equipment efficiencies. The location is important because of both the ambient conditions (primarily dry bulb temperature and humidity) and the utility rates.

3.1 General Modeling Approach

Braun and Mercer (2003a) provide a detailed description of the basic models employed within VSAT along with validation results. The tool is based upon a program developed by Brandemuehl and Braun (2002). Given a physical building description, an occupancy schedule, and thermostat control strategy, the building model provides hourly estimates of the sensible cooling and heating requirements needed to keep the zone temperatures at cooling and heating setpoints.

The building model involves detailed calculations that consider transient conduction through walls using transfer function representations. Predictions of the model compare well with other detailed models from the literature with substantially faster calculation speeds (Braun and Mercer, 2003a).

The space conditioning model follows the approach employed by Brandemuehl and Braun (1999) and employs the use of quasi-steady-state mass and energy balances on the air within the zone and air distribution system. A fixed ventilation effectiveness is employed for the zone to consider short-circuiting of supply air to the return duct. The base case employs a differential enthalpy economizer.

The primary air conditioning units are modeled using an approach similar to that incorporated in ASHRAE's HVAC Toolkit (Brandemuehl et al., 1993). The model for the primary air conditioner utilizes prototypical performance characteristics, which are scaled according to the capacity requirements and efficiency at design conditions. The primary supply fan operates at a fixed speed and is modeled assuming a constant fan/motor efficiency and overall pressure loss.

VSAT was validated by comparing annual equipment loads and power consumptions for similar case studies in Energy-10 (Balcomb, 2002) and TRNSYS (2002). Energy-10 is a design tool developed for the U.S. Department of Energy (DOE) to analyze residential and small commercial buildings. TRNSYS is a complex transient system simulation program that incorporates a detailed building load model (Type-56 multi-zone building component). VSAT was validated for a base case employing the conventional ventilation strategies. In general, the VSAT predictions were within about 5% of the hourly, monthly, and annual predictions from TRNSYS and Energy-10 (Braun and Mercer, 2003).

3.2 Slab and Ground Modeling

The floor slab and ground are important thermal storage elements for building thermal mass control strategies and it is significant to validate their heat transfer model. Unlike walls or roofs, whose heat transfer can be accurately represented by using 1-dimensional model, the slab and ground heat transfer is more complex.

The original version of VSAT incorporated a simplified 1-dimensional, 3-node dynamic heat transfer model for slab floor that was converted to a transfer function. In this model, the floor has the following layers (from the surface to the inner): inside air, carpet (for the office, restaurant and retail store only), 4" or 6" heavyweight concrete slab, and a adiabatic boundary at the bottom. In this model, energy storage capacity was underestimated because the soil below the slab was neglected. The node distribution for heat transfer and energy storage within the slab is represented in Fig. 3.1.

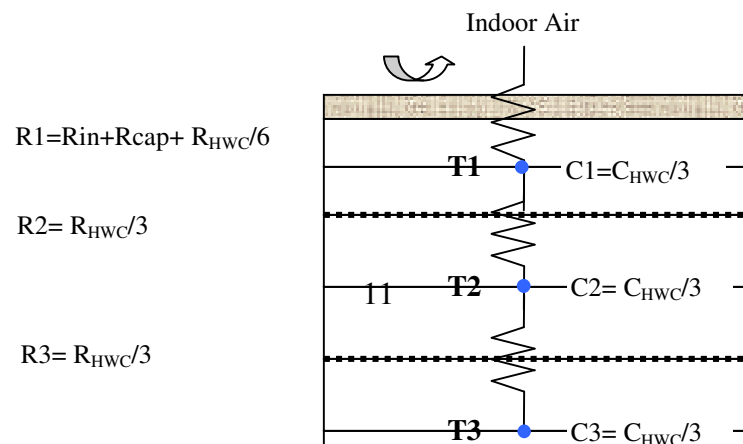


Fig 3.1: Node distribution of the original VSAT slab model

At steady-state, this simple representation does not lead to any heat loss or heat gain from the space. In order to account for steady-state heat loss or heat gain due to the slab, a pure resistance is assumed between zone and ambient air. Wang (1979) and Bligh et al. (1978) found that heat loss from an unheated concrete slab floor is mostly through the perimeter rather than through the floor and into the ground. Total heat loss is nearly proportional to the length of the perimeter, so that the perimeter insulation of a slab-on-grade floor is recommended for comfort and energy conservation by ASHRAE. The periperal heat loss is estimated within VSAT according to:

$$q'' = U_a * P * (T_z - T_a) \quad (3.1)$$

where U_a is the heat loss coefficient per foot of perimeter, P is the length of the perimeter of exposed edge, T_z is the zone temperature, and T_a is the ambient temperature. The original value for U_a within the previous version VSAT was 0.5 Btu/hr-F-ft.

In order to evaluate the accuracy of this slab-ground model and to find the best 1-dimensional heat transfer model, slab and ground heat transfer was studied using a detailed 2-dimensional finite-element model. In the case study, a carpet was not included and 4" heavywright concrete was assumed. The finite-element program *FEHT* (Klein and Beckman, 1996-2001, Version 7.161) was used as reference for comparison with simple 1-dimensional models that were used in VSAT. FEHT is an acronym for **F**inite **E**lement **H**eat **T**ransfer. The element lines and mesh of the slab and ground for the heat transfer in FEHT are shown in Fig. 3.2.

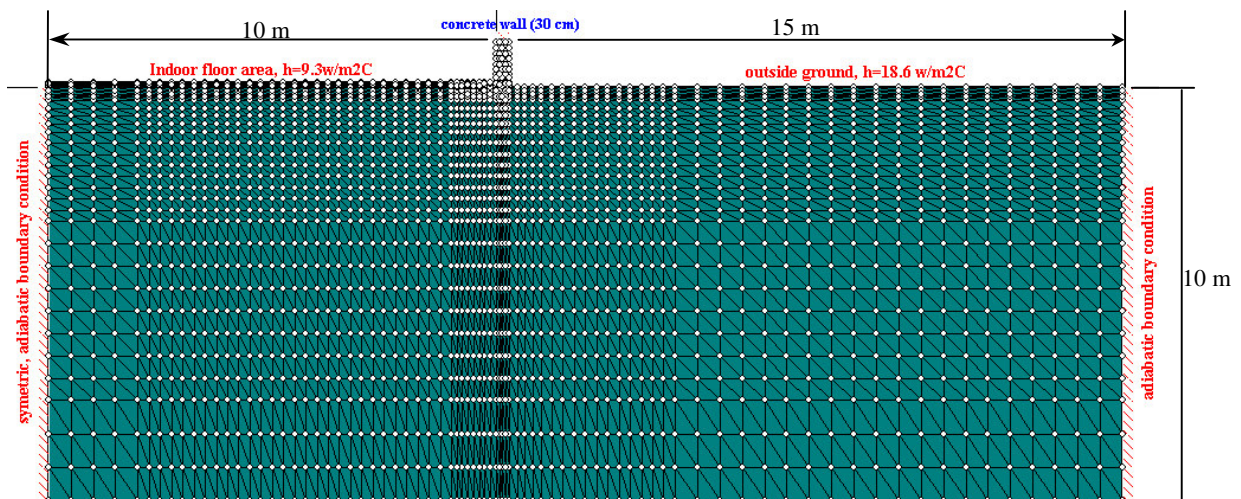
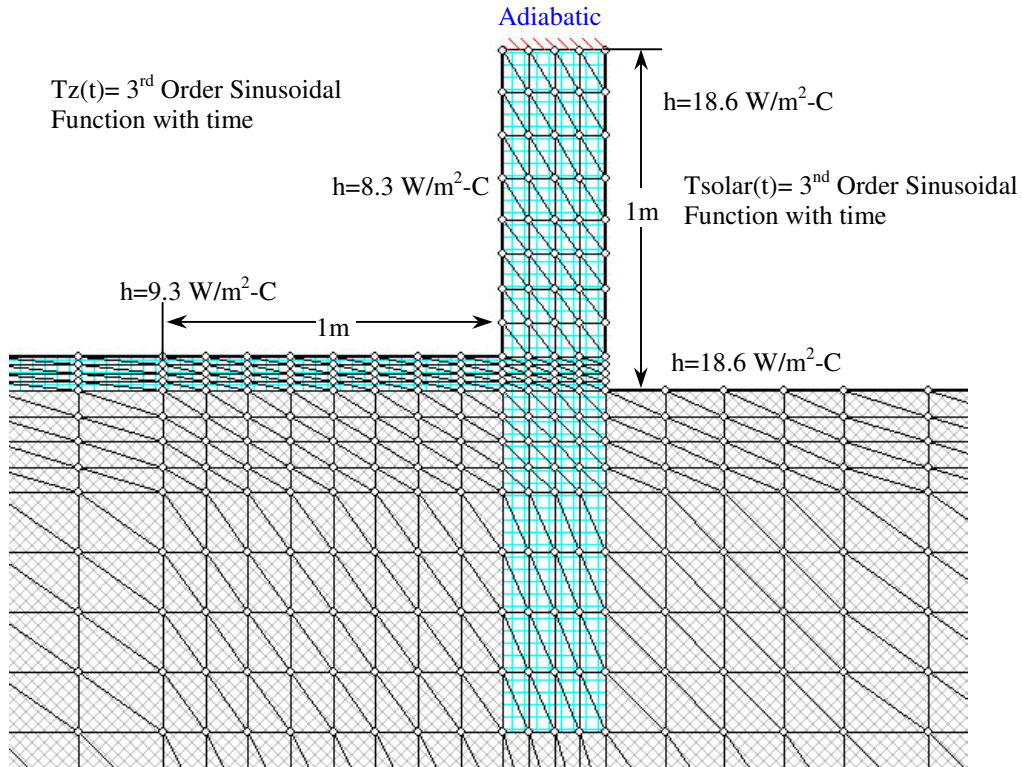


Fig. 3.2: The element lines and mesh for the ground-floor heat transfer in FEHT

Because the temperature profile near the indoor floor edge is quite sensitive to its distance to the exterior wall, high density mesh (up to 8 nodes in 1 meter) was used to minimize the error. The mesh near the wall is shown in Fig. 3.3.



The boundary conditions were as follows:

1. The left side boundary is regarded as adiabatic because of the geometry symmetry;
2. The bottom boundary is regarded as adiabatic because the soil temperature at 10 meters underground is nearly a constant value. This is shown in Fig. 3.4, which is based on the underground soil temperature distribution formula: the Begga's formula (see Popiel, 2001).

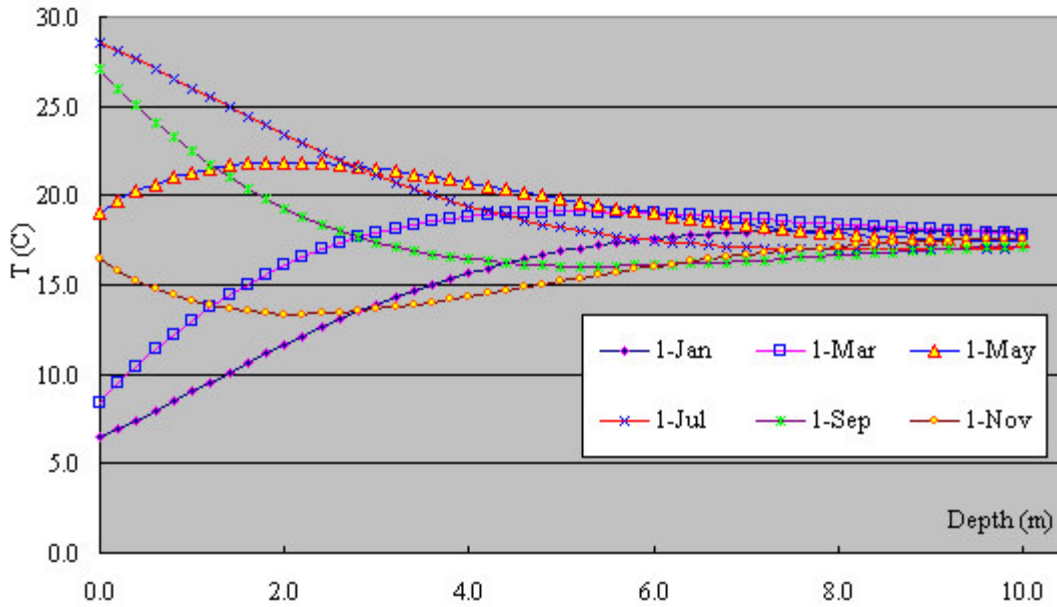
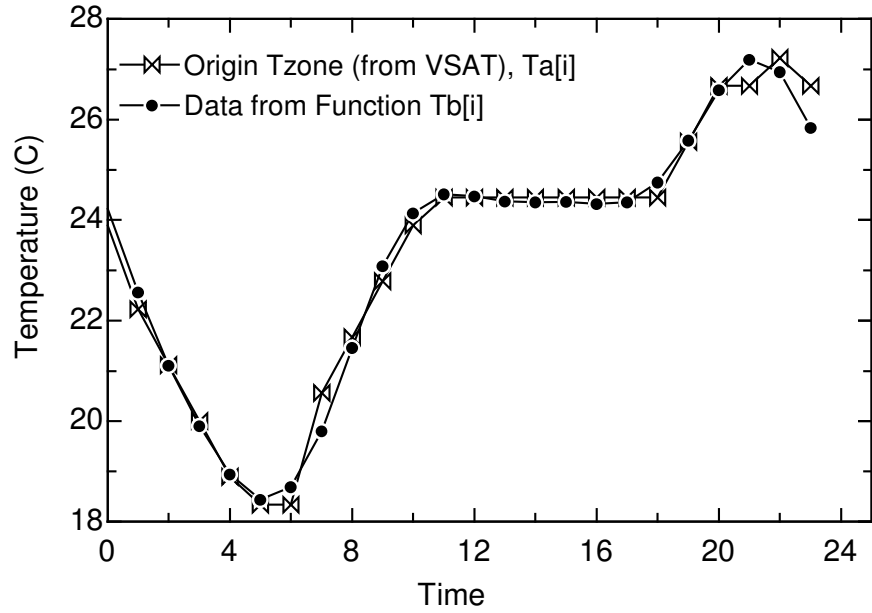


Fig 3.4: Temperature profile of the soil (based on the Begga's formula)

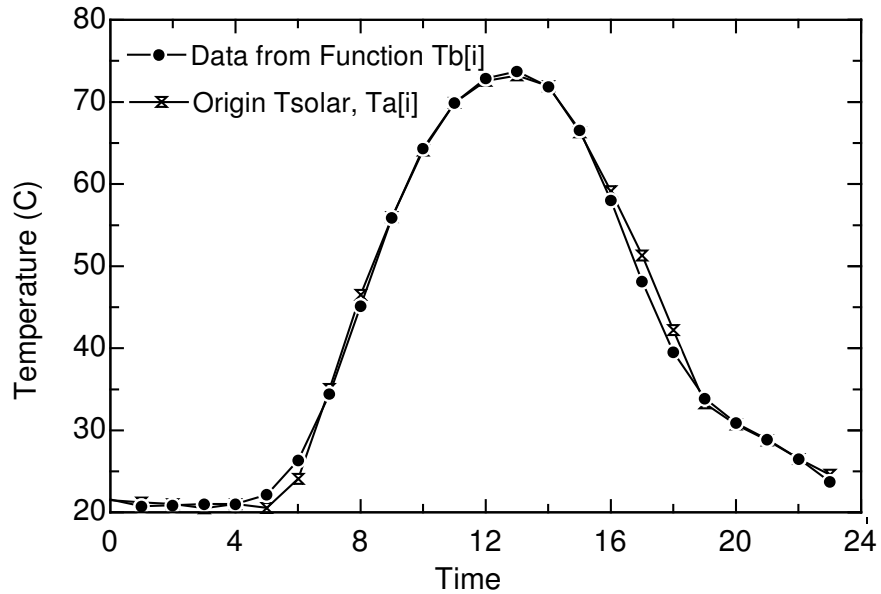
3. The soil temperature distribution on the right side boundary was considered to be adiabatic because it is far enough away from the slab to be unaffected by it;
4. The top surface was under a convective boundary condition. The hourly zone temperature (for the indoor part) and solar air temperature (for outdoor part) were represented using 3rd-order sinusoidal functions in the following format

$$T(t)=T_0+A_1\sin(\omega_1t+\phi_1)+A_2\sin(\omega_2t+\phi_2)+A_3\sin(\omega_3t+\phi_3) \quad (3.2)$$

This function was developed through least-squares regression applied to data generated by VSAT simulations. The ambient solar-air temperature was selected from a typical hot day for CZ10. For this same day, the zone temperature profile was taken from output for the retail store with night ventilation control. Fig. 3.5a and 3.5b show comparisons of the discrete hourly temperatures with temperatures determined with this function.



a. zone temperature (indoor condition)



b. solar-air temperature (outdoor condition)

Fig 3.5 Comparisons of the hourly temperatures from VSAT and equation 3.2

The initial condition for each node was also determined using Begga's formula at the beginning time and its according depth. Up to 50-day cycles were calculated in FEHT in order to achieve a steady-periodic condition. Fig. 3.6 indicates that the effects of the initial conditions were successfully eliminated through this repeated cycling.

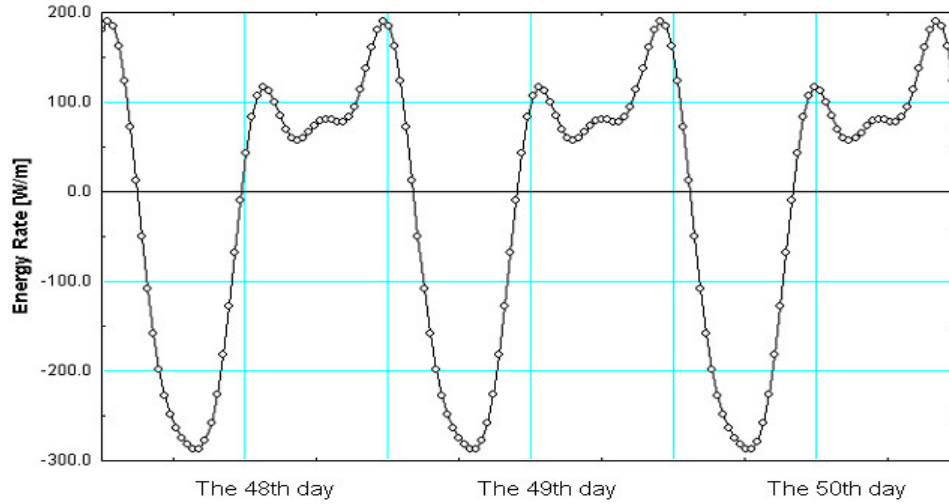


Fig 3.6 Heat transfer rate variations at the inside floor surface (L3W=10m31m)

Fig. 3.7 gives comparisons of the FEHT predictions for average heat flux to the floor from the space with predictions from the original VSAT slab heat transfer model (as shown in Fig. 3.1). Although the original model gives a similar shape for the heat flux variation, the peaks occur at different times and have different magnitudes. This is due to three effects: the original model does not include the soil, which is a big part of thermal mass; the positions of the nodes are not optimized to give the best results; and the 1-dimensional model is a simplification.

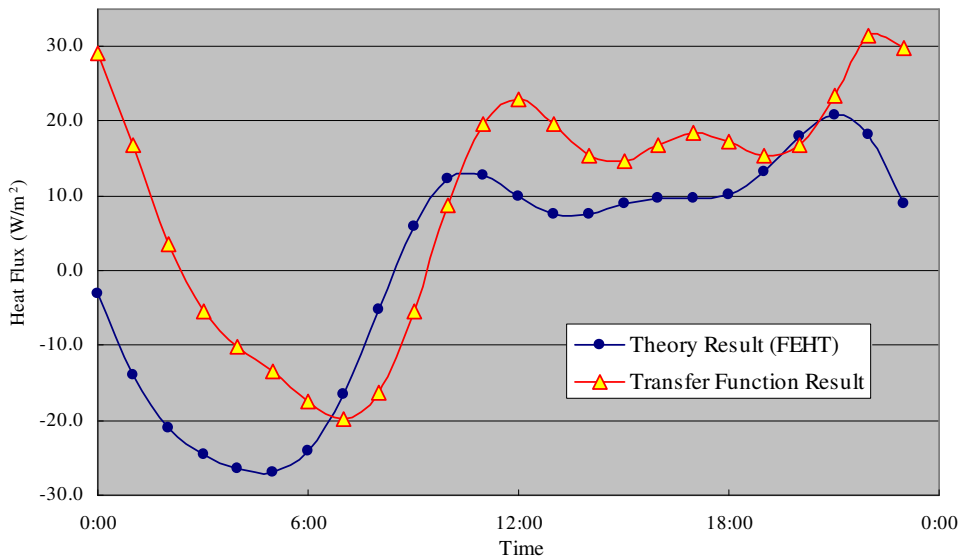


Fig. 3.7: Comparison of the FEHT and original VSAT slab model indoor heat flux results

Fig. 3.8 gives an example underground temperature profile at 17:00. The temperature profiles are such that the ground heat transfer under the internal part of the floor (approximately 8 meters in length) is nearly one dimensional in a direction normal to the floor. However, at the outer edge of the floor (about 2 meters in length) the heat transfer is two dimensional but is dominated by heat transfer in a direction that is normal to the slab edge. As a result, the form of the original slab model within VSAT seems reasonable. However, it is necessary to determine the amount of soil that should be considered and to optimize the node positions and value for the perimeter heat loss factor (U_a).

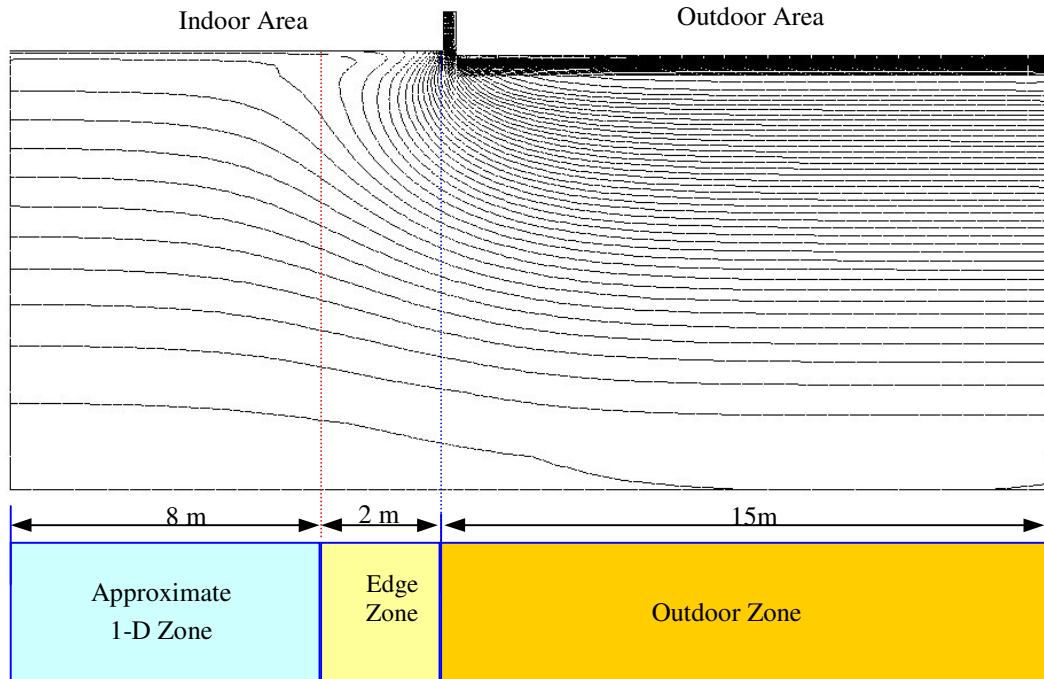


Fig. 3.8: Underground temperature profile (17:00) and zone distribution

Fig. 3.9 shows comparisons of predictions of heat flux from FEHT result and the original VSAT slab model modified to include different depths of soil. The simplified model agrees well with FEHT results for a soil depth of about 0.8 meter (2.5 feet). This is consistent with transient temperature field results from FEHT which indicates that the daily indoor zone temperature wave normally does not penetrate more than 0.8 meter into the soil depth. A soil depth of 0.8 meter was chosen for all subsequent simulation results.

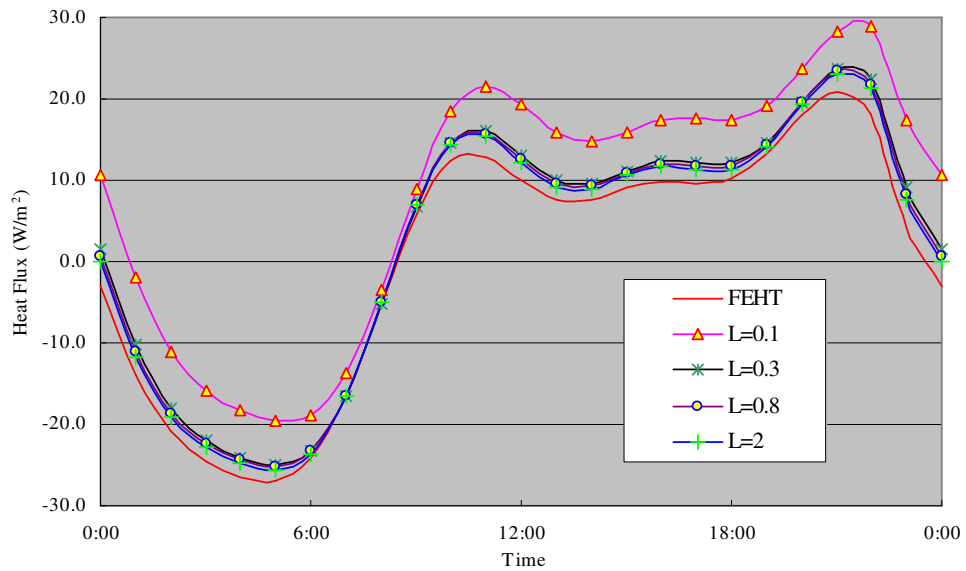
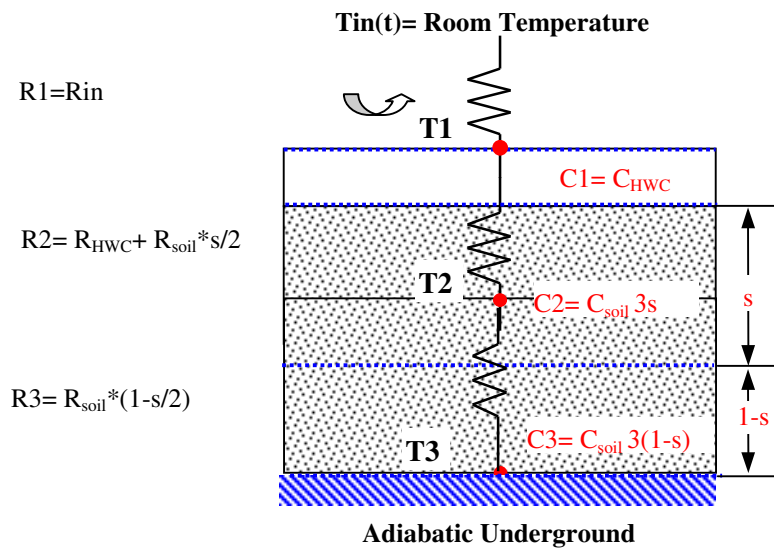


Fig. 3.8: Comparison of the FEHT 1-D result with the result of different depth of soil

A variety of node arrangements were investigated. The configuration shown in Fig. 3.9 was found to work very well with the parameter s determined by minimizing differences between the FEHT and simplified model predictions. Fig. 3.10 shows that $s \approx 1/3$ gives the best performance in terms of mean square and absolute errors.

Fig. 3.9: Nodes distribution configuration



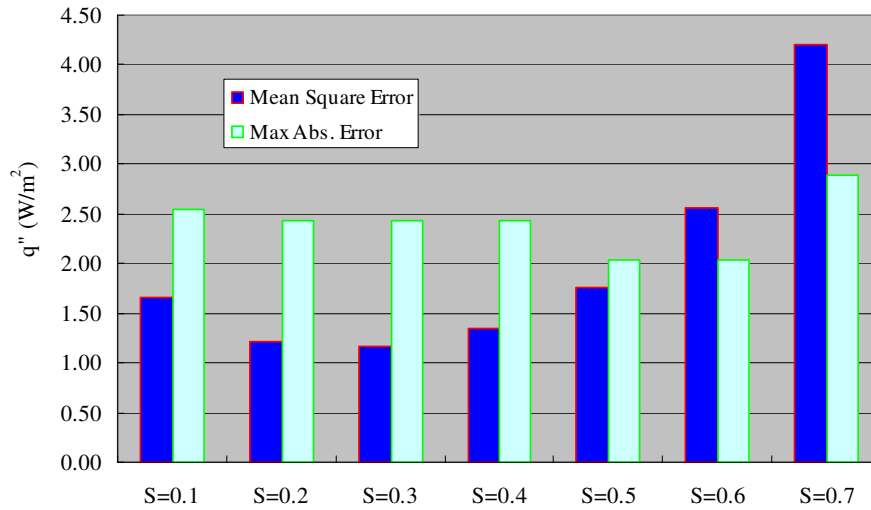


Fig. 3.10: Optimization of the middle layer fraction s

In the results described in the previous paragraph, edge effects were neglected (i.e., $U_a=0$) to study the influence of number of nodes and node location. However, in order to have a complete model the approximate transient 1-D model is combined with a quasi-static edge zone model. The conductance per unit length of perimeter for the edge (U_a) was optimized by minimizing errors with the FEHT overall heat transfer rate. For the floor considered in this study, the minimum error was achieved with $U_a=1.49$ W/m (0.85 Btu/h-ft-F). Fig. 3.11 shows that the simplified 1-D+ $U_a \cdot P$ model agrees very well with the detailed FEHT predictions and is an improvement over the model that neglects edge effects.

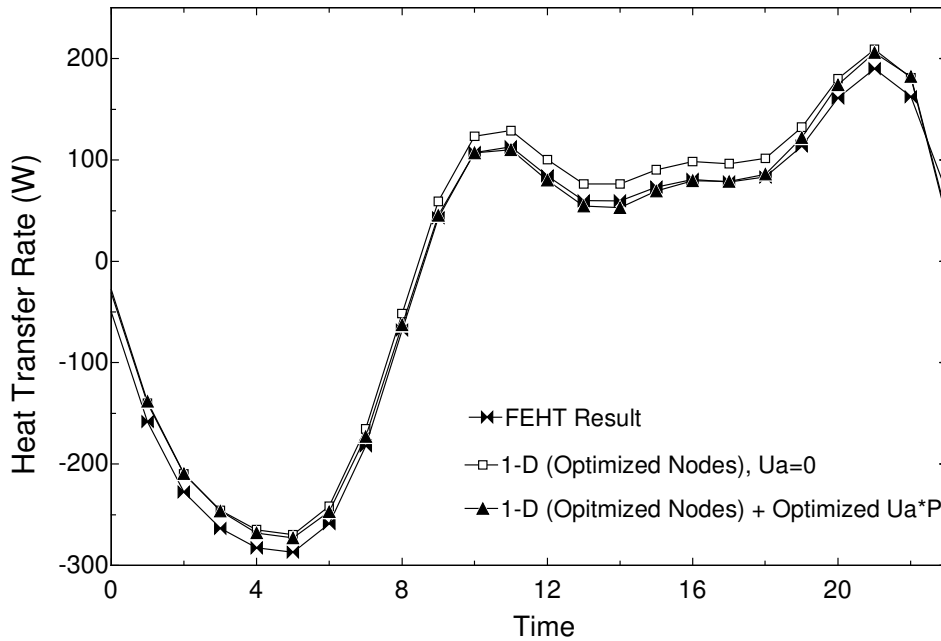


Fig. 3.11: Optimizing the peripheral heat loss factor U_a

3.3 Modeling Parameters

The default parameters in VSAT with the improved slab model were employed for the simulation results presented in this section (medium efficiency equipment index with rated air conditioner EER of 9.5 and gas furnace efficiency of 0.75, supply fan power of 0.4 W/cfm). The slab description is slightly different than that used for the case study presented in section 3.2. The slab model employed within VSAT used 6 inches of pea-gravel and a 2-foot soil layer beneath the heavy weight concrete floor. A carpet and pad were assumed for the small office building and restaurant dining area, but not for any of the other building types. Appendix A contains detailed descriptions with the updated slab description of the prototypical buildings that were employed within VSAT for the night ventilation simulation studies.

3.3 Weather Data

VSAT includes weather data for the California climate zones shown in Figure 3.12. The representative cities for each climate zone (CZ) are given in Table 3.1. The climate zones are based on energy use, temperature, weather and other factors. They are basically a geographic area that has similar climatic characteristics. The California Energy Commission (CEC) originally developed weather data for each climate zone by using unmodified (but error-screened) data for a representative city and weather year

(representative months from various years). The CEC analyzed weather data from weather stations selected for (1) reliability of data, (2) currency of data, (3) proximity to population centers, and (4) non-duplication of stations within a climate zone. There are two sets of climate zone data included in VSAT, the original and a massaged set. In the massaged data, the dry bulb temperature has been modified in an effort to give the file a better "average" across the entire zone. However, because only dry bulb was adjusted, the humidity conditions are affected and therefore, the massaged files are not preferred. The original data set was used for the results presented in this report.

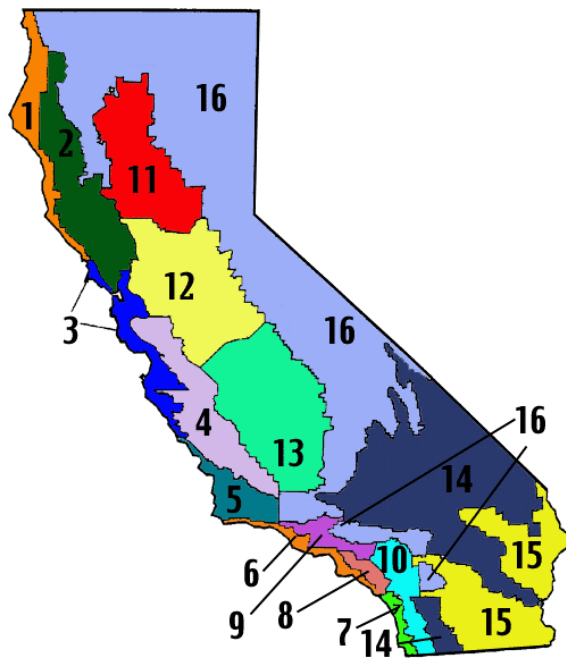


Figure 3.12: California Climate Zones

Table 3.1. Cities Associated with California Climate Zones

CZ 1: Arcata	CZ 5: Santa Maria	CZ 9: Pasadena	CZ13: Fresno
CZ 2: Santa Rosa	CZ 6: Los Angeles	CZ10: Riverside	CZ14: China Lake
CZ 3: Oakland	CZ 7: San Diego	CZ11: Red Bluff	CZ15: El Centro
CZ 4: Sunnyvale	CZ 8: El Toro	CZ12: Sacramento	CZ16: Mount Shasta

3.4 Operating Costs

Operating costs associated with the base case and night ventilation precooling strategy are calculated based on annual electric power and/or gas consumption by the HVAC equipment. Percent savings for night ventilation cooling is assessed by comparing annual operating costs to the base case.

The annual operating costs for an HVAC system within VSAT are calculated assuming a three tiered utility rate structure of on-peak, mid-peak and off-peak rates. These costs are calculated according to

$$C_k = \sum_{m=1}^{m=12} \left\{ r_{d,on,m} \cdot \dot{W}_{peak,on,m} + r_{d,mid,m} \cdot \dot{W}_{peak,mid,m} + r_{d,off,m} \cdot \dot{W}_{peak,off,m} + \sum_{i=1}^{N_m} (r_{e,i,m} \cdot W_{i,m} + r_{g,i,m} \cdot G_{i,m}) \right\} \quad (4)$$

where subscript k denotes the HVAC system associated with a particular ventilation strategy k , m is the month and i is the hour of the year. N_m is the number of hours within month m . For each month m , $r_{d,on,m}$, $r_{d,mid,m}$ and $r_{d,off,m}$ correspond to the utility rates for electricity demand during the on-peak, mid-peak and off-peak time periods (\$/kW). Peak power consumption for the HVAC equipment during the on-peak, mid-peak and off-peak periods is represented as $\dot{W}_{peak,on,m}$, $\dot{W}_{peak,mid,m}$ and $\dot{W}_{peak,off,m}$, respectively. For each hour i of month m , r_e is the utility rate associated with electricity usage (\$/kWh), W corresponds to the amount of electricity consumed (kWh), r_g is the utility rate associated with natural gas usage (\$/therm) and G represents the amount of gas consumed (therm).

Annual electricity costs include both energy (\$/kWh) and demand charges (\$/kW). Gas energy usage costs do not vary with time of the day. However, the user may enter different electric and gas rates for summer and winter periods. The user may also adjust the start month for the summer and winter periods and the times of day associated with on-peak, mid-peak and off-peak periods.

Each ventilation strategy is compared with an assumed base case of fixed ventilation incorporating a setup/ setback thermostat and differential enthalpy economizer. Annual operating cost savings (S_k) for each ventilation strategy k , when compared to the base case, are calculated according to

$$S_k = C_{BASE.CASE} - C_k \quad (5)$$

Annual operating cost percent savings ($\% S_k$) for each ventilation strategy k are calculated according to

$$\%S_k = \left\{ 1 - \frac{C_k}{C_{BASE.CASE}} \right\} \cdot 100\% \quad (6)$$

All utility rates used for economic results assume secondary, firm service (electricity constantly supplied) and a monthly electric demand less than 500 kW. Typical utility rate information was obtained for small commercial service in each of the California climate zones and implemented within VSAT. Table 3.2 summarizes the utility rates that were considered for each climate zone. Pacific Gas and Electricity (PGE), Southern California Edison (SCE), Southern California Gas (SCG) and San Diego Gas and Electricity (SDGE) are the major utility suppliers in California. The utility rates of each supplier differ depending upon time-of-use. Table 3.3 shows the time-of-use associated with each utility provider. The cities associated with climate zones 10 (Riverside) and 15 (El Centro) are served by local energy companies. However, for the electric rate structure within VSAT, Southern California Edison was assumed for both climate zones 10 and 15 because the majority of CZ 10 and approximately half of CZ 15 is territory within the service area of Southern California Edison. Southern California Gas Company was also assumed for most all the southern California climate zones except CZ 07, which is serviced by San Diego Gas and Electricity.

For summer electricity consumption, the demand charge for Pacific Gas and Electricity is higher, almost twice that of Southern California Edison; while Pacific Gas and Electricity's energy charge is low, only half of Southern California Edison's energy charge. For Pacific Gas and Electric, the ratio of on-peak to off-peak demand charges is greater than 5, whereas Southern California Edison does not charge demand fees during off-peak times. For energy charges, both companies have on-peak to off-peak ratios of about 2. San Diego's time-of-use energy charge ratio is much lower.

Table 3.2. Utility Rates in California

CZ	Representative City	Service Provider	Time of Use	Summer	Winter
				Season	Season
1	Arcata		<i>Demand Charge- \$/kW</i>		
2	Santa Rosa		On Peak	\$13.35	N/A
3	Oakland	Pacific Gas	Mid Peak	\$3.70	\$3.65
4	Sunnyvale	And	Off Peak	\$2.55	\$2.55
5	Santa Maria	Electricity	<i>Energy Charge - \$/kWh</i>		
11	Red Bluff	(Schedules E-19	On Peak	0.0877	N/A
12	Sacramento	and G-NR1)	Mid Peak	0.0581	0.0639
13	Fresno		Off Peak	0.0506	0.0504
			<i>Gas Charge - \$/therm</i>		
				\$0.6736	\$0.7422
6	Los Angeles		<i>Demand Charge- \$/kW</i>		
8	El Toro	Southern	On Peak	\$7.75	\$0.00
9	Pasadena	California Edison	Mid Peak	\$2.45	\$0.00
10	Riverside	(Schedule TOU-	Off Peak	\$0.00	\$0.00
14	China Lake	GS-2) and	<i>Energy Charge - \$/kWh</i>		
15	El Centro	Southern	On Peak	0.2960	N/A
16	Mount Shasta	California Gas	Mid Peak	0.1176	0.1296
		(Schedule GN-10)	Off Peak	0.0942	0.0942
			<i>Gas Charge - \$/therm</i>		
				\$0.7079	\$0.7079
7	San Diego		<i>Demand Charge- \$/kW</i>		
			On Peak	\$10.42	\$4.83
		San Diego Gas	Mid Peak	N/A	N/A
		and Electricity	Off Peak	N/A	N/A
		(Schedules AL-	<i>Energy Charge - \$/kWh</i>		
		TOU and EECC	On Peak	\$0.1163	\$0.1151
		and GN-3)	Mid Peak	\$0.0895	\$0.0894
			Off Peak	\$0.0884	\$0.0884
			<i>Gas Charge - \$/therm</i>		
				\$0.6524	\$0.7497

Table 3.3. Time-Of-Use for California Utility Companies

PGE			
Summer:	May 1 - Oct. 31	Winter:	Nov. 1 - April 30
On-Peak	12:00 - 6:00, M - F	On-Peak	N/A
Mid-Peak	8:00 AM - 12:00 & 6:00 PM - 9:00 PM, M - F	Mid-Peak	8:00 AM - 9:00 PM, M - F
Off-Peak	9:00 PM - 8:00 AM, all week	Off-Peak	9:00 PM - 8:00 AM, all week
SCE			
Summer:	June 1 - Sept. 30	Winter:	Oct. 1 - May 31
On-Peak	12:00 - 6:00, M - F	On-Peak	N/A
Mid-Peak	8:00 AM - 12:00 & 6:00 PM - 11:00 PM, M - F	Mid-Peak	8:00 AM - 9:00 PM, M - F
Off-Peak	11:00 PM - 8:00 AM, all week	Off-Peak	9:00 PM - 8:00 AM, all week
SDGE - Electric Rate			
Summer:	May 1 - Sept. 30	Winter:	Oct. 1 - April 30
On-Peak	11:00 - 6:00, M - F	On-Peak	5:00 - 8:00, M - F
Mid-Peak	6:00 AM - 11:00 & 6:00 PM - 10:00 PM, M - F	Mid-Peak	6:00 AM - 5:00 PM & 8:00 PM - 10:00 PM, M - F
Off-Peak	10:00 PM - 6:00 AM, all week	Off-Peak	10:00 PM - 6:00 AM, all week
SDGE - Gas Rate			
Summer:	April 1 - Nov. 30	Winter:	Dec. 1 - March 31
SCG			
Summer:	April 1 - Nov. 30	Winter:	Dec. 1 - March 31

4. Simulated Savings

4.1 Sample Hourly Results

Figure 4.1 shows sample hourly results for the base case (night setup with no economizer) and with Night Ventilation Precooling for the school class wing within early summer in Climate Zone 10 obtained using the default VSAT utility rates (PG&E E-19 and GNR-1). Night ventilation precooling is enabled during the unoccupied mode when the ambient temperature is sufficiently cooler than the zone temperature. For this example, this occurs during the hour from 11-12:00 pm and continues until the occupied mode begins at 5 am. Prior to occupancy the zone temperature is cooled to around 20°C. At occupancy, the economizer keeps the zone temperature at a lower economizer setpoint until 8 am when the temperature begins to rise. The temperature reaches the setpoint for mechanical cooling at 11:00 am.

Figure 4.1: Simulated hourly temperatures for night ventilation precooling and the base case (class school wing during early summer in California Climate Zone 10).

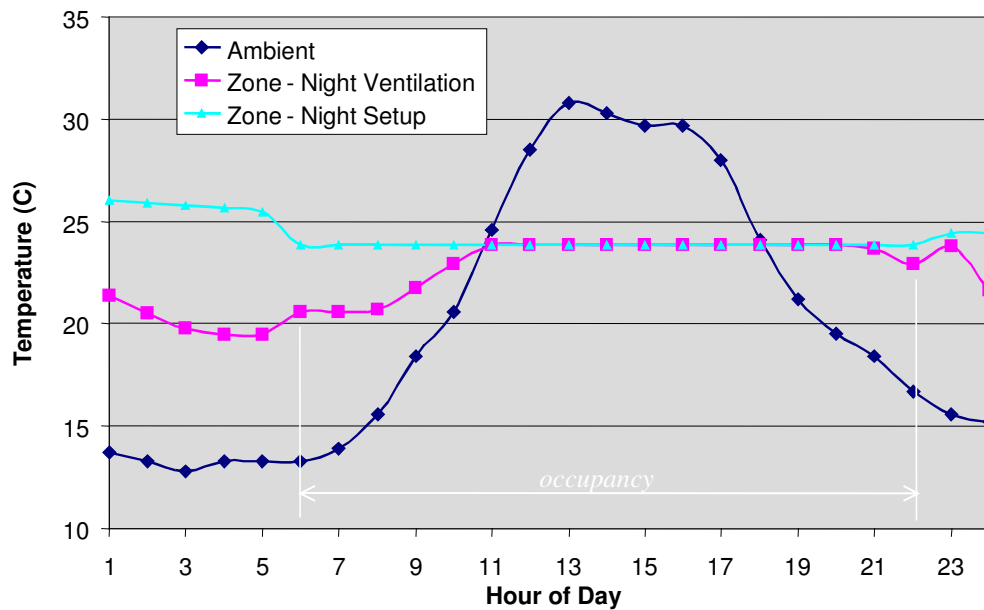
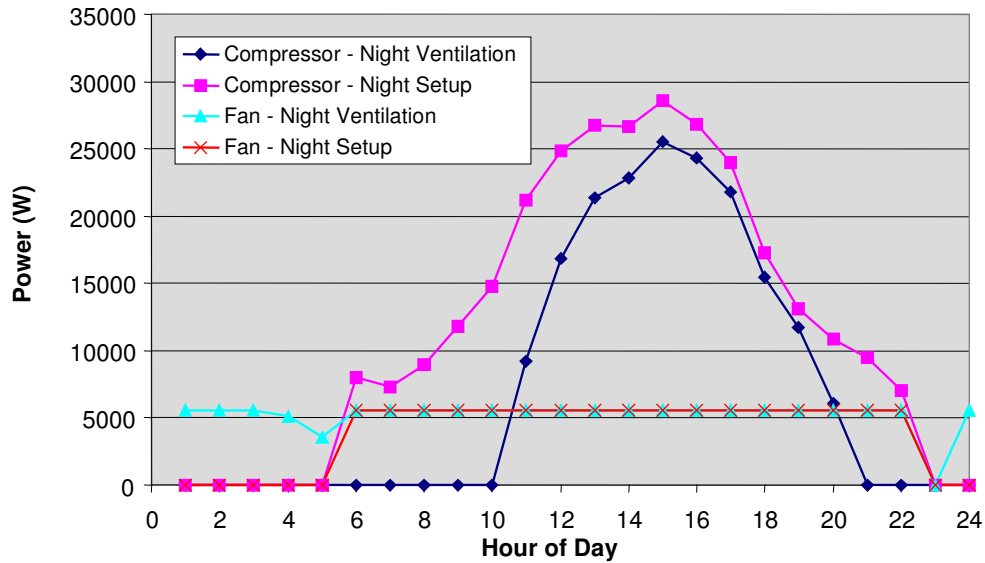


Figure 4.2 shows hourly fan and compressor power comparisons for the situation considered for Figure 4.1. Additional fan energy is utilized during the early morning hours with night ventilation precooling, but this leads to a reduction in compressor energy over much of the day. Part of the savings is due to the low zone setpoint for the economizer, which acts to maintain a cool building thermal mass during the morning hours. For the night ventilation control, mechanical cooling is not needed until 11 am. Clearly, the night

ventilation control requires significantly less compressor energy and has slightly lower peak electrical demand at the expense of additional fan energy.

Figure 4.2: Simulated hourly power for night ventilation precooling and the base case (class school wing during early summer in California Climate Zone 10).

Figure 4.3 gives annual electrical energy usage for the class school wing in California



Climate Zone 10 for three ventilation strategies: 1) a base case with a night setup thermostat, 2) case 1 with the addition of a differential enthalpy-based economizer, and 3) case 2 with the addition of the night ventilation precooling algorithm. Compared to the base case, the economizer results in a savings in compressor energy of 19.3%. The combined compressor and fan savings are about 13.2%. Compared to the economizer, the addition of the night ventilation algorithm leads to an additional savings of about 13.6% in compressor energy. However, the fan energy increases by about 13.5%, and because the compressor energy is the major consumption, the energy saved in compressor is more than the additional consumption by fan, the combined savings about 3.8% is achieved compared to the economizer only.

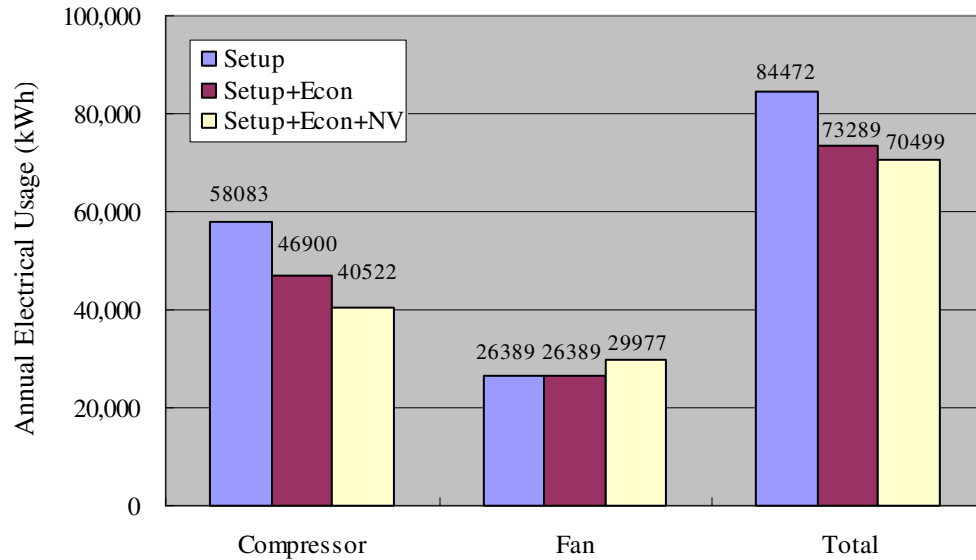


Figure 4.3: Simulated electrical energy usage for different ventilation strategies (class school wing in California Climate Zone 10).

4.2 Annual Cost Savings

Tables 4.1 - 4.4 give annual results for economizer and night ventilation control in all climate zones for the small office, retail store, restaurant dining area, and school class wing with the default supply air fan power of 0.40 W/Cfm. The results include compressor, supply air fan, and total air conditioning electrical usage, costs for electrical energy and demand associated with air conditioning, total air conditioning costs, and percent savings associated with air conditioning compressor energy usage, demand costs, and total costs. The percentage savings in electrical costs are also shown on a map of California in Figure 4.4 for the four featured buildings. The savings are all relative to a base case that includes a night setup thermostat with a differential enthalpy economizer.

The savings in compressor energy ranged from about 0 to 53% depending on the location and building type. However, the savings in total air conditioning electrical energy usage are much smaller than the compressor savings due to an increase in fan energy. The electrical energy savings varied between about 0 and 8%. However, the ventilation algorithm is based upon reducing total energy costs, including the effects of differences between on-peak and off-peak electrical rates. In addition, there are demand cost reductions. The electrical demand cost savings associated with night ventilation varied

between about 0 and 28%, whereas the total electrical cost savings ranged from about 0 to 17%.

Generally, the greatest percentage compressor and total cost savings occur in coastal climates with relatively mild ambient temperatures. However, the compressor savings are also significant in hot inland climates having larger total loads. The savings are considerably smaller for the restaurant than for the other buildings. Compared to the other buildings, the restaurant has less thermal mass, smaller internal gains, a longer occupancy schedule, and greater ventilation requirements.

In some limited cases, penalties occur when night ventilation is employed. Compressor savings occurred in all locations, but overall electrical cost savings were slightly negative for three of the buildings in CZ07 (San Diego) because of the hot climate. In some other cases, the total electrical energy savings were negative but cost savings occurred because of reduced on-peak energy usage and demand.

Table 4.1: Night ventilation air conditioning savings for small office (default parameters)

Climate	Control	Comp. (kWh)	Fan (kWh)	Elec. (kWh)	Elec. Cost (\$)	Dem. Cost (\$)	Total Cost (\$)	Comp. Sav. (%)	Elec. Sav. (%)	Dem. \$ Sav. (%)	Cost \$ Sav. (%)
CZ01	EC	775	5,944	6,719	437	979	1,416	□	□	□	□
	EC+NV	366	6,377	6,743	422	772	1,194	52.8%	-0.4%	21.1%	15.7%
CZ02	EC	17,953	11,670	29,622	2,047	3,123	5,170	□	□	□	□
	EC+NV	14,750	13,585	28,336	1,944	3,050	4,994	17.8%	4.3%	2.3%	3.4%
CZ03	EC	6,269	7,184	13,453	919	1,725	2,644	□	□	□	□
	EC+NV	3,618	8,936	12,554	823	1,612	2,434	42.3%	6.7%	6.6%	7.9%
CZ04	EC	9,890	9,096	18,986	1,293	2,214	3,507	□	□	□	□
	EC+NV	6,881	11,022	17,904	1,188	2,079	3,267	30.4%	5.7%	6.1%	6.8%
CZ05	EC	6,614	9,543	16,157	1,072	2,385	3,457	□	□	□	□
	EC+NV	4,767	10,612	15,379	993	2,237	3,231	27.9%	4.8%	6.2%	6.5%
CZ06	EC	18,218	9,055	27,273	4,456	822	5,278	□	□	□	□
	EC+NV	14,956	11,248	26,204	4,247	814	5,061	17.9%	3.9%	1.0%	4.1%
CZ07	EC	17,461	10,882	28,343	2,805	1,333	4,138	□	□	□	□
	EC+NV	15,288	13,190	28,478	2,798	1,360	4,159	12.4%	-0.5%	-2.0%	-0.5%
CZ08	EC	18,499	9,722	28,221	4,580	835	5,415	□	□	□	□
	EC+NV	15,839	11,491	27,330	4,394	823	5,216	14.4%	3.2%	1.4%	3.7%
CZ09	EC	19,858	9,949	29,807	4,878	924	5,803	□	□	□	□
	EC+NV	16,707	11,933	28,640	4,647	913	5,560	15.9%	3.9%	1.2%	4.2%
CZ10	EC	23,776	11,435	35,211	5,817	1,093	6,910	□	□	□	□
	EC+NV	20,173	13,498	33,671	5,540	1,075	6,615	15.2%	4.4%	1.6%	4.3%
CZ11	EC	25,964	14,441	40,405	2,716	3,842	6,559	□	□	□	□
	EC+NV	22,483	17,313	39,796	2,659	3,755	6,414	13.4%	1.5%	2.3%	2.2%
CZ12	EC	20,543	12,033	32,576	2,238	3,218	5,456	□	□	□	□
	EC+NV	16,823	14,490	31,313	2,136	3,106	5,243	18.1%	3.9%	3.5%	3.9%
CZ13	EC	27,126	11,363	38,489	2,603	3,363	5,966	□	□	□	□
	EC+NV	22,832	13,853	36,685	2,483	3,265	5,748	15.8%	4.7%	2.9%	3.7%
CZ14	EC	35,277	12,691	47,968	7,712	1,226	8,938	□	□	□	□
	EC+NV	31,761	15,362	47,123	7,564	1,220	8,784	10.0%	1.8%	0.5%	1.7%
CZ15	EC	51,092	14,033	65,126	9,997	1,418	11,415	□	□	□	□
	EC+NV	47,970	16,741	64,711	9,890	1,416	11,307	6.1%	0.6%	0.1%	0.9%
CZ16	EC	10,588	10,738	21,327	3,569	876	4,445	□	□	□	□
	EC+NV	8,660	12,218	20,878	3,430	860	4,289	18.2%	2.1%	1.8%	3.5%

Table 4.2: Night ventilation air conditioning savings for retail store (default parameters)

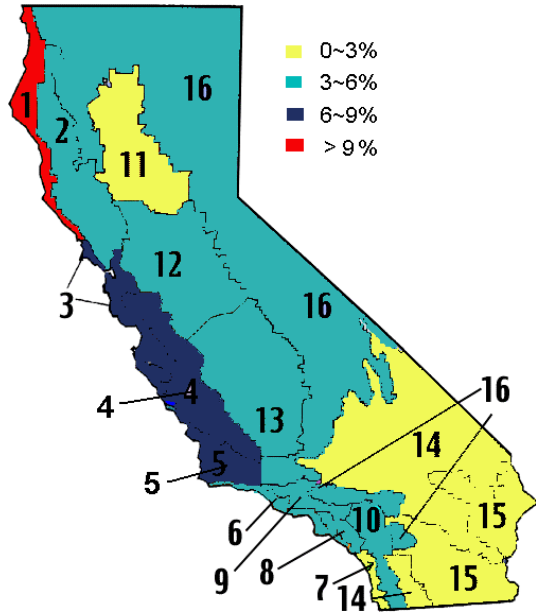
Climate	Control	Comp. (kWh)	Fan (kWh)	Elec. (kWh)	Elec. Cost (\$)	Dem. Cost (\$)	Total Cost (\$)	Comp. Sav. (%)	Elec. Sav. (%)	Dem. \$ Sav. (%)	Cost \$ Sav. (%)
CZ01	EC	3,495	85,191	88,686	5,430	7,189	12,618	□	□	□	□
	EC+NV	2,238	91,793	94,031	5,637	5,137	10,774	36.0%	-6.0%	28.5%	14.6%
CZ02	EC	237,564	202,277	439,842	28,792	35,888	64,679	□	□	□	□
	EC+NV	193,740	223,767	417,507	27,017	34,333	61,350	18.4%	5.1%	4.3%	5.1%
CZ03	EC	64,793	112,075	176,868	11,403	17,997	29,400	□	□	□	□
	EC+NV	31,116	132,133	163,249	10,010	15,504	25,514	52.0%	7.7%	13.9%	13.2%
CZ04	EC	103,920	175,710	279,630	17,846	25,398	43,244	□	□	□	□
	EC+NV	69,789	198,156	267,946	16,491	23,307	39,798	32.8%	4.2%	8.2%	8.0%
CZ05	EC	53,543	166,344	219,887	13,833	25,888	39,721	□	□	□	□
	EC+NV	38,859	176,842	215,701	13,205	22,631	35,836	27.4%	1.9%	12.6%	9.8%
CZ06	EC	216,802	154,447	371,249	56,138	9,752	65,890	□	□	□	□
	EC+NV	174,297	180,233	354,530	52,752	9,605	62,357	19.6%	4.5%	1.5%	5.4%
CZ07	EC	204,243	187,842	392,086	38,122	15,433	53,555	□	□	□	□
	EC+NV	183,655	213,482	397,136	38,344	15,182	53,525	10.1%	-1.3%	1.6%	0.1%
CZ08	EC	218,372	163,942	382,314	57,548	9,943	67,491	□	□	□	□
	EC+NV	184,315	183,899	368,214	54,586	9,646	64,232	15.6%	3.7%	3.0%	4.8%
CZ09	EC	248,565	193,797	442,363	66,340	11,452	77,792	□	□	□	□
	EC+NV	212,654	216,991	429,645	63,233	11,220	74,452	14.4%	2.9%	2.0%	4.3%
CZ10	EC	319,776	204,839	524,614	79,572	13,287	92,859	□	□	□	□
	EC+NV	275,728	228,424	504,152	75,480	13,016	88,496	13.8%	3.9%	2.0%	4.7%
CZ11	EC	368,296	256,551	624,847	40,047	43,976	84,023	□	□	□	□
	EC+NV	334,682	285,352	620,034	39,382	42,816	82,198	9.1%	0.8%	2.6%	2.2%
CZ12	EC	271,272	204,728	476,000	31,052	36,868	67,920	□	□	□	□
	EC+NV	223,329	231,211	454,540	29,299	35,612	64,911	17.7%	4.5%	3.4%	4.4%
CZ13	EC	375,148	193,641	568,789	36,700	37,935	74,635	□	□	□	□
	EC+NV	328,775	220,048	548,823	35,208	37,092	72,301	12.4%	3.5%	2.2%	3.1%
CZ14	EC	493,264	224,749	718,013	106,927	14,624	121,551	□	□	□	□
	EC+NV	461,409	248,232	709,642	105,240	14,586	119,826	6.5%	1.2%	0.3%	1.4%
CZ15	EC	731,641	252,117	983,758	142,220	17,445	159,666	□	□	□	□
	EC+NV	701,175	278,141	979,315	140,922	17,442	158,364	4.2%	0.5%	0.0%	0.8%
CZ16	EC	138,302	175,180	313,482	46,943	10,017	56,959	□	□	□	□
	EC+NV	115,372	190,208	305,580	44,645	9,767	54,412	16.6%	2.5%	2.5%	4.5%

Table 4.3: Night ventilation air conditioning savings for restaurant (default parameters)

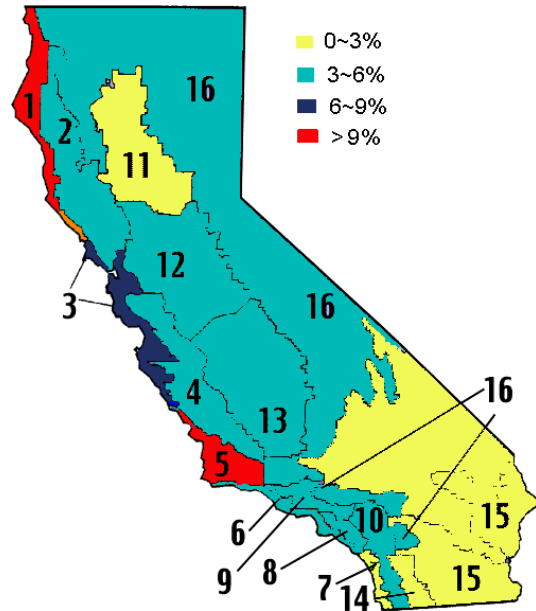
Climate	Control	Comp. (kWh)	Fan (kWh)	Elec. (kWh)	Elec. Cost (\$)	Dem. Cost (\$)	Total Cost (\$)	Comp. Sav. (%)	Elec. Sav. (%)	Dem. \$ Sav. (%)	Cost \$ Sav. (%)
CZ01	EC	312	9,612	9,924	590	718	1,308	□	□	□	□
	EC+NV	312	9,612	9,924	590	718	1,308	0.0%	0.0%	0.0%	0.0%
CZ02	EC	22,608	23,154	45,762	2,944	3,630	6,574	□	□	□	□
	EC+NV	21,180	24,075	45,255	2,895	3,586	6,481	6.3%	1.1%	1.2%	1.4%
CZ03	EC	4,823	14,108	18,931	1,177	1,824	3,001	□	□	□	□
	EC+NV	3,825	14,904	18,729	1,139	1,722	2,861	20.7%	1.1%	5.6%	4.7%
CZ04	EC	8,799	22,354	31,153	1,927	2,595	4,522	□	□	□	□
	EC+NV	7,897	23,223	31,120	1,894	2,474	4,367	10.3%	0.1%	4.7%	3.4%
CZ05	EC	4,935	21,245	26,180	1,597	2,743	4,340	□	□	□	□
	EC+NV	4,630	21,430	26,060	1,582	2,670	4,252	6.2%	0.5%	2.7%	2.0%
CZ06	EC	22,924	19,677	42,601	6,325	1,194	7,518	□	□	□	□
	EC+NV	21,030	20,893	41,924	6,148	1,170	7,317	8.3%	1.6%	2.0%	2.7%
CZ07	EC	17,095	23,942	41,036	3,959	1,594	5,553	□	□	□	□
	EC+NV	16,438	25,086	41,524	3,989	1,568	5,556	3.8%	-1.2%	1.6%	-0.1%
CZ08	EC	23,619	20,814	44,432	6,546	1,223	7,768	□	□	□	□
	EC+NV	22,506	21,596	44,102	6,439	1,207	7,646	4.7%	0.7%	1.3%	1.6%
CZ09	EC	27,831	24,596	52,427	7,699	1,412	9,111	□	□	□	□
	EC+NV	26,447	25,617	52,064	7,563	1,392	8,955	5.0%	0.7%	1.4%	1.7%
CZ10	EC	36,781	25,501	62,282	9,286	1,626	10,912	□	□	□	□
	EC+NV	35,151	26,661	61,812	9,130	1,608	10,738	4.4%	0.8%	1.1%	1.6%
CZ11	EC	37,126	30,585	67,711	4,256	4,442	8,698	□	□	□	□
	EC+NV	35,610	32,282	67,892	4,246	4,381	8,627	4.1%	-0.3%	1.4%	0.8%
CZ12	EC	26,033	26,132	52,165	3,337	3,786	7,123	□	□	□	□
	EC+NV	24,468	27,326	51,794	3,291	3,709	7,001	6.0%	0.7%	2.0%	1.7%
CZ13	EC	37,017	23,477	60,494	3,840	3,843	7,683	□	□	□	□
	EC+NV	35,020	25,043	60,063	3,798	3,797	7,595	5.4%	0.7%	1.2%	1.1%
CZ14	EC	59,898	27,222	87,120	12,708	1,742	14,450	□	□	□	□
	EC+NV	58,481	28,585	87,066	12,658	1,739	14,397	2.4%	0.1%	0.2%	0.4%
CZ15	EC	90,638	31,210	121,847	17,212	2,106	19,318	□	□	□	□
	EC+NV	89,263	32,813	122,076	17,188	2,105	19,293	1.5%	-0.2%	0.0%	0.1%
CZ16	EC	15,825	21,496	37,320	5,421	1,192	6,613	□	□	□	□
	EC+NV	14,731	22,227	36,958	5,311	1,175	6,486	6.9%	1.0%	1.4%	1.9%

Table 4.4: Night ventilation air conditioning savings for school class wing (default parameters)

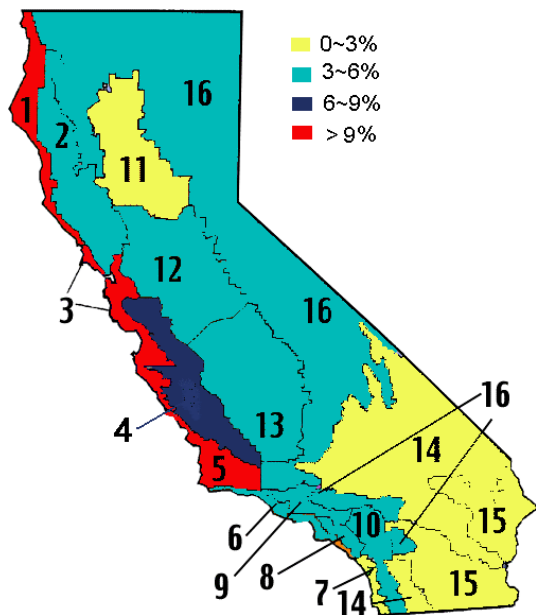
Climate	Control	Comp. (kWh)	Fan (kWh)	Elec. (kWh)	Elec. Cost (\$)	Dem. Cost (\$)	Total Cost (\$)	Comp. Sav. (%)	Elec. Sav. (%)	Dem. \$ Sav. (%)	Cost \$ Sav. (%)
CZ01	EC	1,388	13,424	14,812	944	1,660	2,604	□	□	□	□
	EC+NV	991	14,448	15,439	948	1,211	2,159	28.6%	-4.2%	27.0%	17.1%
CZ02	EC	34,796	26,594	61,390	4,152	5,640	9,793	□	□	□	□
	EC+NV	28,782	29,994	58,775	3,920	5,352	9,271	17.3%	4.3%	5.1%	5.3%
CZ03	EC	10,735	17,130	27,865	1,856	3,150	5,006	□	□	□	□
	EC+NV	5,983	20,535	26,518	1,676	2,706	4,382	44.3%	4.8%	14.1%	12.5%
CZ04	EC	18,060	20,273	38,333	2,554	3,965	6,519	□	□	□	□
	EC+NV	11,938	23,767	35,705	2,301	3,594	5,895	33.9%	6.9%	9.4%	9.6%
CZ05	EC	11,366	21,998	33,364	2,161	4,314	6,475	□	□	□	□
	EC+NV	8,536	23,926	32,462	2,031	3,790	5,820	24.9%	2.7%	12.1%	10.1%
CZ06	EC	40,731	21,942	62,673	9,942	1,804	11,746	□	□	□	□
	EC+NV	33,542	26,062	59,603	9,315	1,759	11,075	17.6%	4.9%	2.5%	5.7%
CZ07	EC	33,442	27,066	60,508	5,935	2,500	8,435	□	□	□	□
	EC+NV	31,413	31,170	62,582	6,080	2,451	8,530	6.1%	-3.4%	2.0%	-1.1%
CZ08	EC	41,508	23,075	64,583	10,166	1,840	12,006	□	□	□	□
	EC+NV	35,729	26,238	61,968	9,611	1,797	11,408	13.9%	4.0%	2.3%	5.0%
CZ09	EC	45,194	21,365	66,559	10,606	1,956	12,562	□	□	□	□
	EC+NV	38,029	24,865	62,894	9,904	1,918	11,823	15.9%	5.5%	1.9%	5.9%
CZ10	EC	55,695	26,389	82,083	13,161	2,351	15,512	□	□	□	□
	EC+NV	48,106	30,003	78,109	12,390	2,293	14,683	13.6%	4.8%	2.5%	5.3%
CZ11	EC	51,523	32,013	83,535	5,528	6,646	12,174	□	□	□	□
	EC+NV	46,459	36,495	82,954	5,431	6,401	11,833	9.8%	0.7%	3.7%	2.8%
CZ12	EC	39,384	28,159	67,543	4,554	5,796	10,349	□	□	□	□
	EC+NV	32,645	32,421	65,066	4,323	5,480	9,803	17.1%	3.7%	5.5%	5.3%
CZ13	EC	53,766	26,576	80,341	5,347	5,998	11,345	□	□	□	□
	EC+NV	46,885	30,750	77,634	5,135	5,803	10,938	12.8%	3.4%	3.3%	3.6%
CZ14	EC	82,079	28,775	110,854	17,395	2,571	19,967	□	□	□	□
	EC+NV	75,875	32,889	108,764	17,011	2,560	19,571	7.6%	1.9%	0.4%	2.0%
CZ15	EC	120,647	31,922	152,569	23,066	3,038	26,104	□	□	□	□
	EC+NV	115,031	36,320	151,351	22,772	3,036	25,808	4.7%	0.8%	0.1%	1.1%
CZ16	EC	24,292	22,716	47,008	7,574	1,815	9,390	□	□	□	□
	EC+NV	20,235	25,150	45,385	7,145	1,772	8,917	16.7%	3.5%	2.4%	5.0%



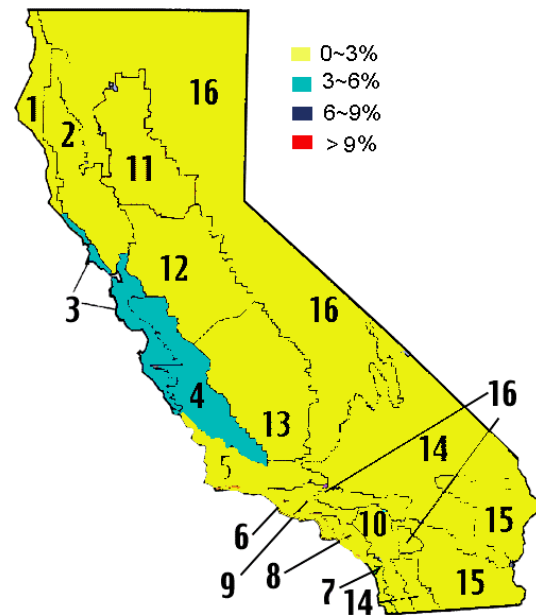
a. Office



b. Retail Store



c. School Class Wing



d. Restaurant

Figure 4.4: Cost savings in California for different buildings

4.3 Impact of Fan Efficiency

Fan and fan motor efficiencies have a very significant effect on the savings potential for night ventilation. Fan power for packaged air conditioning equipment generally varies between about 0.2 W/cfm and 0.7 W/cfm. A value of 0.7 W/cfm typically corresponds to a unit with a very low fan efficiency (e.g., 10%).

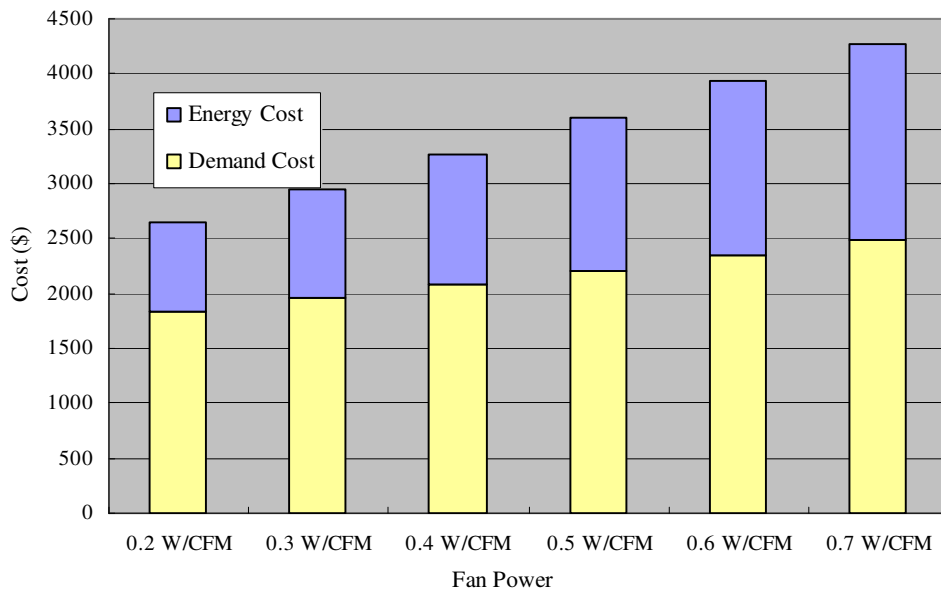
Table 4.5 gives annual results for the small office building where the supply air fan power has been cut in half to 0.25 W/cfm. In this case, the maximum energy, demand, and cost savings are about 15%, 22%, and 19 %. Thus, it is important to utilize efficient fans and fan motors in combination with night ventilation precooling. Even greater savings would be possible if efficient, variable-speed fan motors were employed.

Fig. 4.5a and 4.5b give comparisons of total cost and savings percentage for night ventilation precooling as a function of fan power for the small office building model in CZ04 climate (utility provided by PGE). The total costs (electricity energy cost + demand costs) are very sensitive to the fan efficiency. For this utility rate, the demand charge is quite high, but the energy charge is fairly low so that the demand cost is the majority of total cost. The percentage savings in total cost decreases almost linearly with the fan power (efficiency).

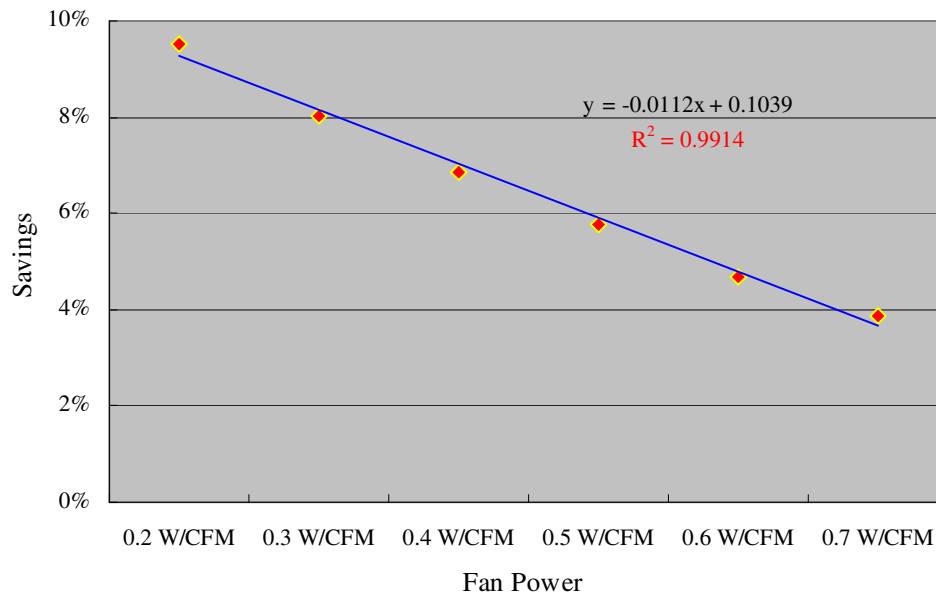
Fig. 4.6a and 4.6b give the same comparisons for the office in CZ06 (utility provided by SCE). Since SCE's demand charge rate is low and its energy charge rate is much higher than PGE, energy costs are the major part of the total costs. Overall, the savings are lower than for CZ04, but are significant when efficient fans are employed.

Table 4.5: Night ventilation air conditioning savings for school class wing
(supply fan power of 0.25 W/cfm)

Climate	Control	Comp. (kWh)	Fan (kWh)	Elec. (kWh)	Elec. Cost (\$)	Dem. Cost (\$)	Total Cost (\$)	Comp. Sav. (%)	Elec. Sav. (%)	Dem. \$ Sav. (%)	Cost \$ Sav. (%)
CZ01	EC	725	3,620	4,345	287	860	1,147	□	□	□	□
	EC+NV	341	3,879	4,220	266	669	935	53.0%	2.9%	22.2%	18.5%
CZ02	EC	17,290	7,158	24,448	1,721	2,873	4,594	□	□	□	□
	EC+NV	14,131	8,322	22,453	1,582	2,799	4,381	18.3%	8.2%	2.6%	4.6%
CZ03	EC	6,031	4,372	10,403	727	1,577	2,303	□	□	□	□
	EC+NV	3,394	5,424	8,819	595	1,463	2,058	43.7%	15.2%	7.2%	10.6%
CZ04	EC	9,449	5,537	14,986	1,041	2,019	3,060	□	□	□	□
	EC+NV	6,486	6,690	13,176	899	1,893	2,792	31.4%	12.1%	6.2%	8.8%
CZ05	EC	6,199	5,853	12,052	813	2,181	2,994	□	□	□	□
	EC+NV	4,425	6,495	10,920	718	2,025	2,743	28.6%	9.4%	7.2%	8.4%
CZ06	EC	17,478	5,583	23,061	3,854	771	4,625	□	□	□	□
	EC+NV	14,283	6,919	21,202	3,571	762	4,334	18.3%	8.1%	1.2%	6.3%
CZ07	EC	13,967	6,665	20,632	2,050	1,043	3,094	□	□	□	□
	EC+NV	12,205	8,050	20,255	2,002	1,065	3,067	12.6%	1.8%	-2.1%	0.9%
CZ08	EC	17,760	5,968	23,729	3,937	780	4,716	□	□	□	□
	EC+NV	15,136	7,060	22,196	3,691	767	4,458	14.8%	6.5%	1.7%	5.5%
CZ09	EC	19,118	6,037	25,155	4,210	862	5,072	□	□	□	□
	EC+NV	15,965	7,239	23,205	3,905	851	4,756	16.5%	7.8%	1.3%	6.2%
CZ10	EC	22,893	7,005	29,898	5,055	1,025	6,080	□	□	□	□
	EC+NV	19,290	8,266	27,557	4,701	1,007	5,707	15.7%	7.8%	1.8%	6.1%
CZ11	EC	25,023	8,839	33,862	2,306	3,532	5,838	□	□	□	□
	EC+NV	21,449	10,689	32,138	2,191	3,441	5,632	14.3%	5.1%	2.6%	3.5%
CZ12	EC	19,795	7,383	27,179	1,898	2,965	4,863	□	□	□	□
	EC+NV	16,068	8,875	24,944	1,747	2,854	4,601	18.8%	8.2%	3.7%	5.4%
CZ13	EC	26,315	6,963	33,278	2,277	3,124	5,401	□	□	□	□
	EC+NV	21,943	8,526	30,469	2,105	3,025	5,131	16.6%	8.4%	3.2%	5.0%
CZ14	EC	34,236	7,771	42,007	6,857	1,151	8,008	□	□	□	□
	EC+NV	30,596	9,538	40,134	6,610	1,144	7,754	10.6%	4.5%	0.6%	3.2%
CZ15	EC	49,576	8,593	58,170	9,008	1,333	10,341	□	□	□	□
	EC+NV	46,266	10,491	56,758	8,804	1,331	10,135	6.7%	2.4%	0.2%	2.0%
CZ16	EC	10,197	6,579	16,776	2,917	815	3,732	□	□	□	□
	EC+NV	8,269	7,504	15,773	2,724	798	3,522	18.9%	6.0%	2.1%	5.6%

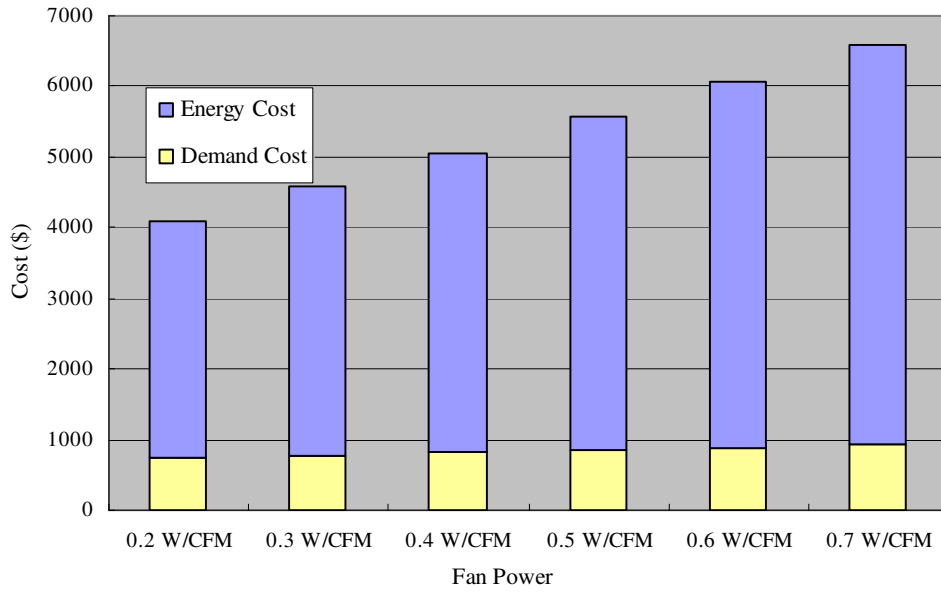


a.) Impact of fan efficiency on costs

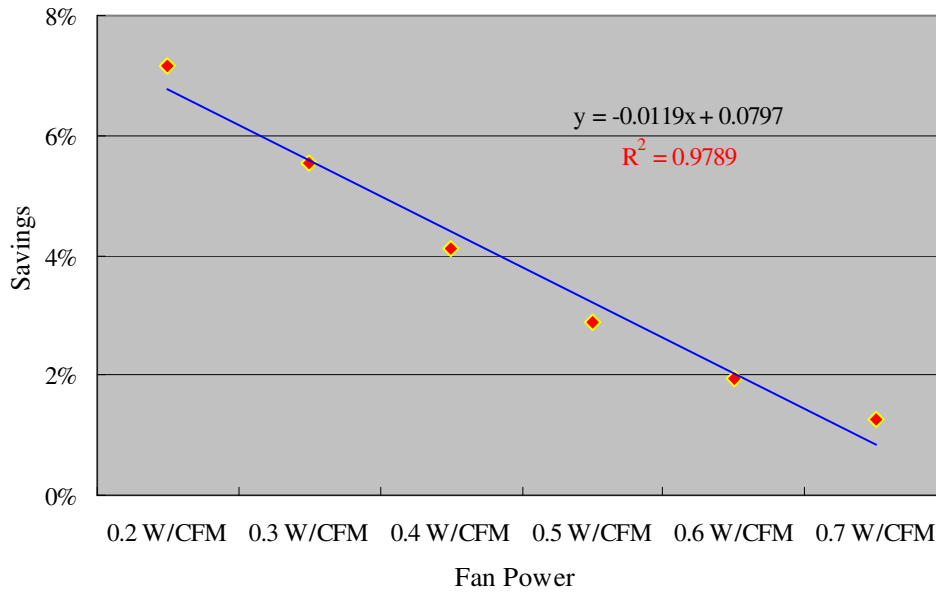


b.) Impact of fan efficiency on saving percentages

Fig. 4.5: Impact of fan efficiency on costs and savings for night ventilation precooling (Office, CZ04, PG&E)



a.) Impact of fan efficiency on costs



b.) Impact of fan efficiency on savings percentages

Fig. 4.6: Impact of fan efficiency on costs and savings for night ventilation precooling (Office, CZ06, SCE)

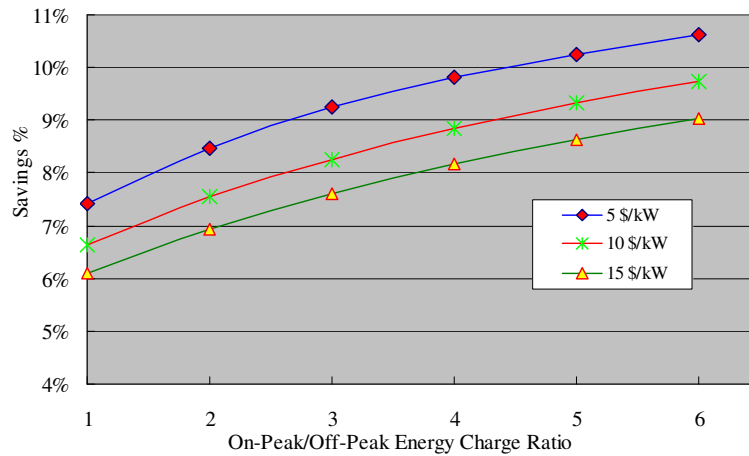
4.4 Impact of Utility Rates

The major utility providers in California (PGE and SCE) have very different utility rates. For the results previously presented, simulations were performed using utility rates for the most common providers in each of the climate zones. In order to separate the effects of climate and utility rates, the effect of energy and demand rates are considered for a single building type (office) and climate zone (CZ04) where a significant potential exists for night ventilation precooling. In order to study this issue, on-peak energy and demand rates were varied for three different cases: 1) equal mid-peak and off-peak rates, 2) mid-peak rates that are halfway between on-peak and off-peak rates, and 3) equal mid-peak and on-peak rates. The off-peak energy charge was fixed at 0.05\$/kWh, whereas the off-peak demand charge was 2.5\$/kW. Table 4.6 describes the three different utility rate structures that were considered with example values. On-peak demand charges of 5\$/kW, 10\$/kW and 15\$/kW were considered and the ratio of on-peak to off-peak energy charges were varied from 1 to 6.

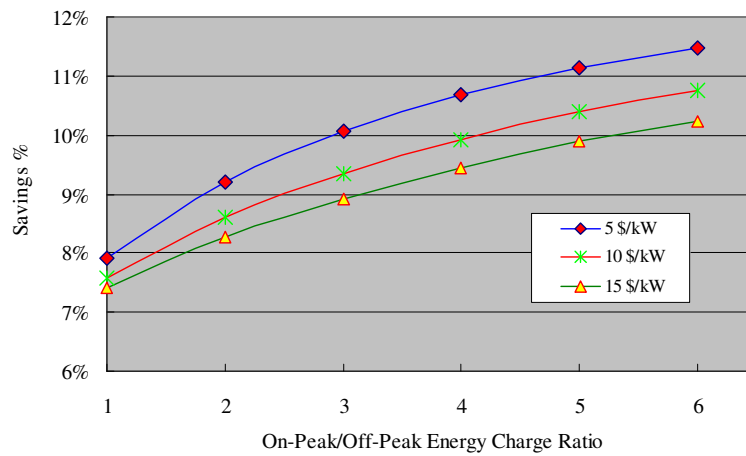
Table 4.6: Utility structure under comparison
(example for on-peak/off-peak energy charge ratio=3, on-peak demand charge=10\$/kW)

Schedule	Summer	Apr.1-Nov.30		Winter	Dec.1-Mar 31	
	Off-Peak	9:00 PM ~ 8:00 AM		Off-Peak	9:00 PM ~ 8:00 AM	
	Mid-Peak	6:00 PM ~ 9:00 PM 8:00 AM ~ 12:00 PM		Mid-Peak	8:00 AM ~ 9:00 PM	
	On-Peak	12:00 PM ~ 6:00 PM		On-Peak	Not Available (N/A)	
Utility	Summer	Enrg. Charge (\$/kWh)	Dmnd. Charge (\$/kW)	Winter	Enrg. Charge (\$/kWh)	Dmnd. Charge (\$/kW)
Rate 1	Off-Peak	0.05	2.5	Off-Peak	0.05	2.5
[Mid-Peak = Off-Peak]	Mid-Peak	0.05	2.5	Mid-Peak	0.05	2.5
	On-Peak	0.15	10	On-Peak	N/A	N/A
Rate 2	Off-Peak	0.05	2.5	Off-Peak	0.05	2.5
[Mid-Peak = ½ (Off-Peak + On-Peak)]	Mid-Peak	0.10	6.25	Mid-Peak	0.10	6.25
	On-Peak	0.15	10	On-Peak	N/A	N/A
Rate 3	Off-Peak	0.05	2.5	Off-Peak	0.05	2.5
[Mid-Peak = On-Peak]	Mid-Peak	0.15	10	Mid-Peak	0.15	10
	On-Peak	0.15	10	On-Peak	N/A	N/A

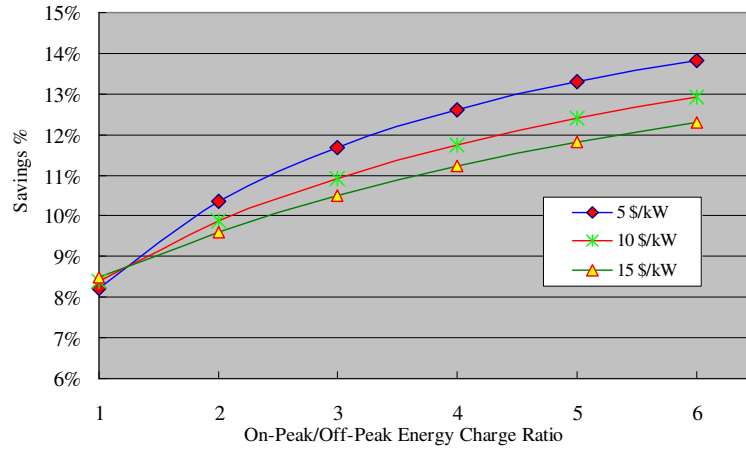
Fig. 4.7 shows the impact of utility rates on savings for the office building in CZ04 (default parameters except for the utility rate follows Table 4.6). The percent savings increase with the ratio of on-peak to off-peak energy charges in all three cases and the relative savings are larger for longer on-peak periods (Rate 3 vs. Rate1) or higher mid-peak rates. Somewhat surprisingly, the percent savings decrease with increase on-peak demand charges. However, the absolute savings increase with the demand charge. It's just that the savings relative to the base case decrease because the base case costs also increase with demand charge.



a: equal mid-peak and off-peak rates (Rate1)



b: mid-peak rates halfway between on-peak and off-peak rates (Rate2)



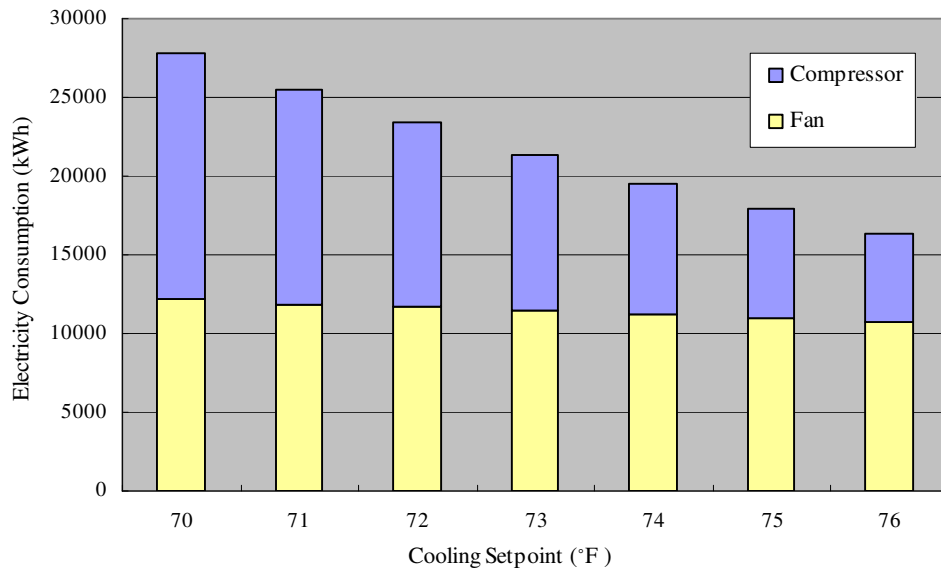
c: equal mid-peak and on-peak rates (Rate3)

Fig. 4.7c: Impact of utility rates on night ventilation precooling savings

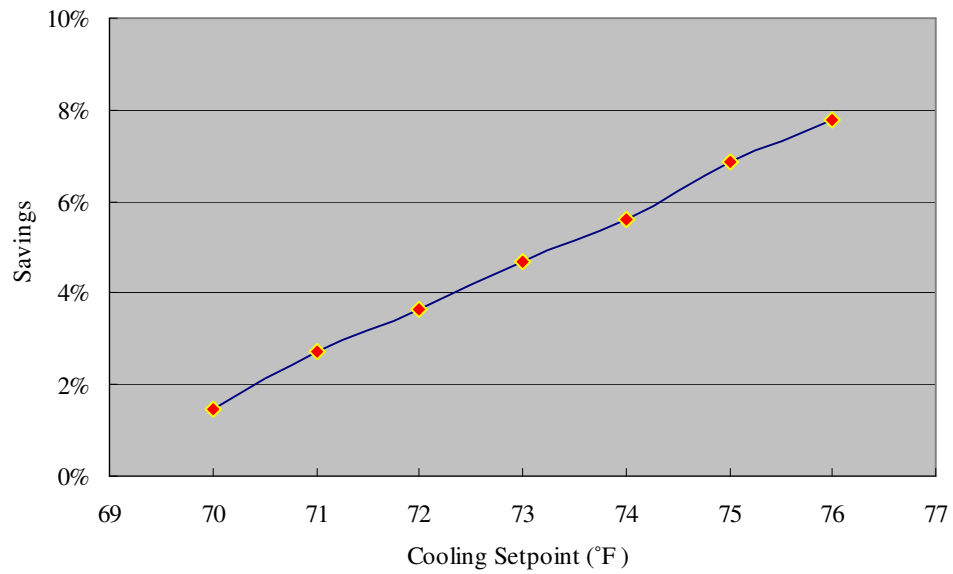
4.5 Impact of Occupied Period Cooling Setpoint

The cooling setpoint during the occupied period has a large impact on the savings associated with night ventilation precooling. Increasing the cooling setpoint can delay the startup of mechanical cooling and utilize building thermal mass when it's most effective in the early part of the occupied period.

Generally, the comfort region includes cooling setpoints between about 70°F and 76°F. For this range, Fig. 4.8a shows the effect of occupied period setpoint for cooling on the compressor and total energy for cooling associated with the night ventilation algorithm applied to the office in CZ04. A higher cooling setpoint leads a reduction in the compressor energy consumption because of two effects: 1) reduced gains to the space and 2) greater energy storage capacity of the thermal mass in response to night ventilation. Fig. 4.8b gives relative savings as a function of the occupied period setpoint. To make the comparison fair, the occupied period setpoint for the base case was also varied. For this example, the savings are sensitive to the setpoint varying between about 2% and 8%.



a. night ventilation energy consumption



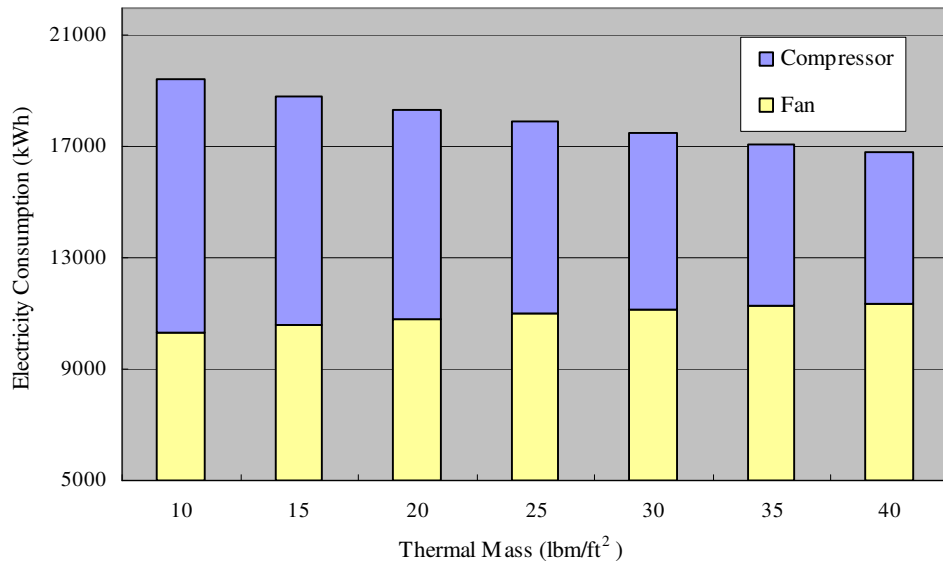
b. night ventilation cost savings

Fig. 4.8: Impact of occupied period cooling setpoint on energy consumption and savings for night ventilation precooling (office, CZ04)

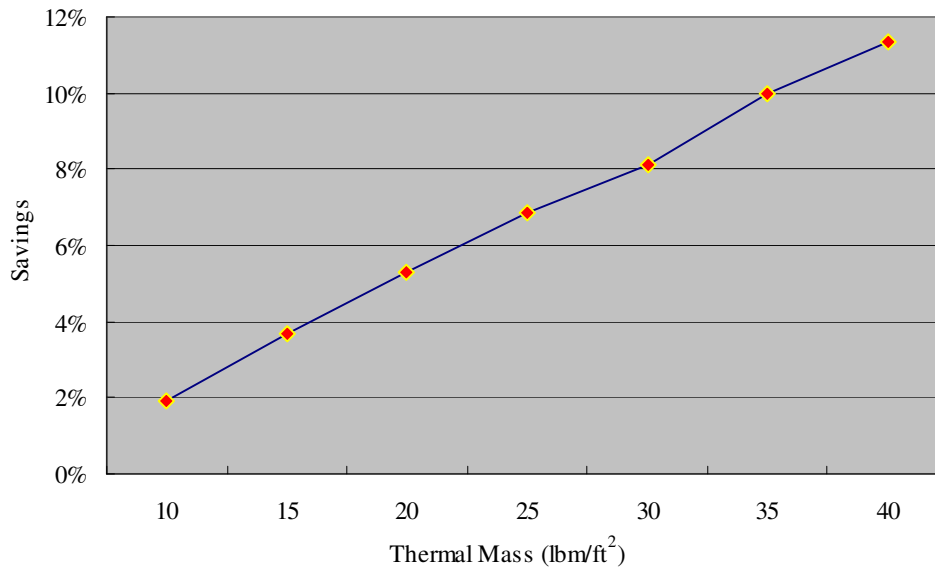
4.6 Impact of Internal Thermal Mass Level

Internal thermal mass includes interior partition walls, furniture and the other materials inside the zone except the exterior building structure. Internal thermal mass is modeled within VSAT using a single lumped element with a default value of 25 lbm per square foot of floor area. Simulations were performed to study the influence of internal thermal mass for the office building located in CZ04.

Fig. 4.9a shows the effect of internal thermal mass on compressor, fan, and total energy usage associated with night ventilation precooling. The fan energy increases slightly with thermal mass because it takes longer for the building mass to be precooled and therefore the fan cycles less during the precooling period. This increase is more than offset by a decrease in compressor energy so that the total energy consumption decreases with internal thermal mass. Higher levels of internal thermal mass also lead to higher savings in total electrical costs as shown in Fig. 4.9b. These results indicate that the savings are very sensitive to internal thermal mass.



a. Impact of thermal mass on electricity consumption



b. Impact of thermal mass on savings percentage

Fig. 4.9: Impact of thermal mass level on energy consumption and savings for night ventilation precooling (office, CZ04)

4.7 Impact of Ground Coupling and Carpeting

The presence of a carpet has a strong impact on heat transfer for a floor slab. Fig. 4.10 shows a comparison of the heat transfer rates with and without a carpet determined using FEHT for a typical day with night ventilation precooling. Fig. 4.10 indicates that carpet has a significant effect on the rates at which energy can be added or removed from the floor turning a typical diurnal cycle.

To further investigate the effects of carpet and pea gravel, system simulations was carried out for the retail store in CZ04. Table 4.6 gives compressor and fan energy consumption for different slab-ground descriptions for the base case and night ventilation strategies. The pea-gravel has a slight effect on the energy usage for both the base and night ventilation cases. For the base case, the carpet also has a relatively small impact on energy usage. However, the carpet does have a significant impact on energy usage for the night ventilation case. This is because the slab floor represents a significant part of the building thermal storage and the carpet impedes heat transfer between the air and the concrete.

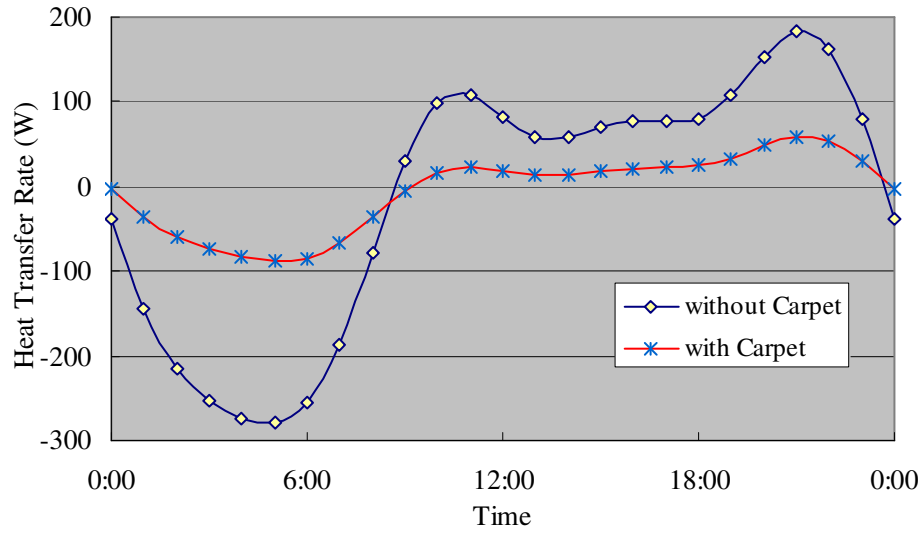


Fig. 4.10: Slab ground heat transfer condition for night ventilation precooling with/without carpet (retail store, CZ04)

Table 4.7: Comparison of the energy consumption under different slab ground conditions (retail store, CZ04)

Slab Ground Condition	EC		NV+EC	
	Compressor (kWh)	Fan (kWh)	Compressor (kWh)	Fan (kWh)
without carpet, only soil	104105	175770	70173	198097
without carpet, with gravel	103920	175710	69789	198156
with carpet, with gravel	106263	178819	80595	197286

5. Prototype Development and Implementation

5.1 General description

A simplified version of the control algorithm described in section 2 was implemented and tested at two field sites. Figure 5.1 shows the measured variables that are used with the ventilation precooling algorithm. These include the ambient temperature (T_{amb}) and relative humidity (H_{amb}), zone temperature (T_z), return air temperature (T_{ra}), and supply air temperature (T_{sa}). When night ventilation precooling is enabled, the damper opens and the fan operates to precool the zone at a prescribed setpoint.

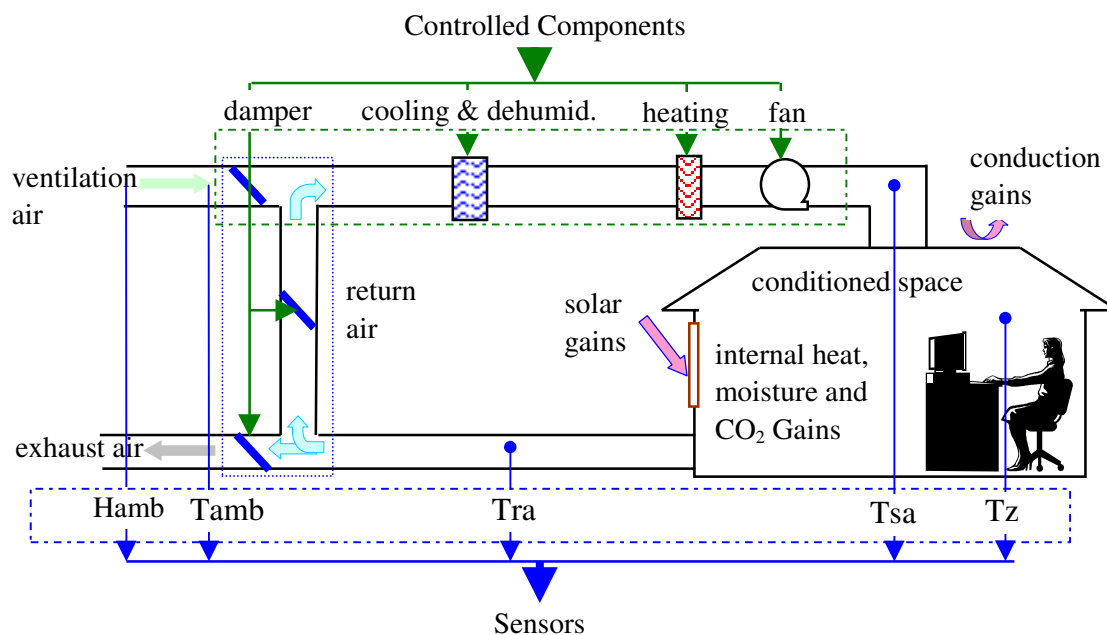


Figure 5.1: Controller input variables

The control algorithm was implemented within an FDSI Virtual Mechanic (VM) platform. The VM interfaces to a Honeywell economizer and DCV controller as depicted in Figure 5.2. The DCV controller normally utilizes the thermostat outputs along with DCV and economizer input measurements to determine the status of the fan, primary cooling and heating equipment, and the damper position. When ventilation precooling is enabled, the VM provides an override to the Honeywell controller, which then provides the primary control signals for opening the damper and turning on the fan. Sensor information from the DCV controller is fed back to the VM for use in the precooling algorithm. The

VM also incorporates a network and modem connection for downloading data from the site.

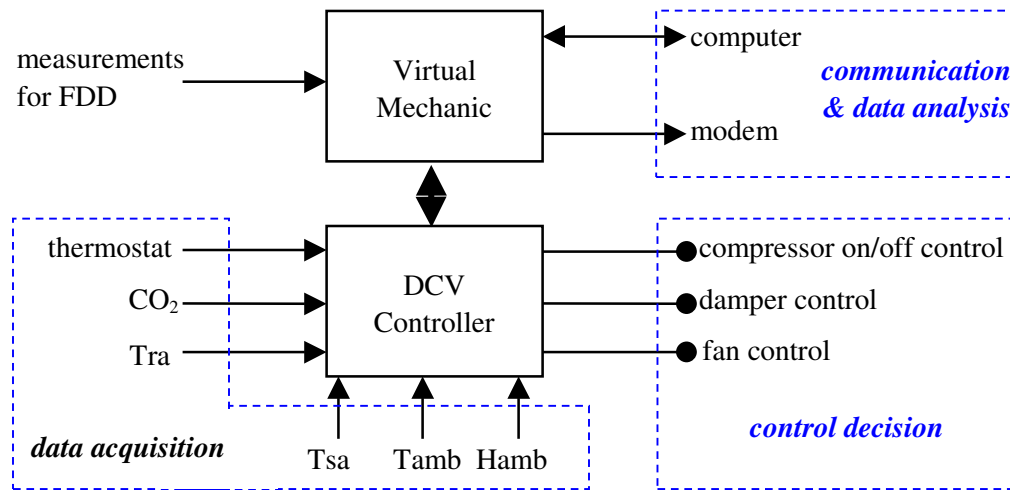


Figure 5.2: Interface between VM and DCV controller

The zone temperature is not measured directly by the VM or DCV controller, but is assumed to be equal to the return air temperature. However, the return air temperature is only an accurate indicator of the zone temperature when the fan is operating. As a result, it is necessary to turn on the fan at night to sample the return air temperature in order to evaluate whether night ventilation precooling should be enabled.

5.2 Description of the main control variables

This section describes the main variables utilized within the software that is implemented in the VMs. In addition to night ventilation, the algorithm allows for mechanical precooling. However, this feature can be disabled remotely.

In the control program, there are 5 sensor channels that collect data for the aim of night ventilation control, namely:

Tamb: ambient dry-bulb temperature;
Hamb: ambient relative humidity;
Tz: zone dry-bulb temperature;
Tra: return air dry-bulb temperature;
Tsa: supply air dry-bulb temperature.

There are 3 controlled components that have the following states:

FanState: state of the fan, Normal/On;
DamperState: state of the damper, Normal/Open/Closed;
CoolState; state of the mechanical cooling machine Normal/On;

The Normal state refers to a normal control condition in the absence of an override from the VM.

During night ventilation, there are four control states, namely:

CS_FANSAMPLING: start the fan and circulate air to sample the return air temperature;
CS_VENT: night ventilation precooling working condition;
CS_MECH: mechanical precooling working condition;
CS_NORMAL: normal working condition (setback), when night ventilation or mechanical precooling is not permitted;

The possible component states under different control states are listed in Table 5.1. Fan sampling is needed before a night ventilation or mechanical precooling decision is made. In the fan sampling mode, the RTU compressor is off, the fan is on, and the outdoor air damper is closed. If all the requirements for night ventilation are met, then the control state is locked in ventilation mode, and mechanical precooling is locked out for the remaining hours before the occupancy. If the night ventilation requirements can not be met, then mechanical precooling could be activated in the early morning, unless it is disabled. In mechanical precooling, the fan is on, the outdoor air damper is closed, and the RTU operates to maintain a prescribed zone temperature setpoint. When neither ventilation nor mechanical precooling is activated, the control state is set to normal.

Table 5.1: Component states under different control states

Control	Fan	Damper	Cool State	Operate
Sampling	ON	Closed	Normal	Sampling
Vent	ON	Open(damper open)	Normal	Vent
Mech	ON	Close(damper 100% closed)	ON (full cooling capacity)	Mech
Normal	Normal	Normal	Normal	Normal

There is an alarm mechanism to safeguard the system when problems happen such as the precooling condition is not met, or a sensor has failed. The 9 alarms are:

ALM_FREEZE_DANGER: Danger of freezing
 ALM_HIGH_HUMIDITY: High ambient humidity;
 ALM_SUFFICIENT_VENT_CAPACITY_TOACHIEVE_SETPOINT:
 This alarm will shut down ventilation precooling if the temperature difference between the return and ambient air is too low for a sufficiently long period of time. No more fan sampling will occur for the rest of the night.
 ALM_MECH_COLDOUTSIDE: Too cold for applying mechanical cooling;
 ALM_TZ_ERROR: Zone temperature sensor failure;
 ALM_TAMB_ERROR: Ambient temperature sensor failure;
 ALM_HAMB_ERROR: Humidity sensor failure;
 ALM_HEAT_DELTAT: The smallest ΔT for night ventilation;
 ALM_HEAT_DIGIN: User demand for heating after precooling.

There are four possible system responses to an alarm, from least severe to worst:

AS_CLEARED: confirmed OK, do not need another response, clear alarm;
 AS_PENDING: don't know, waiting for information;
 AS_WAITING: suspected danger;
 AS_LATCHED: confirmed danger.

The following defaults for the precooling schedule are implemented:

Mechanical precooling: start time 4:00 AM
 Ventilation precooling: start time 12:00 AM
 Warmup period: start time 7:00 AM

These variables can be changed remotely. In addition, default values for some other control variables are:

freezeLimitAmbientTemperature = 50 °F

maximumAmbientHumidity	= 55 °F (dewpoint temperature)
ventEnableSetpointTempDiff	= 10 °F
mechMinAmbientTemperature	= 60 °F
enableTzSetpoint	= 67 °F
disableTzSetpoint	= 67 °F
enableDeltaTSetpoint	= 10 °F
disableDeltaTSetpoint	= 6 °F

5.3 Description of control algorithm

In the first step, the ventilation and mechanical precooling scheduling is evaluated as depicted in Figures 5.3 and 5.4.

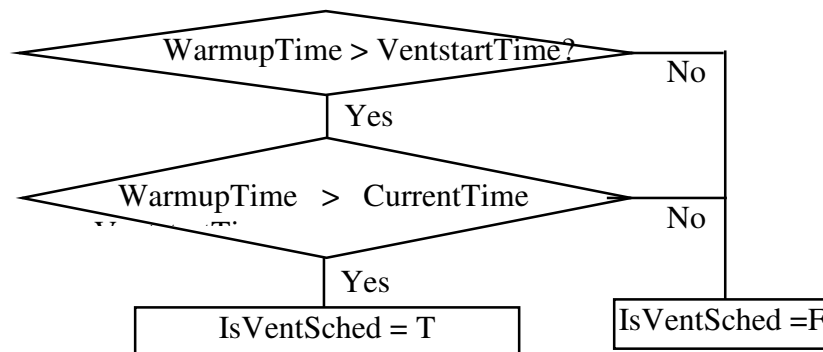


Figure 5.3: Scheduling condition for Night Ventilation Precooling

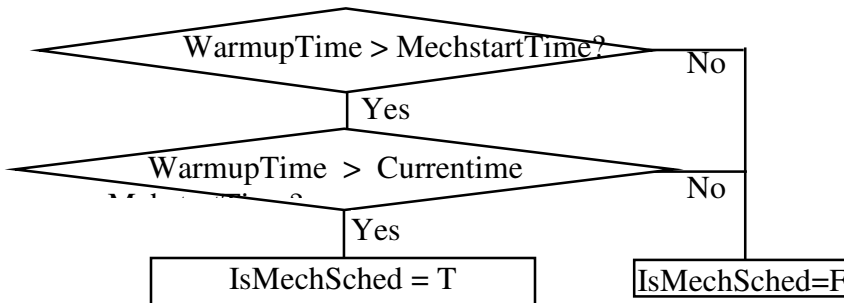


Figure 5.4: Scheduling condition for Mechanical Precooling

In the second step, the thermal conditions for ventilation and mechanical precooling are evaluated as shown in Figures 5.5 and 5.6. The specific conditions used in the evaluations are configurable with defaults shown in these figures.

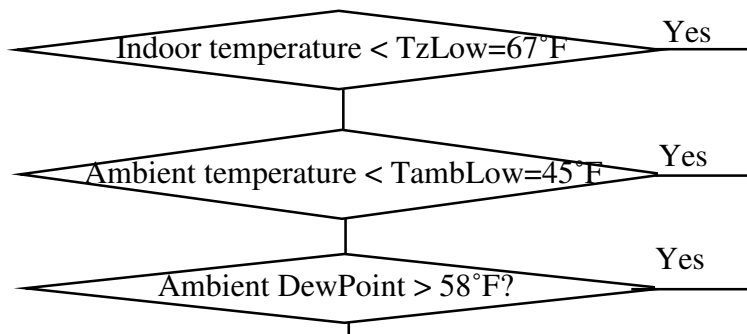


Figure 5.5: The flow diagram for Night Ventilation thermal conditions

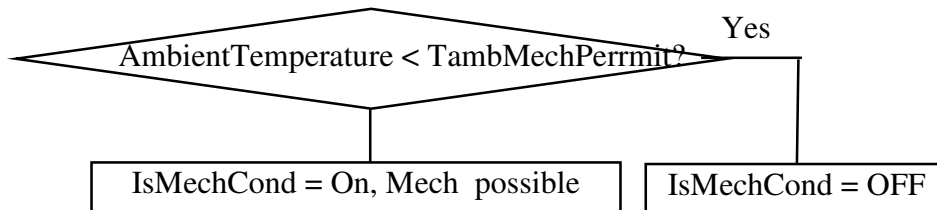


Fig. 5.6: The flow diagram for evaluating Mechanical Precooling thermal conditions

Both the scheduling and thermal conditions must be satisfied for precooling to occur. For multiple RTUs at a site, each VM operates independently to enable ventilation or mechanical precooling.

5.4 Logic simulation tests

Prior to implementation, logic simulations were applied to test the precooling control algorithm through time with constant inputs. The results of these tests are also useful in understanding implementation of the algorithm and will be presented in this section. Three working conditions were considered: 1. wet and cold ambient condition, in which both precooling should not be applied; 2. dry and cool ambient condition, in which ventilation precooling should be applied; and 3. wet and warm ambient condition, in which mechanical precooling should be applied.

1. Wet and cold ambient conditions

Given a condition where $T_z = T_{ra} = 72^\circ\text{F}$, ambient dewpoint $= 48^\circ\text{F}$, and $T_{amb} = 50^\circ\text{F}$, the ambient is too cold for either night ventilation or mechanical precooling. Table 5.2 shows control variables at different times for this situation. At 2:00 AM, the night ventilation schedule is satisfied, $IsVentSched = T$. Then, the system turns on the fan for sensor

sampling, $RequestSensorSampling=T$, and the states of the Tz, Tamb, and Hamb sensor error alarms change from Cleared to Pending, so that $State(Tz\ Error)$, $State(Tamb\ Error)$, $State(Hamb\ Error) = Pending$. The freeze danger, high ambient humidity and sufficient ventilation alarms also change from Cleared to Pending, $State(Freeze\ Danger)$, $State(High\ Humidity)$, $State(Sufficient\ vent\ capacity)=Pending$. The system changes to a fan sampling condition, $operateState=Fan\ Sampling$, the fan is on, $Fanstate=on$, the damper is closed, $damperState=closed$ and $fan\ Verify=T$. Accordingly, Tz, Tamb and Hamb are sampled and the alarm for sensor reading data error is cleared. After the data are acquired, $State(Freeze\ Danger)$, $State(High\ humidity)=Waiting$. Since the ambient dry bulb temperature is too low, the system will set the State(Freeze Danger) to Latched and night ventilation will not be applied during this night.

At 4:00 AM, the Mechanical cooling schedule is satisfied, $IsMechSched=T$, then a request is sent to turn on the fan for the sensor sampling, $requestSensorSampling=T$, and the alarm to detect whether the ambient is too cold to apply mechanical precooling is in a waiting state, $State(Too\ Cold\ Mech)=Waiting$. Since the ambient temperature is too cold, $State(Too\ Cold\ Mech)=Latched$, so mechanical precooling will not be applied during this unoccupied period.

At 8:00AM, the system goes back to a normal working condition. The mechanical and ventilation precooling schedule expires, $IsMechSched$, $IsVentSched= False$, and all the alarms are cleared. FanState, CoolingState, DamperState, ControlState and OperateState are all set to normal during the occupied hours.

2. Dry and cool ambient conditions

Given a condition where $Tz=Tra=72^{\circ}F$, ambient dewpoint= $32^{\circ}F$, and $Tamb=58^{\circ}F$, the ambient is appropriate for the night ventilation precooling. Table 5.3 gives control variables at different times for this case. At 2:00 AM, the night ventilation schedule is satisfied, $IsVentSched=T$, then $requestSensorSampling=T$ (system request for the fan to turn on for sampling), and the states of Tz, Tamb, and Hamb sensor error alarms change from Cleared to Pending, so that $State(Tz\ Error)$, $State(Tamb\ Error)$, $State(Hamb\ Error)=Pending$. The freeze danger, high ambient humidity and sufficient ventilation alarms also change from Cleared to Pending, $State(Freeze\ Danger)$, $State(High\ Humidity)$, $State(Sufficient\ vent\ capacity)=Pending$. Accordingly, the system changes to a fan sampling condition, $operateState=Fan\ Sampling$, and the fan is on, $Fanstate=on$, the

damper is closed, *damperState=closed*, and *fan Verify=T*. *Tz*, *Tamb* and *Hamb* are measured and the alarms for sensor reading data errors are cleared. Once the data are acquired, then the conditions are met for ventilation precooling and *State(Freeze Danger)*, *State(High humidity)*, *State(Sufficient vent capacity) =cleared*. In this case, both the schedule requirement and the thermal condition requirement are met, and *controlState=Vent*, *operateState=Vent*, *fanstate=on*, *damperState=Open*, *coolstate=Normal*.

At 4:00 AM, the Mechanical cooling schedule is satisfied, *IsMechSched=T*, while the system is running, so that fan sampling is not needed, *requestSensorSampling=F*. Since ventilation precooling is on, mechanical precooling will not be applied. The states *controlState=Vent*, *operateState=Vent*, *fanstate=on*, *damperState=Open*, *coolstate=Normal* will keep their values until just prior to occupancy.

At 8:00AM, the system returns to its normal operating condition. *IsMechSched* and *IsVentSched* are set back to False, and all the alarms are cleared. *fanState*, *coolingState*, *damperState*, *controlState* and all operating states are set to Normal during the occupied period.

3. Wet and warm ambient conditions

Given a condition where *Tz=Tra=72°F*, ambient dewpoint=*62°F*, and *Tamb=65°F*, the ambient conditions are appropriate for mechanical precooling. Table 5.4 shows control variables for this case. At 2:00 AM, the night ventilation schedule is satisfied, *IsVentSched=T*, then *requestSensorSampling=T*, *State(Tz Error)*, *State(Tamb Error)*, *State(Hamb Error)=Pending*, and *State(Freeze Danger)*, *State(High Humidity)*, *State(Sufficient vent capacity)=Pending*. The system changes to a fan sampling condition, *operateState=Fan Sampling*, the fan is on, *Fanstate=on*, and the damper closes, *damperState=closed*, so *fan Verify=T*. Accordingly, *Tz*, *Tamb* and *Hamb* are sampled and the alarm for a sensor reading data error is cleared. Once the data are acquired, the alarms *State(Freeze Danger)= Cleared*, *State(High humidity)=Waiting*, *State(Sufficient vent capacity) =Waiting*. For this example, the humidity is too high, so the high humidity alarm responds, *State(High humidity)=Latched*. Since the high humidity is latched, the system will not attempt to apply night ventilation anymore during the unoccupied period and *controlState=Normal*, *operateState=Normal*, *fanstate=OFF*, *damperState=Closed*, *coolstate=Normal*.

At 4:00 AM, the Mechanical cooling schedule is satisfied, *IsMechSched=T*, the system requests fan sampling, *requestSensorSampling=T*. Since both the schedule and the thermal condition requirements are met, mechanical precooling will be applied: *controlState=Mech, operateState=Mech, fanstate=on, damperState=Closed, coolstate=On*.

At 8:00AM, the system returns to its normal operating condition. *IsMechSched* and *IsVentSched* are set back to False, and all the alarms are cleared. The *fanstate*, *coolingstate*, *damperstate*, *controlstate* and *operate state* are all set to normal during occupancy.

Table 5.2: Control variables for a wet and cold ambient condition

Time	2:00:00	2:00:00	2:00:00	2:00:00	2:00:00	2:00:00	2:00:00	2:00:00	2:03:15	2:03:15	2:03:15	2:03:15	2:03:15	2:03:15	2:18:15	4:00:00	4:00:00	4:15:00	8:00:00	8:00:00	8:00:00
IsVentSched	T	T	T	T	T	T	T	T	T	T	T	T	T	T	T	T	T	T	F	F	F
IsMechSched	F	F	F	F	F	F	F	F	F	F	F	F	F	F	F	T	T	T	T	F	F
ControlState	Nml																				
OperateState	Nml	Smplg																			
FanState	Nml	On																			
DamperState	Nml	Closed																			
CoolState	Nml																				
FanVerify	F	F	F	F	F	F	F	F	T	T	T	T	T	T	T	T	T	T	T	T	T
Sensor Sampling	F	T	T	T	T	T	T	T	T	T	T	T	T	T	T	F	T	T	F	F	F
Value(Tz)	Err	72	72	72	72	72	72	72	72	72	72	72	72	72							
Value(Tamb)	Err	50	50	50	50	50	50	50	50	50	50	50	50								
Value(Hamb-Dewp)	Err	48	48	48	48	48	48	48	48	48	48	48									
Value(Tra)	Err																				
Value(Tsa)	Err																				
State(Tz Err)	Clr	Pnd	Clr																		
State(Tamb Err)	Clr	Clr	Pnd	Clr																	
State(Hamb Err)	Clr	Clr	Clr	Pnd	Clr																
State(Freeze Danger)	Clr	Clr	Clr	Clr	Pnd	Wting	Wting	Wting	Ltch	Ltch	Ltch	Ltch	Ltch	Ltch							
State(High Hamb)	Clr	Clr	Clr	Clr	Clr	Pnd	Wting														
State(Sufficient vent capacity)	Clr	Clr	Clr	Clr	Clr	Clr	Pnd	Clr													
State(TooColdMech)	Clr	Wting	Ltch	Ltch	Ltch	Clr															
State(Heat DeltaT)	Clr																				
State(Heat Digin)	Clr																				

Note: Clr--Cleared, Pnd--Pending, Wting--Waiting, Ltch--Latched, Err--Error, T--True, F--Fall, Nml--Normal, Smplg--Fan Sampling

Table 5.3: Control variables for a dry and cold condition

Time	2:00:00	2:00:00	2:00:00	2:00:00	2:00:00	2:00:00	2:00:00	2:00:00	2:03:15	2:03:15	2:03:15	2:03:15	2:03:15	2:03:15	2:05:00	4:00:00	8:00:00	8:00:00	8:00:00
isVentSched	T	T	T	T	T	T	T	T	T	T	T	T	T	T	T	T	F	F	F
isMechSched	F	F	F	F	F	F	F	F	F	F	F	F	F	F	F	T	T	F	F
controlState	Nml	Vent	Vent	Vent	Vent	Nml													
operateState	Nml	Smplg	Vent	Vent	Vent	Vent	Nml												
fanState	Nml	On	Nml																
damperState	Nml	Closed	Open	Open	Open	Open	Nml												
coolState	Nml																		
fanVerify	F	F	F	F	F	F	F	F	T	T	T	T	T	T	T	T	T	T	T
Sensor Sampling	F	T	T	T	T	T	T	T	T	T	T	T	T	T	T	T	F	F	F
Value(Tz)	Err	72	72	72	72	72	72	72	72	72	72	72							
Value(Tamb)	Err	58	58	58	58	58	58	58	58	58	58	58							
Value(Hamb-Dewp)	Err	32	32	32	32	32	32	32	32	32	32								
Value(Tra)	Err																		
Value(Tsa)	Err																		
State(Tz Error)	Clr	Pnd	Clr																
State(Tamb Error)	Clr	Clr	Pnd	Pnd	Pnd	Pnd	Pnd	Pnd	Clr										
State(Hamb Error)	Clr	Clr	Clr	Pnd	Pnd	Pnd	Pnd	Pnd	Pnd	Clr									
State(Freeze Danger)	Clr	Clr	Clr	Clr	Pnd	Clr													
State(High Hamb)	Clr	Clr	Clr	Clr	Clr	Pnd	Clr												
State(Sufficient vent capacity)	Clr	Clr	Clr	Clr	Clr	Clr	Pnd	Clr	Clr	Clr	Clr	Clr	Clr						
State(TooColdMech)	Clr																		
State(Heat DeltaT)	Clr																		
State(Heat Digin)	Clr																		

Note: Clr--Cleared, Pnd--Pending, Wting--Waiting, Ltch--Latched, Err--Error, T--True, F--Fall, Nml--Normal, Smplg--Fan Sampling

Table 5.4: Control variables for a wet and warm condition

Time	2:00:00	2:00:00	2:00:00	2:00:00	2:00:00	2:00:00	2:00:00	2:00:00	2:03:15	2:03:15	2:03:15	2:03:15	2:03:15	2:03:15	2:18:15	4:00:00	4:00:00	8:00:00	8:00:00	8:00:00
isVentSched	T	T	T	T	T	T	T	T	T	T	T	T	T	T	T	T	T	F	F	F
isMechSched	F	F	F	F	F	F	F	F	F	F	F	F	F	F	F	T	T	T	F	F
controlState	Nml	Mech	Mech	Mech	Nml															
operateState	Nml	Smplg	Smpplg	Mech	Mech	Mech	Nml													
fanState	Nml	On																		
damperState	Nml	Closed																		
coolState	Nml	On	On	On	Nml															
FanVerify	F	F	F	F	F	F	F	F	T	T	T	T	T	T	T	T	T	T	T	T
Sensor Sampling	F	T	T	T	T	T	T	T	T	T	T	T	T	T	T	F	T	F	F	F
Value(Tz)	Err	72	72	72	72	72	72	72	72	72	72	72	72							
Value(Tamb)	Err	65	65	65	65	65	65	65	65	65	65	65								
Value(Hamb-DewP)	Err	62	62	62	62	62	62	62	Err	Err	Err									
Value(Tra)	Err																			
Value(Tsa)	Err																			
State(Tz Err)	Clr	Pnd	Clr																	
State(Tamb Err)	Clr	Clr	Pnd	Pnd	Pnd	Pnd	Pnd	Pnd	Clr											
State(Hamb Err)	Clr	Clr	Clr	Pnd	Pnd	Pnd	Pnd	Pnd	Pnd	Clr										
State(Freeze Danger)	Clr	Clr	Clr	Clr	Pnd	Clr														
State(High Hamb)	Clr	Clr	Clr	Clr	Clr	Pnd	Wting	Wting	Ltch	Ltch	Ltch	Ltch	Ltch	Clr						
State(Sufficient vent capacity)	Clr	Clr	Clr	Clr	Clr	Clr	Pnd	Wting	Wting	Wting	Wting	Wting	Wting	Clr						
State(TooCold Mech)	Clr																			
State(Heat DeltaT)	Clr																			
State(Heat Digin)	Clr																			

Note: Clr--Cleared, Pnd--Pending, Wting--Waiting, Ltch--Latched, Err--Error, T--True, F--False, Nml--Normal, Smpplg--Fan Sampling

6. Field test results

6.1 Overview of the field sites

One field site is the headquarters for Field Diagnostic Services, Inc. (FDSI) and is located outside of Philadelphia, PA. This site was used primarily to debug the implementation, since it is relatively easy to monitor and update the algorithm. The FDSI field site utilizes 2 rooftop units (RTUs). However, only one VM is installed and connected to one of the RTUs (RTU #1). The control of the second RTU is a slave to the first.

The second site is a Walgreens drug store located in Rialto, CA. Figure 6.1 shows a floorplan for the Walgreens store in Rialto. At this site, 5 VMs have been installed on 5 RTUs. Although there are 6 RTUs, only the 5 which serve the sales zone were implemented with night ventilation precooling. One of the VMs serves as the master controller, while the other units act as slaves. Tables 6.1 and 6.2 provide details concerning the building and rooftop units. Figure 6.2 shows one of the rooftop units. The field measurements for HVAC equipment included electric power, integrated electrical energy, and ambient, return, and mixed air temperature and humidity.

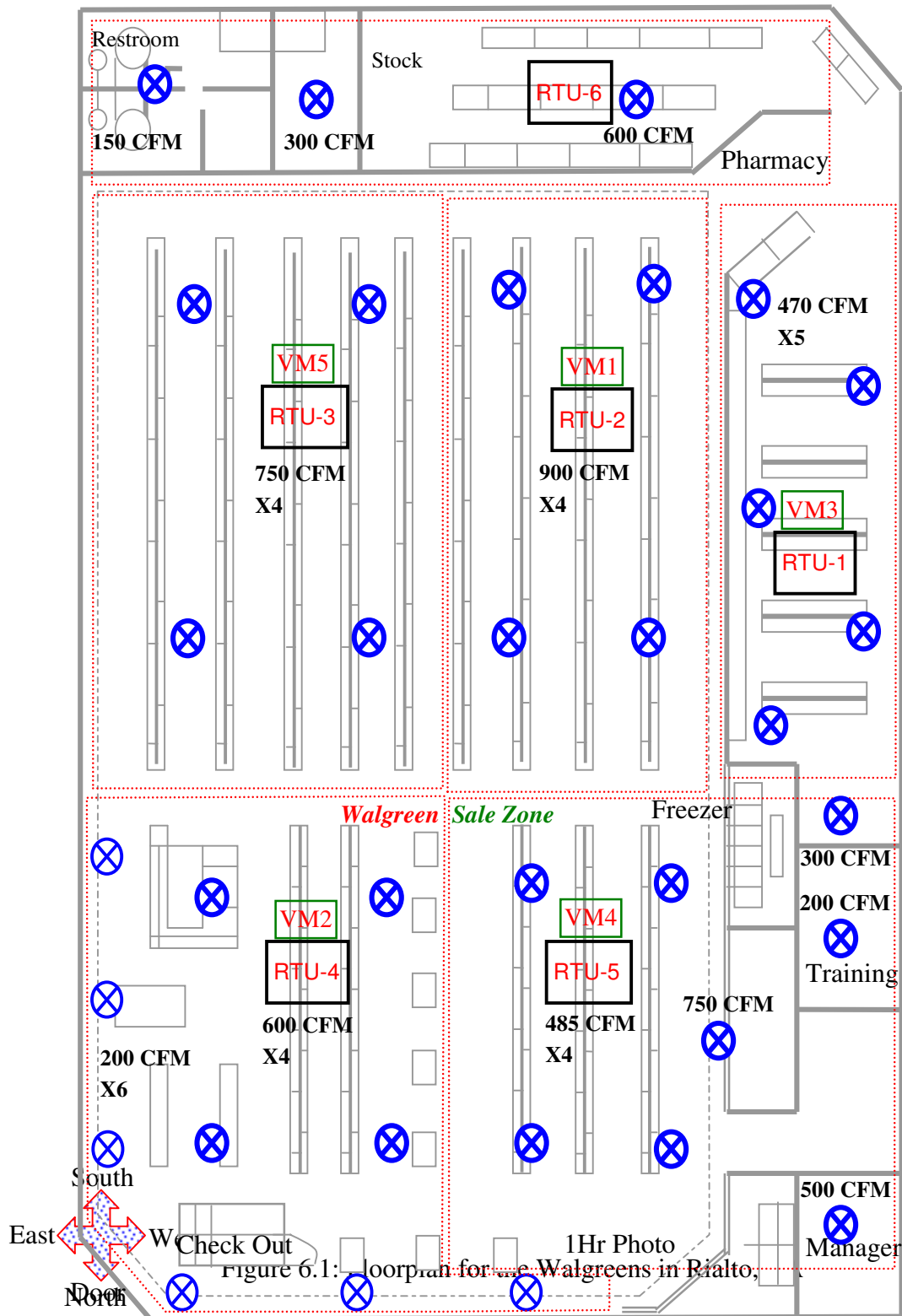


Figure 6.1: Floor plan for the Walgreens in Rialto.

Table 6.1: Rialto Store Description

<p>Floor Area</p>	<p>100 feet by 90 feet (9,000 sq. ft.) in retail store space, 40 feet by 20 feet in the pharmacy. An additional 35 feet by 90 feet of backroom storage and 20 feet by 100 feet for office and equipment that is not part of the DCV study.</p>
--------------------------	--

Building Orientation	Generally north - south, with front door on northeast corner.
Wall Construction	Brick and stucco exterior.
Windows/ Shading	A total of 20 windows on the two exterior walls to the retail store area. Windows are 5 feet by 8 feet, tinted, double-pane with ¼” air gap. Windows are on the east and north walls. A five-foot overhang covers the sidewalk and shades the exterior windows.
Roof/Ceiling Construction	Flat roof with light store coating.
Floor	Floor tiles over concrete slab.
Lighting	Retail store has total of 170 fixtures with 2 bulbs, 8-foot long fluorescent lights. Pharmacy has 33 fixtures of 2 bulbs, four-foot long fixtures.
Other Loads and Equipment	Refrigerated drink and food open to store, 25 feet linear feet. Freezer section with doors, 20 feet long. Photo processing machine plus two cash registers.
Occupancy Patterns	Store hours are 8 am to 10 pm, seven days a week.

Table 6.2: Rialto Rooftop Unit Description

Manufacturer	Trane
Model	WFD090C30BBC - Retail Store WFD075C30BBC - Pharmacy
Nominal Cooling Capacity	Retail store units - 7½ tons Retail store units - 6¼ tons
Number of Stages	1
SEER / HSPF	8.9 EER
Electrical	Three phase, 208 V
Supply Fan Performance	2,500 nominal supply airflow @ 0.5 in. w.c. - 6¼ tons 3,000 nominal supply airflow @ 0.5 in. w.c. - 7½ tons



Fig. 6.2: Trane rooftop heat pump installed on Walgreen's Rialto store

6.2 Web-Based Interface

Data were downloaded from the sites every day across phone lines and were accessible from a website. The website also allowed many different parameters of the control algorithm to be changed. For instance, it was possible to change the control mode between night setback, night ventilation, and night mechanical cooling. In addition, zone setpoints could be specified for each hour of the day. Also, the conditions necessary for enabling night ventilation could be changed.

6.3 Results for the FDSI site

The FDSI site has been primarily used to debug the precooling algorithm and not to evaluate energy savings. The algorithm was first implemented in August 2002 and relatively little data are available yet for documenting the performance of ventilation precooling. Figure 6.3 shows ambient and return air temperatures for a day where relatively little night ventilation precooling was performed. During occupancy, the return air temperature was about 71 °F. During the early morning hours, ventilation precooling occurred for about 30 minutes. This is evident because both the return air and ambient temperature sensor outputs dropped. During other times within the unoccupied period, both the return air and ambient temperatures are not meaningful because the fan is off. Another drop in the measured ambient temperature occurred

after the system returned to normal occupied mode since the fan turned on and the damper opened.

Figure 6.4 shows ambient temperature, return air temperature, fan control status, and compressor control status for a Monday where significant night ventilation precooling occurred. At 2 pm, the conditions were met for ventilation precooling and the fan turned on. The fan operated continuously until the return air temperature reached the setpoint of 67 °F at around 5:30 am. Then the fan cycled to maintain this setpoint until 7:30 am. At 7:30 am, the system returned to its normal operating condition, which means that the fan operates continuously and control reverts to the two-stage thermostat (1st stage for economizer and 2nd stage for compressor). It appears that compressor turned on briefly at this transition point, but then remained off until after 9 am. During the occupied period, the return air temperature was maintained at around 72 °F. However, there is a gap in the data between about 1 pm and 5 pm. The unoccupied mode began at 6 pm. At this point, the fan turned off, the zone temperature setpoint was raised, and the temperature floated. Again, it should be noted that the return air temperature is not meaningful when the fan is off.

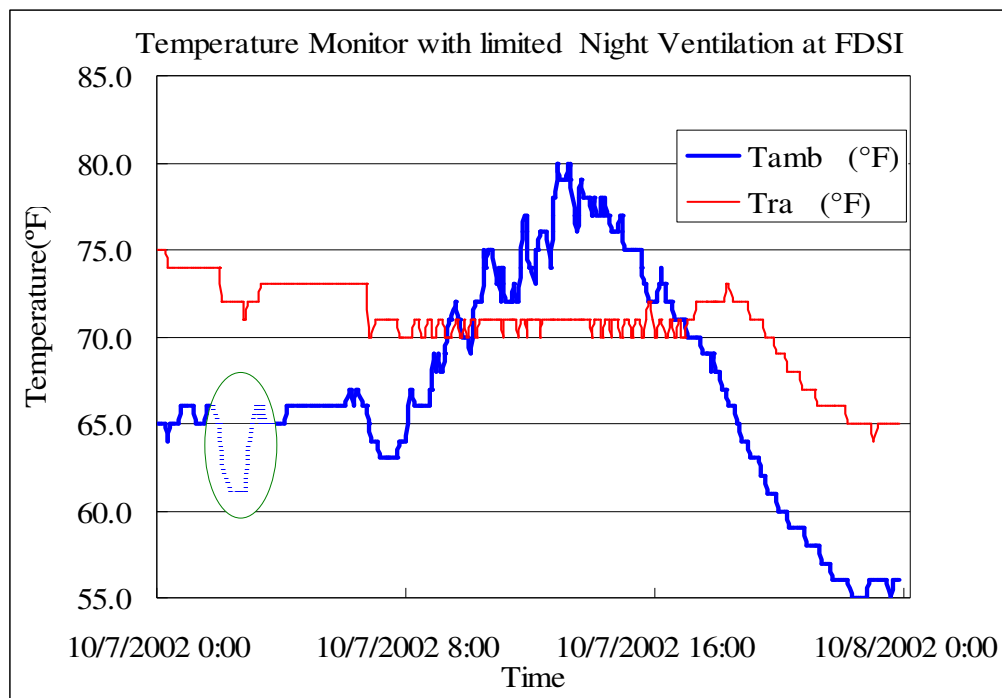


Figure 6.3: Ambient and return air temperatures with limited night ventilation precooling

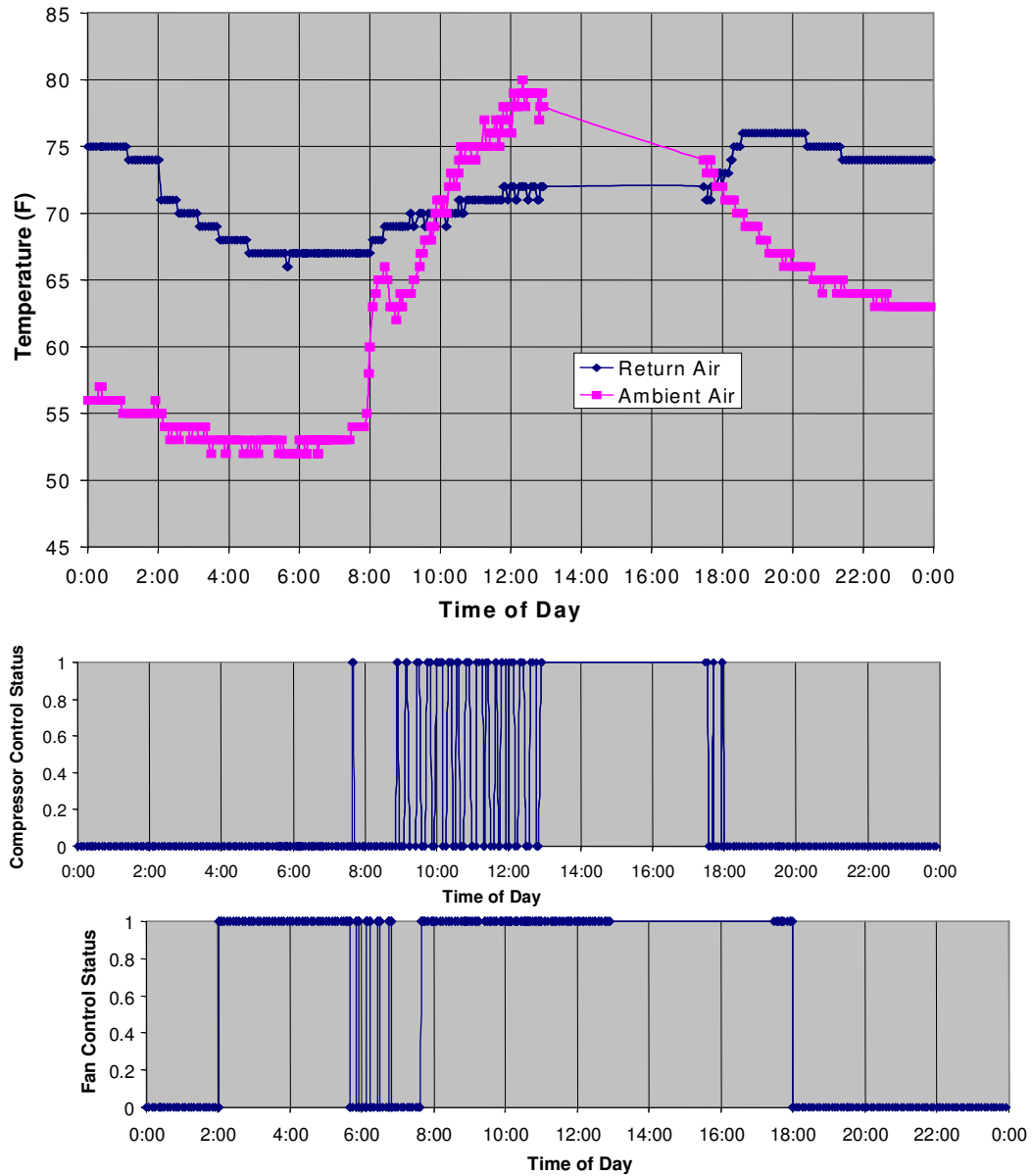


Figure 6.4: Night ventilation precooling results for Monday, 09/30/2002 at FDSI

6.4 Results from the Walgreen's

6.4.1 Resolution of Control and Data Acquisition Problems

There have been a number of problems at the Walgreen's field site, which were described in Deliverables 3.2.2a and 3.2.3a. The problems included: 1) intermittent communication failures and 2) inconsistent ambient and return air sensor readings and control decisions for the different units at the site.

Various testing and repairs were performed in late February and early March. New EPROM chips (CEC 030214 PRE D) were installed on the RTU at the Walgreen's. Most of the problems were rectified, including:

1. Consistent communication was restored;
2. Sensors installations were checked and corrected and have been working adequately;
3. The ambient temperature sensor used to evaluate whether night ventilation should be enabled was changed from a sensor in the ventilation air duct to a sensor at the inlet to the condenser coil. In addition, a backup algorithm was developed that utilizes the duct ventilation air sensor but opens the ventilation damper during the fan sampling mode. The sampling method can be switched using the web-based interface.
4. The algorithm used to coordinate control decisions for the different rooftop units was changed to allow a master/slave relationship.

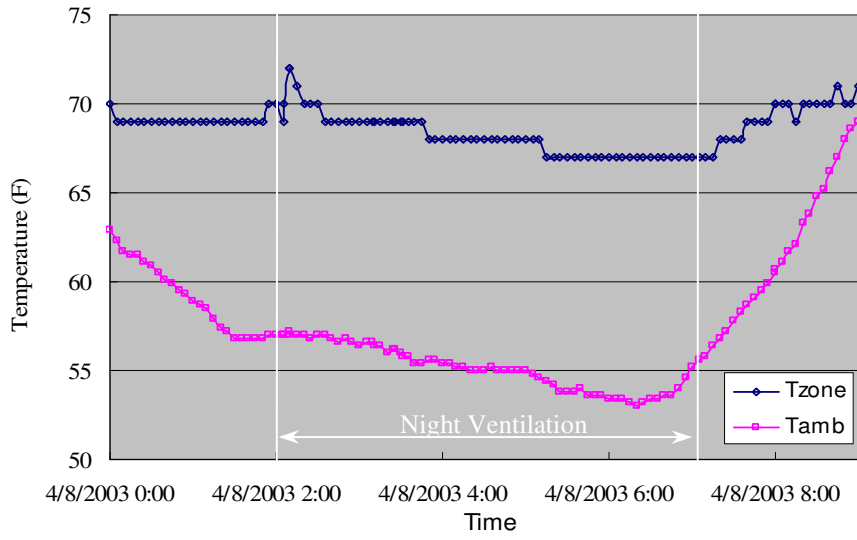
As a result of these changes, the control algorithm has been working properly. Table 6.3 provides a typical night ventilation control logic record for one of the units (VM1) at the Walgreen's on April 8, 2003. At 2:00 am, the night ventilation schedule criteria was met, and then at 2:04 AM, the control mode was changed to Night Ventilation, a Fan Sampling request was sent to turn on the fan, and the sensors' readings were collected. When the night ventilation requirements were met ($T_{zone} \geq 67^{\circ}\text{F}$, $T_{amb} \geq 50^{\circ}\text{F}$, $T_{zone} - T_{amb} \geq 10^{\circ}\text{F}$ and dewpoint of ambient air $\geq 55^{\circ}\text{F}$), the night ventilation was turned ON, and the damper changed to be OPEN. At 3:11 am, a sensor reading error occurred ($T_z = -46.4^{\circ}\text{F}$) which led to the night ventilation algorithm shutting down. However, after 15 minutes (the default time interval for another round of fan sampling), a second fan sampling request was sent and at this time the T_z reading was correct and another round of night ventilation was performed. Fig. 6.5a shows ambient and zone temperatures during the nighttime for VM1 on this day.

Night ventilation occurred during a 5-hour period where the ambient temperature was between about 57°F and 54°F. The zone temperature reached the setpoint of 67°F after about 3 hours and was maintained for the rest of the period. Fig. 6.5b shows ambient and zone temperatures during the daytime period, while Fig. 6.5c shows the power associated with the rooftop unit. The use of night ventilation precooling kept the zone temperature below the occupied period setpoint until about 10:00 am and the unit did not turn on until that time.

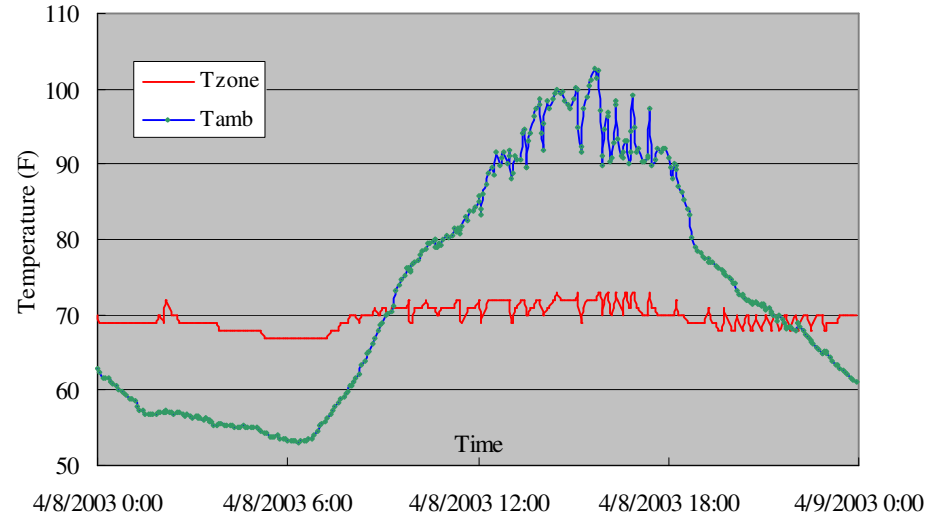
Table 6.3: Night Ventilation Control Logic record of VM1 at the Walgreen's

VM	Timestamp	IsVent	Control	Operate	FanState	Damper	Fan	Sampling	Tamb	Tz
1	4/8/2003 2:00	T	Nrm	Nrm	Nrm	Nrm	F	F	Err	Err
1	4/8/2003 2:04	T	Vent	FSmp	On	Closed	F	T	Err	Err
1	4/8/2003 2:09	T	Vent	Vent	On	Open	T	F	57.2	72.2
1	4/8/2003 3:11	T	Vent	Nrm	Nrm	Nrm	T	F	56.4	-46.4*
1	4/8/2003 3:26	T	Vent	FSmp	On	Closed	F	T	56.2	Err
1	4/8/2003 3:31	T	Vent	Vent	On	Open	T	F	55.8	69.8
1	4/8/2003 4:00	T	Vent	Vent	On	Open	T	F	55.4	68.6
1	4/8/2003 7:00	F	Vent	Vent	On	Open	T	F	55.2	67.4
1	4/8/2003 7:00	F	Vent	Vent	On	Open	T	F	55.2	67.4
1	4/8/2003 7:00	F	Nrm	Nrm	Nrm	Nrm	T	F	55.2	67.4

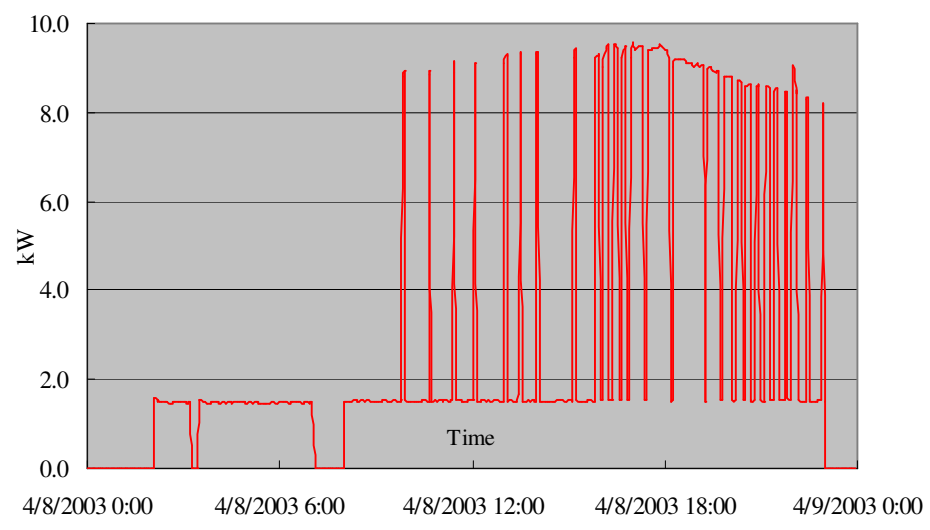
Note*: unreasonable data due to sensor temporary error



a. precooling conditions for VM1



b. daytime conditions for VM1



c. rooftop unit power

Fig. 6.5: Night ventilation precooling conditions for VM1 at the Walgreen's

Table 6.4 illustrates coordination of the 5 VMs at the Walgreen's. When the master VM (VM1) sent a Fan Sampling request, as expected, the slave VMs followed the master so that the whole system began fan sampling at the same time. All the VMs met the ventilation precooling requirement and then all the VMs ran in night ventilation precooling operation. However, there was an unreasonable Tz sensor reading at 3:11 am that broke the night ventilation requirements for VM1. However, night ventilation precooling was only stopped for VM1, while the slave VMs continued night ventilation. Once night ventilation has begun, the slave VMs use their own sensors to determine if the precooling condition is met. 15 minutes later after the bad sensor reading, VM1 began a new Fan Sampling and returned night ventilation mode. When one of the slave VMs (e.g, VM4 at 5:52 am) achieves the zone setpoint, the other units can continue to precool.

Table 6.4: Coordination of the VMs at the Walgreen's

VM	timestamp	isVent	control	operate	fanState	Damper	Cool	Fan	Sampling	Tamb	Tz
1	4/8/2003 2:00	T	Nrm	Nrm	Nrm	Nrm	Nrm	F	F	Err	Err
1	4/8/2003 2:04	T	Vent	FSmp	On	Closed	Nrm	F	T	Err	Err
1	4/8/2003 2:09	T	Vent	Vent	On	Open	Nrm	T	F	57.2	72.2
1	4/8/2003 3:11	T	Vent	Nrm	Nrm	Nrm	Nrm	T	F	56.4	-46.4*
1	4/8/2003 3:26	T	Vent	FSmp	On	Closed	Nrm	F	T	56.2	Err
1	4/8/2003 4:00	T	Vent	Vent	On	Open	Nrm	T	F	55.4	68.6
1	4/8/2003 7:00	F	Vent	Vent	On	Open	Nrm	T	F	55.2	67.4
2	4/8/2003 2:00	T	Nrm	Nrm	Nrm	Nrm	Nrm	F	F	Err	Err
2	4/8/2003 2:08	T	Vent	FSmp	On	Closed	Nrm	F	T	Err	Err
2	4/8/2003 2:13	T	Vent	Vent	On	Open	Nrm	T	F	57.4	72.4
2	4/8/2003 4:00	T	Vent	Vent	On	Open	Nrm	T	F	56	69.2
2	4/8/2003 7:00	F	Vent	Vent	On	Open	Nrm	T	F	54.8	68.2
3	4/8/2003 2:00	T	Nrm	Nrm	Nrm	Nrm	Nrm	F	F	Err	Err
3	4/8/2003 2:08	T	Vent	FSmp	On	Closed	Nrm	F	T	Err	Err
3	4/8/2003 2:13	T	Vent	Vent	On	Open	Nrm	T	F	58.1	72.2
3	4/8/2003 4:00	T	Vent	Vent	On	Open	Nrm	T	F	56.8	71
3	4/8/2003 7:00	F	Vent	Vent	On	Open	Nrm	T	F	62.7	69.4
4	4/8/2003 2:00	T	Nrm	Nrm	Nrm	Nrm	Nrm	T	F	Err	Err
4	4/8/2003 2:08	T	Vent	FSmp	On	Closed	Nrm	T	F	57.8	71.8
4	4/8/2003 4:00	T	Vent	Vent	On	Open	Nrm	T	F	56.6	68.2
4	4/8/2003 5:52	T	Vent	Nrm	Nrm	Nrm	Nrm	T	F	55.2	67
4	4/8/2003 7:00	F	Vent	Nrm	Nrm	Nrm	Nrm	T	F	56.4	67.8
5	4/8/2003 2:00	T	Nrm	Nrm	Nrm	Nrm	Nrm	F	F	Err	Err
5	4/8/2003 2:08	T	Vent	FSmp	On	Closed	Nrm	F	T	Err	Err
5	4/8/2003 2:14	T	Vent	Vent	On	Open	Nrm	T	F	57.9	72
5	4/8/2003 4:00	T	Vent	Vent	On	Open	Nrm	T	F	55.8	68.6
5	4/8/2003 7:00	F	Vent	Vent	On	Open	Nrm	T	F	55	67.8

Note*: unreasonable data due to sensor temporary error

6.4.2 Evaluating Energy Savings

Comparison field tests were designed whereby the control strategy would switch on a weekly basis between night ventilation precooling and conventional night setup. Week by week tests were started at the Rialto Walgreens on Monday, April 7, 2003. The goal was to compare energy consumption with and without night ventilation. During the first week the system was setup to run under night ventilation precooling and the second week the system reverted to night setup control. Each RTU's daily electricity consumption and the daily electricity consumption summation for these two weeks are listed in Table 6.5.

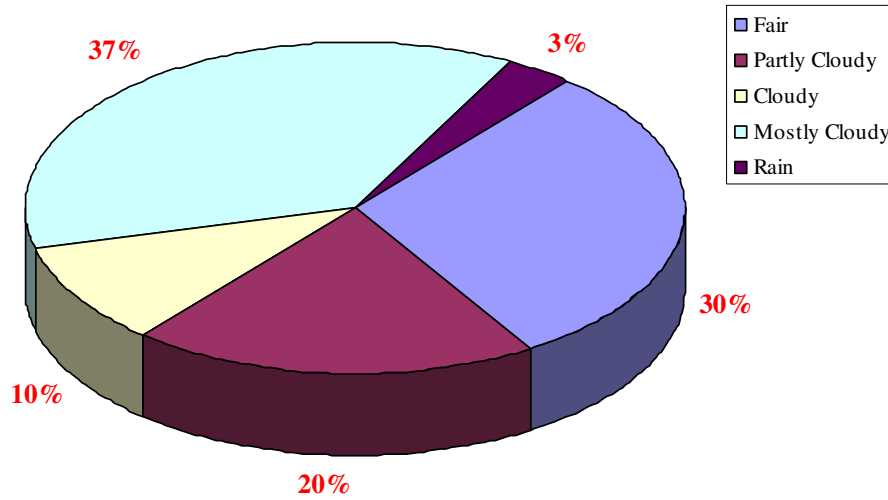
Table 6.5: Comparison Test results (the first two weeks) at the Walgreen's, Rialto

Operation	Time		Tamb_hi (°F)	Tamb_low (°F)	VM1 (kWh)	VM2 (kWh)	VM3 (kWh)	VM4 (kWh)	VM5 (kWh)	Sum (kWh)
Week 1 with Night Vent.	8-Apr	Tue	85	50	67.4	27.4	5.2	62.5	102.7	265.2
	9-Apr	Wed	81	50	94.7	26.8	5.2	43.1	99.8	269.6
	10-Apr	Thu	74	48	66.9	25.2	9.7	39.4	87.1	228.3
	11-Apr	Fri	70	47	47.6	23.4	5.1	39.2	72.7	188
	12-Apr	Sat	68	47	40.8	23.8	6.1	41.4	73.8	185.9
	13-Apr	Sun	65	47	40.7	22.9	4.4	37.6	69.6	175.2
	14-Apr	Mon	62	44	25.1	22.7	4.4	40.1	25.8	118.1
Week 2 w/o Night Vent.	15-Apr	Tue	65	44	24.3	21	1.4	48.5	31.3	126.5
	16-Apr	Wed	69	46	28.1	20.2	1.5	38.7	59.6	148.1
	17-Apr	Thu	64	45	26.4	19.1	0.8	35.6	34.2	116.1
	18-Apr	Fri	67	46	25.2	19.2	0	58.6	31.7	134.7
	19-Apr	Sat	67	46	44.8	18.9	0.6	37.4	77	178.7
	20-Apr	Sun	67	46	58	18.7	0.7	38.3	88.6	204.3
	21-Apr	Mon	69	45	40.6	18.6	0.5	37	46.5	143.2

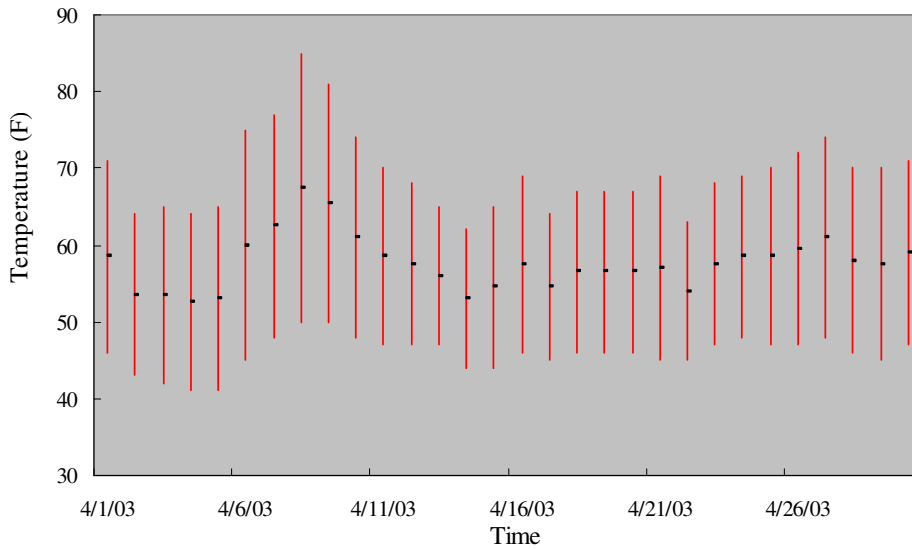
At the very beginning of the first week, the weather conditions were favorable for night ventilation. However, it got very cool after April 10th and the conditions were no longer appropriate for night ventilation. Fig. 6.6 shows weather statistics for Rialto during April. Most of the weather was cloudy with low ambient temperatures. The average daily high temperature for April was 69.4°F, whereas the average daily low was 45.9°F. This is much cooler than usual. Because of the low ambient temperatures, the economizer could handle most of the cooling load and night ventilation was not particularly effect.

The original goal was to find two comparable weeks of weather where the energy consumption of night ventilation and night setup control could be compared. However, cloudy and rainy weather lasted for more than one month, and in the middle of May,

the temperature increased sharply to the point where significant night ventilation precooling was not possible.



a. sky conditions at Rialto during April



b. temperature conditions (average, high, and low) at Rialto during April

Figure 6.6: Weather statistics for Rialto during April, 2003

In addition, to the weather conditions not being favorable for night ventilation precooling comparisons, there were other problems that make it difficult to perform comparative tests for night ventilation precooling at this site:

1. Lack of a Return Air Damper

There are no return air dampers equipped on the RTUs at this site. As a result, it is not possible to get 100% outside air during ventilation precooling. This severely limits the potential for precooling at this site. Fig. 6.7 shows ambient, zone, and supply air temperature during a night having successful night ventilation. Because of the lack of return air damper, return air is mixed with ambient air and the supply air temperature is much higher than the ambient temperature.

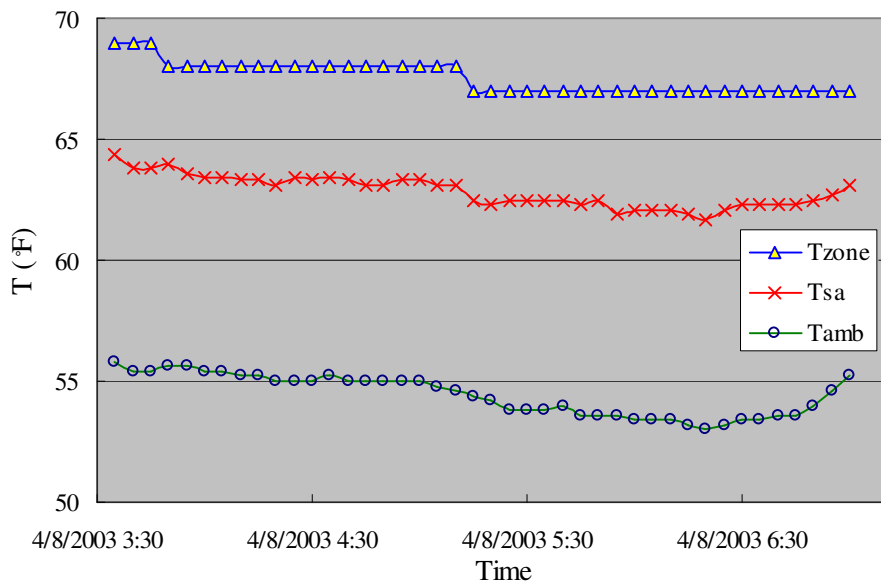


Fig. 6.7: Night ventilation precooling for VM1 at the Walgreen's

Precooling data are listed in Table 6.6 for this nighttime period. The night ventilation precooling capacity was calculated using air flow rate from the manufacturers data, so that

$$\dot{Q} = \dot{V} \times \rho \times cp \times (T_{zone} - T_{sa}) \quad (6.1)$$

Table 6.6 shows example values for precooling capacity at 5-minute intervals at selected times during the night. These data were also used to compute a total precooling effect, which is the integrated precooling due to night ventilation at any time during the night. Precooling effect data are also shown in Table 6.7 for this particular night. An equivalent COP is defined as the ratio of the total precooling effect during the night ventilation period divided by the integrated fan electrical consumption. For this day, the equivalent COP for night ventilation precooling was estimated to be 3.8.

Much better precooling effects and COPs would be achieved if the system were equipped with a return air damper that would close during night ventilation precooling.

Table 6.6 presents calculated maximum precooling capacities and effects determined using the data assuming 100% outside air for ventilation precooling. For this case, the equivalent COP increases to 8.5. A return air damper is necessary to achieve significant savings with night ventilation precooling.

Table 6.6: Night ventilation precooling of VM1 at Walgreen's

TIME	Tamb (°F)	Tsa (°F)	Tzone (°F)	Fan Power (kW)	Electr. Energy (kWh)	Precooling Capacity (kW)	Precooling Effect (kWh)	Max Precooling Capacity (kW)*	Max Precooling Effect (kWh)*
4/8/2003 3:35	55.8	64.4	69	1.5	0.0	5.15	0.00	12.53	0.00
4/8/2003 3:40	55.4	63.8	69	1.48	0.1	5.82	0.43	12.98	1.04
4/8/2003 3:45	55.4	63.8	69	1.46	0.3	5.82	0.91	12.98	2.13
4/8/2003 3:50	55.6	64	68	1.47	0.4	4.47	1.40	11.63	3.21
4/8/2003 3:55	55.6	63.6	68	1.48	0.5	4.92	1.77	11.63	4.18
4/8/2003 4:00	55.4	63.4	68	1.48	0.6	5.15	2.18	11.86	5.15
4/8/2003 4:05	55.4	63.4	68	1.49	0.7	5.15	2.61	11.86	6.13
4/8/2003 4:10	55.2	63.3	68	1.47	0.8	5.26	3.04	12.08	7.12
.....
4/8/2003 6:40	53.6	62.3	67	1.47	4.3	5.26	16.79	12.75	40.65
4/8/2003 6:45	53.6	62.3	67	1.45	4.4	5.26	17.23	12.75	41.67
4/8/2003 6:50	54	62.5	67	1.49	4.5	5.03	17.65	12.31	42.64
4/8/2003 6:55	54.6	62.7	67	1.47	4.7	4.81	18.05	11.63	43.56
4/8/2003 7:00	55.2	63.1	67	1.48	4.8	4.36	18.41	10.96	40.65
Equivalent COP						3.8		8.5	

*Note: 2°F fan temperature increase has been taken into account, as $T_{sa} = T_{amb} + 2$

2. Floating occupied period thermostat cooling setpoints

Honeywell T7300 Series commercial thermostats are employed at the test site. Fig. 6.8 shows zone temperature and daily power condition of VM1 at the Walgreen's. Originally, the occupied cooling setpoints were set to be 74°F for all 5 VMs. However, from the daily zone temperature records, it could be found that the cooling setpoints changed randomly. If the Tstat cooling setpoints are not constant, it is more difficult to perform meaningful comparative tests for night ventilation and night setup. Some remedies were tried, such as updating the Tstat settings remotely on a daily basis, but the results were not significantly improve. All the Tstats appear to have this problem.

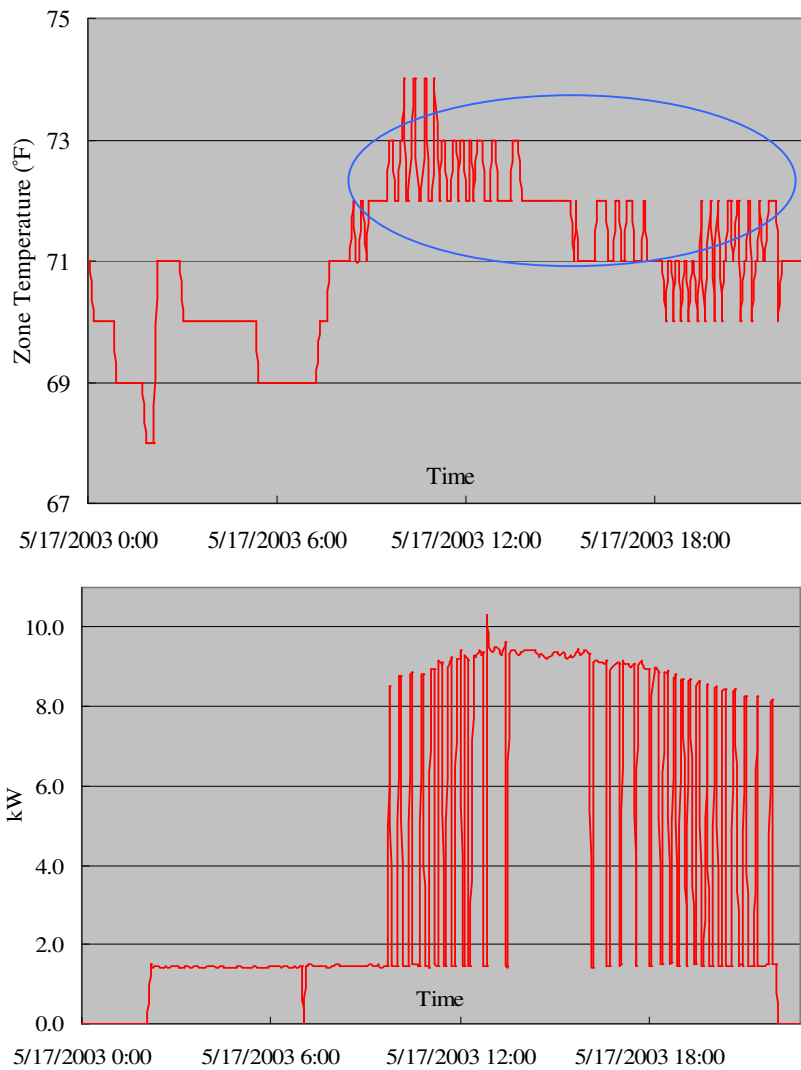


Fig. 6.8: Zone temperatures and RTU power for VM1 at Walgreen's

3. Damper Failure

The dampers for VM3 and VM4 have malfunctioned recently. As illustrated in Table 6.7, VM3's damper stays at 20% and VM4's damper is completely closed regardless of time and other conditions. It appears that damper relay for VM3 is broken. The problem with the VM4 damper appears to be in the control board.

Table 6.7: VM3 and VM4's damper condition

VM	TIME	Ta_cond	Tamb	Hamb	Tzone	Hzone	Tsa	KW	KWh	Damper	FAN1	COOL1
3	5/21/2003 2:15	69	68	45	76	39	75.1	1.17	170	20	0	0
3	5/21/2003 2:16	69	67	47	76	39	75.1	1.18	170.1	20	0	0
3	5/21/2003 2:20	69	67	50	76	40	74.9	1.18	170.1	20	0	0
3	5/21/2003 2:25	68.6	66	52	76	41	75.1	1.16	170.2	20	0	0
3	5/21/2003 2:30	68.4	66	53	76	41	75.1	1.16	170.3	20	0	0
4	5/21/2003 11:10	99.6	101	23	74	40	82.2	1.57	1785.9	0	1	1
4	5/21/2003 11:15	101.4	101	23	74	40	82.4	1.59	1786	0	1	1
4	5/21/2003 11:20	101.7	101	23	74	41	82.2	1.56	1786.1	0	1	1
4	5/21/2003 11:25	102.6	101	23	74	41	82.2	1.59	1786.2	0	1	1
4	5/21/2003 11:30	102.4	102	22	74	41	82.4	1.54	1786.3	0	1	1
4	5/21/2003 11:35	103.5	102	22	75	41	82.8	1.57	1786.4	0	1	1

4. Low refrigerant charge

The RTU associated with VM2 appears to be very low on refrigerant charge and has been shutting down due to low suction pressure. Fig. 6.9 shows an example for May 31, 2003. The zone temperature floats to fairly high values and yet the compressor does not stay on. Walgreens is aware of the problem, but it has yet to be fixed.

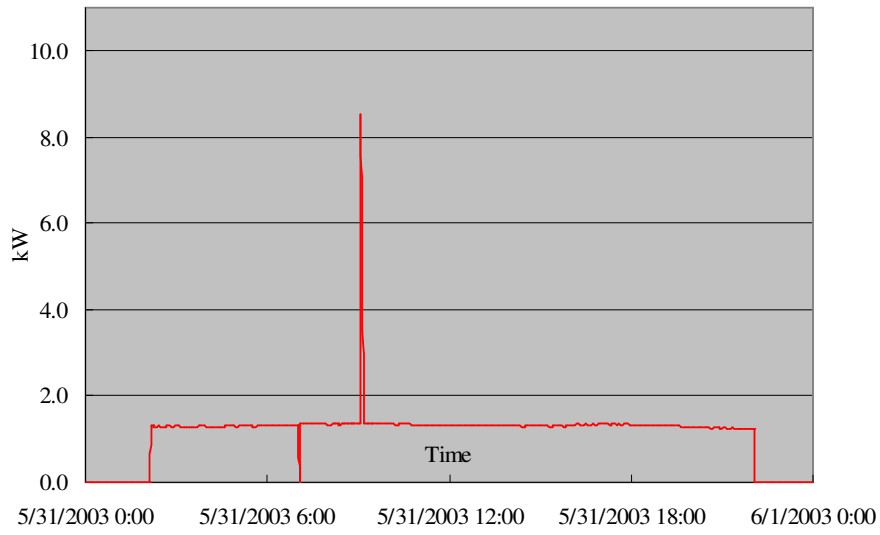
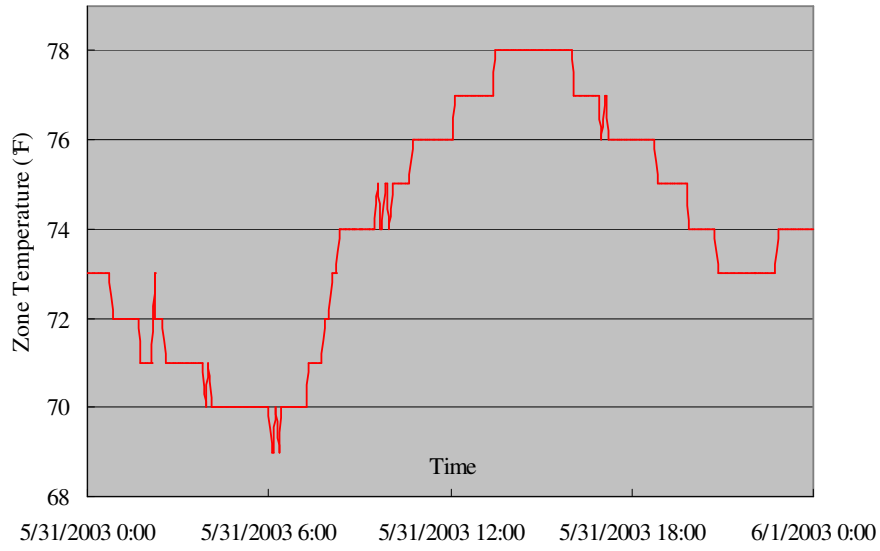


Fig. 6.9: Zone temperature and daily power condition of VM2 at Walgreen's

7. Summary

A simple night ventilation precooling algorithm was developed. Simulation results obtained using the default parameters in VSAT indicate that there are very significant (up to 53%) savings in compressor energy. However, the compressor savings are offset by increased fan energy and the overall electrical energy savings are relatively small (less than 8%). With time-of-use electricity and demand rates, the reductions in air conditioning demand costs (up to 28%) and total air conditioning costs (up to 17%) can be very significant. Fan and fan motor efficiencies have a very significant effect on the savings potential for night ventilation. Typically, fans that are employed within packaged equipment have very poor efficiencies (e.g., 15%). In many cases, the cost savings can nearly double if the fan efficiency is doubled. Thus, it is important to utilize efficient fans and fan motors in combination with night ventilation precooling. Even greater savings would be possible if efficient, variable-speed fan motors were employed.

The savings are also very sensitive to the utility rates. Greater savings are possible with higher ratios of on-peak to off-peak charges and on-peak periods that start earlier in the day. In addition, higher occupied period cooling setpoints, higher levels of internal thermal mass and the elimination of carpets increase savings.

The strategy can be implemented using the same sensors and control hardware employed within a economizer controller. Therefore, it should be cost effective to integrate night ventilation control with economizers for packaged equipment used in small commercial buildings. Even greater savings should be possible for packaged equipment that utilizes variable-speed fan control.

A simplified version of the control algorithm was implemented within two field sites. The first field site, located at the Field Diagnostic Services, Inc. (FDSI) headquarters near Philadelphia, PA, was used primarily for initial debugging of the implementation. Correct operation of the basic algorithm embedded in the controller was demonstrated using data from this site. The second field site is a Walgreens located in Rialto, CA. The Walgreens site employs five rooftop units (RTUs) each with a controller that provides ventilation precooling under the appropriate conditions. The algorithm was shown to work properly, but there were difficulties in demonstrating energy savings at the site due to several problems, including: 1) unfavorable weather conditions for night ventilation this past spring, 2) lack of a return air damper limited the amount of ventilation precooling that is possible, 3) uncontrolled changes in occupied period setpoints, 4) service problems with the RTUs.

Currently, the site is being used to explore the potential for use of mechanical precooling with demand-limiting during the on-peak period.

8. References

- Andresen, I. and Brandemuehl, M.J., 1992, "Heat storage in building thermal mass: a parametric study," *ASHRAE Transactions*, Vol. 98, Part 1.
- Andrews, J.W., Piraino, M., and Strasser, J. 1993. "Laboratory Testing of Control Strategies to Reduce Peak Air-Conditioning Loads," *ASHRAE Transactions*, Vol. 98, Part 1, pp. 910-918.
- ASHRAE, ANSI/ASHRAE Standard 62-1999 - Ventilation for Acceptable Indoor Air Quality (1999). Atlanta: American Society of Heating, Refrigerating and Air-Conditioning Engineers, Inc.
- Balcomb, J. D. (2002), *Mastering Energy-10: A User Manual for Version 1.5*, National Renewable Energy Laboratory, Golden, CO.
- Brandemuehl, M.J. and Braun, James E. (2002), *The Savings Estimator*, Honeywell International Inc., Morristown, NJ., <http://thermal.ies.lafayette.in.us/savest>
- Braun, J.E., 1990, "Reducing energy costs and peak electrical demand through optimal control of building thermal storage," *ASHRAE Transactions*, Vol. 96, Pt. 2, pp. 876-888.
- Braun, J.E., Montgomery, K.W., and Chaturvedi, N., 2001, "Evaluating the performance of building thermal mass control strategies," *International Journal of Heating, Ventilating, Air-Conditioning and Refrigeration Research*, Vol. 7, No. 4, pp. 403-428.
- Braun, J.E., Lawrence, T.M, Klaassen, C.J., and House, J.M., 2002, "Demonstration of load shifting and peak load reduction with control of building thermal mass," Proceedings of the 2002 ACEEE Conference on Energy Efficiency in Buildings, Monterey, CA.
- Braun, J.E., and Mercer, K., 2003. VSAT-Ventilation Strategy Assessment Tool, Deliverables 3.1.2, 3.2.1 and 4.2.2 to California Energy Commission.
- Braun, J.E., and Zhong, Z., 2003. Development and Initial Evaluation of a Night Ventilation Precooling Algorithm, Deliverables 3.2.2a and 3.2.3a to California Energy Commission.
- Geros, V., 1999. "Experimental evaluation of night ventilation phenomena," *Energy and Buildings*, 29, 141-154.
- Givoni, B., 1998. "Effectiveness of mass and night ventilation in lowering the indoor daytime temperature - Part I," *Energy and Buildings*, 28, 25-32.
- Keeney, K.R. and Braun, J.E., 1995. Building characteristics and control strategies for use of building thermal mass in cooling, Technical Report 734-RP, Atlanta: American Society of Heating, Refrigerating and Air-Conditioning Engineers, Inc.
- Keeney, K.R. and Braun, J.E., 1997, "Application of building precooling to reduce peak cooling requirements," *ASHRAE Transactions*, Vol. 103, Pt. 1, pp. 463-469.

- Klein, S.A. and Beckman, W.A., 1996-2001, FEHT- Finite Element Heat Transfer, Version 7.161.
- Kolokotroni, M. and Aronis, A., 1999. "Cooling-energy reduction in air-conditioned offices by using night ventilation," *Applied Energy*, 63, 241-253.
- Morris, F.B., Braun, J.E., and Treado, S.J., 1994, "Experimental and simulated performance of optimal control of building thermal storage," *ASHRAE Transactions*, Vol. 100, Pt. 1, pp. 402-414.
- Popiel, C.O., 2001, "Measurement of temperature distribution in ground", *Experimental thermal and fluid science*, Vol. 25, pp. 301-309.
- Rabl, A. and Norford, L.K., 1991, "Peak load reduction by preconditioning buildings at night," *International Journal of Energy Research* 15: 781-798.
- Shaviv, E., 2001. "Thermal mass and night ventilation as passive cooling design strategy," *Renewable Energy*, 24, 445-452.
- Snyder, M.E. and Newell, T.A., 1990, "Cooling cost minimization using building mass for thermal storage," *ASHRAE Transactions*, Vol. 96, Pt. 2, pp. 830-838.
- TRNSYS (2000), *TRNSYS Users Guide: A Transient Simulation Program*, Solar Energy Laboratory, University of Wisconsin-Madison. <http://sel.me.wisc.edu/trnsys/>
- Zhong, Z. 2001. "Study on the thermal performance of PCM wallboard rooms under night Ventilation," Masters Degree Thesis, Tsinghua University, China.

APPENDIX A – PROTOTYPICAL BUILDING DESCRIPTIONS

Seven different types of buildings are considered in VSAT: small office, school class wing, retail store, restaurant dining area, school gymnasium, school library, and school auditorium. Descriptions for these buildings were obtained from prototypical building descriptions of commercial building prototypes developed by Lawrence Berkeley National Laboratory (Huang, et al. 1990 & Huang, et al. 1995). These reports served as the primary sources for prototypical building data. However, additional information was obtained from DOE-2 input files used by the researchers for their studies.

Tables A.1 – A.7 contain information on the geometry, construction materials, and internal gains used in modeling the different buildings. Although not given in these tables, the walls, roofs and floors include inside air and outside air thermal resistances. The window R-value includes the effects of the window construction and inside and outside air resistances. Table 8 lists the properties of all construction materials and the air resistances. The geometry of each of the buildings is assumed to be rectangular with four sides and is specified with the following parameters: 1) floor area, 2) number of stories, 3) aspect ratio, 4) ratio of exterior perimeter to total perimeter, 5) wall height and 6) ratio of glass area to wall area. The aspect ratio is the ratio of the width to the length of the building. However, exterior perimeter and glass areas are assumed to be equally distributed on all sides of the building, giving equal exposure of exterior walls and windows to incident solar radiation. The four exterior walls face north, south, east, and west.

The user can specify occupancy schedules, but default values are based upon the original LBNL study. In the LBNL study, the occupancy was scaled relative to a daily average maximum occupancy density (people per 1000 ft²). In VSAT, the user can specify a peak design occupancy density (people per 1000 ft²) that is used for determining fixed ventilation requirements (no DCV). This same design occupancy density is used as the scaling factor for the hourly occupancy schedules. As a result, the original LBNL occupancy schedules were rescaled using the default peak design occupancy densities.

The heat gains and CO₂ generation per person depend upon the type of building (and associated activity). Design internal gains for lights and equipment also depend upon the building and are scaled according to specified average daily minimum and maximum gain fractions. For all of the buildings, the lights and equipment are at their average maximum values whenever the building is occupied and are at their average minimum values at all other times.

Zone thermostat setpoints can be set for both occupied and unoccupied periods. The default occupied setpoints for cooling and heating are 75°F and 70°F, respectively. The default unoccupied setpoints for cooling (setup) and heating (setback) are 85°F and 60°F, respectively. The lights are assumed to come on one hour before people arrive and stay on one hour after they leave. The occupied and unoccupied setpoints follow this same schedule.

Table A.1. Office Building Characteristics

Windows		
R-value, hr-ft ² -F/Btu	1.58	
Shading Coefficient	0.75	
Area ratio (window/wall)	0.15	
Exterior Wall Construction		
Layers	1" stone R-5.6 insulation R-0.89 airspace 5/8" gypsum	
Roof Construction		
Layers	Built-up roof (3/8") 4" lightweight concrete R-12.6 insulation R-0.92 airspace 1/2" acoustic tile	
Floor		
Layers	Carpet and pad 4" heavyweight concrete 6" pea gravel 2' soil	
Slab perimeter loss factor, Btu/h-ft-F	0.5	
General		
Floor area, ft ²	6600	
Wall height, ft	11	
Internal mass, lb/ft ²	25	
Number of stories	1	
Aspect Ratio	0.67	
Ratio of exterior perimeter to floor perimeter	1.0	
Design equipment gains, W/ft ²	0.5	
Design light gains, W/ft ²	1.7	
Ave. daily min. lights/equip. gain fraction	0.2	
Ave. daily max. lights/equip. gain fraction	0.9	
Sensible people gains, Btu/hr-person	250	
Latent people gains, Btu/hr-person	250	
CO ₂ people generation, L/min-person	0.33	
Design occupancy for vent., people/1000 ft ²	7	
Design ventilation, cfm/person	20	
Average weekday peak occupancy, ft ² /person	470	
Default average weekday occupancy schedule * Values given relative to average peak	Hours	Values
	1-7	0.0
	8	0.33
	9	0.66
	10-16	1.0
	17	0.5
	18-24	0.0
Default average weekend occupancy schedule * Values given relative to average peak	Hours	Values
	1-8	0.0
	9	0.15
	10-12	0.2
	12-13	0.15
	13-24	0.0
Monthly occupancy scaling * relative to daily occupancy schedule	Month	Value
	1-12	1.0

Table A.2. Restaurant Dining Area Characteristics

Windows		
R-value, hr-ft ² -F/Btu	1.53	
Shading Coefficient	0.8	
Area ratio (window/wall)	0.15	
Exterior Wall Construction		
Layers	3" face brick ½" plywood R-4.9 insulation 5/8" gypsum	
Roof Construction		
Layers	Built-up roof (3/8") ¾" plywood R-13.2 insulation R-0.92 airspace ½" acoustic tile	
Floor		
Layers	Carpet and pad 4" heavyweight concrete 6" pea gravel 2' soil	
Slab perimeter loss factor, Btu/h-ft-F	0.5	
General		
Floor area, ft ²	5250	
Wall height, ft	10	
Internal mass, lb/ft ²	25	
Number of stories	1	
Aspect Ratio	1.0	
Ratio of exterior perimeter to floor perimeter	0.75	
Design equipment gains, W/ft ²	0.0	
Design light gains, W/ft ²	2.0	
Ave. daily min. lights/equip. gain fraction	0.2	
Ave. daily max. lights/equip. gain fraction	1.0	
Sensible people gains, Btu/hr-person	250	
Latent people gains, Btu/hr-person	275	
CO ₂ people generation, L/min-person	0.35	
Design occupancy for vent., people/1000 ft ²	30	
Design ventilation, cfm/person	20	
Average weekday peak occupancy, ft ² /person	50	
Default average weekday occupancy schedule * Values given relative to average peak	Hours	Values
	1-6	0.0
	7-12	0.2,0.3,0.1,0.05,0.2,0.5
	13-24	0.5,0.4,0.2,0.05,0.1,0.4, 0.6,0.5,0.4,0.2,0.1,0.0
Default average weekend occupancy schedule * Values given relative to average peak	Hours	Values
	1-6	0.0
	7-12	0.3,0.4,0.5,0.2,0.2,0.3
	13-24	0.5,0.5,0.5,0.35,0.25, 0.5,0.8,0.8,0.7,0.4,0.2, 0.0
Monthly occupancy scaling * relative to daily occupancy schedule	Month	Value
	1-5	1.0
	6-8	0.5
	9-12	1.0

Table A.3. Retail Store Characteristics

Windows		
R-value, hr-ft ² -F/Btu	1.5	
Shading Coefficient	0.76	
Area ratio (window/wall)	0.15	
Exterior Wall Construction		
Layers	8" lightweight concrete R-4.8 insulation R-0.89 airspace 5/8" gypsum	
Roof Construction		
Layers	Built-up roof (3/8") 1.25" lightweight concrete R-12 insulation R-0.92 airspace 1/2" acoustic tile	
Floor		
Layers	4" heavyweight concrete 6" pea gravel 2' soil	
Slab perimeter loss factor, Btu/h-ft-F	0.5	
General		
Floor area, ft ²	80,000	
Wall height, ft	15	
Internal mass, lb/ft ²	25	
Number of stories	2	
Aspect Ratio	0.5	
Ratio of exterior perimeter to floor perimeter	1.0	
Design equipment gains, W/ft ²	0.4	
Design light gains, W/ft ²	1.6	
Ave. daily min. lights/equip. gain fraction	0.2	
Ave. daily max. lights/equip. gain fraction	0.9	
Sensible people gains, Btu/hr-person	250	
Latent people gains, Btu/hr-person	250	
CO ₂ people generation, L/min-person	0.33	
Design occupancy for vent., people/1000 ft ²	25	
Design ventilation, cfm/person	15	
Average weekday peak occupancy, ft ² /person	390	
Default average weekday occupancy schedule * Values given relative to average peak	Hours	Values
	1-7	0.0
	8	0.33
	9	0.66
	10-20	1.0
	21	0.5
Default average weekend occupancy schedule * Values given relative to average peak	Hours	Values
	1-7	0.0
	8	0.33
	9	0.66
	10-20	1.0
	21	0.5
Monthly occupancy scaling * relative to daily occupancy schedule	Month	Value
	1-12	1.0

Table A.4. School Class Wing Characteristics

Windows		
R-value, hr-ft ² -F/Btu	1.7	
Shading Coefficient	0.73	
Area ratio (window/wall)	0.18	
Exterior Wall Construction		
Layers	8" concrete block R-5.7 insulation 5/8" gypsum	
Roof Construction		
Layers	Built-up roof (3/8") 3/4" plywood R-13.3 insulation R-0.92 airspace 1/2" acoustic tile	
Floor		
Layers	6" heavyweight concrete 6" pea gravel 2' soil	
Slab perimeter loss factor, Btu/h-ft-F	0.5	
General		
Floor area, ft ²	9600	
Internal mass, lb/ft ²	25	
Wall height, ft	10	
Number of stories	2	
Aspect Ratio	0.5	
Ratio of exterior perimeter to floor perimeter	0.875	
Design equipment gains, W/ft ²	0.3	
Design light gains, W/ft ²	2.2	
Ave. daily min. lights/equip. gain fraction	0.1	
Ave. daily max. lights/equip. gain fraction	0.95	
Sensible people gains, Btu/hr-person	250	
Latent people gains, Btu/hr-person	200	
CO ₂ people generation, L/min-person	0.3	
Design occupancy for vent., people/1000 ft ²	25	
Design ventilation, cfm/person	15	
Average weekday peak occupancy, ft ² /person	50	
Default average weekday occupancy schedule * Values given relative to average peak	Hours	Values
	1-6	0.0
	7	0.1
	8-11	0.9
	12-15	0.8
	16	0.45
	17	0.15
	18	0.05
	19-21	0.33
22-24	0.0	
Default average weekend occupancy schedule * Values given relative to average peak	Hours	Value
	1-9	0.0
	10-13	0.1
	14-24	0.0
Monthly occupancy scaling * relative to daily occupancy schedule	Month	Value
	1-5	1.0
	6-8	0.5
	9-12	1.0

Table A.5. School Gymnasium Characteristics

Windows		
R-value, hr-ft ² -F/Btu	1.7	
Shading Coefficient	0.73	
Area ratio (window/wall)	0.18	
Exterior Wall Construction		
Layers	8" concrete block R-5.7 insulation 5/8" gypsum	
Roof Construction		
Layers	Built-up roof (3/8") 3/4" plywood R-13.3 insulation R-0.92 airspace 1/2" acoustic tile	
Floor		
Layers	6" heavyweight concrete 6" pea gravel 2' soil	
Slab perimeter loss factor, Btu/h-ft-F	0.5	
General		
Floor area, ft ²	7500	
Internal mass, lb/ft ²	25	
Wall height, ft	32	
Number of stories	1	
Aspect Ratio	0.86	
Ratio of exterior perimeter to floor perimeter	0.86	
Design equipment gains, W/ft ²	0.2	
Design light gains, W/ft ²	0.65	
Ave. daily min. lights/equip. gain fraction	0.0	
Ave. daily max. lights/equip. gain fraction	0.9	
Sensible people gains, Btu/hr-person	250	
Latent people gains, Btu/hr-person	550	
CO ₂ people generation, L/min-person	0.55	
Design occupancy for vent., people/1000 ft ²	30	
Design ventilation, cfm/person	20	
Average weekday peak occupancy, ft ² /person	180	
Default average weekday occupancy schedule * Values given relative to average peak	Hours	Value
	1-7	0.0
	8-15	1.0
Default average weekend occupancy schedule * Values given relative to average peak	Hours	Value
	1-24	0.0
	Month	Value
Monthly occupancy scaling * relative to daily occupancy schedule	1-5	1.0
	6-8	0.1
	9-12	1.0

Table A.6. School Library Characteristics

Windows		
R-value, hr-ft ² -F/Btu	1.7	
Shading Coefficient	0.73	
Area ratio (window/wall)	0.18	
Exterior Wall Construction		
Layers	8" concrete block R-5.7 insulation 5/8" gypsum	
Roof Construction		
Layers	Built-up roof (3/8") ¾" plywood R-13.3 insulation R-0.92 airspace ½" acoustic tile	
Floor		
Layers	6" heavyweight concrete 6" pea gravel 2" soil	
Slab perimeter loss factor, Btu/h-ft-F	0.5	
General		
Floor area, ft ²	1500	
Internal mass, lb/ft ²	25	
Wall height, ft	10	
Number of stories	1	
Aspect Ratio	0.2	
Ratio of exterior perimeter to floor perimeter	0.75	
Design equipment gains, W/ft ²	0.4	
Design light gains, W/ft ²	1.5	
Ave. daily min. lights/equip. gain fraction	0.1	
Ave. daily max. lights/equip. gain fraction	0.95	
Sensible people gains, Btu/hr-person	250	
Latent people gains, Btu/hr-person	250	
CO ₂ people generation, L/min-person	0.33	
Design occupancy for vent., people/1000 ft ²	20	
Design ventilation, cfm/person	15	
Average weekday peak occupancy, ft ² /person	100	
Default average weekday occupancy schedule * Values given relative to average peak	Hours	Value
	1-6	0.0
	7	0.1
	8-11	0.9
	12-15	0.8
	16	0.45
	17	0.15
	18	0.05
	19-21	0.33
	22-24	0.0
Default average weekend occupancy schedule * Values given relative to average peak	Hours	Value
	1-9	0.0
	10-13	0.1
	14-24	0.0
Monthly occupancy scaling * relative to daily occupancy schedule	Month	Value
	1-5	1.0
	6-8	0.5
	9-12	1.0

Table A.7. School Auditorium Characteristics

Windows		
R-value, hr-ft ² -F/Btu	1.7	
Shading Coefficient	0.73	
Area ratio (window/wall)	0.18	
Exterior Wall Construction		
Layers	8" concrete block R-5.7 insulation 5/8" gypsum	
Roof Construction		
Layers	Built-up roof (3/8") 3/4" plywood R-13.3 insulation R-0.92 airspace 1/2" acoustic tile	
Floor		
Layers	6" heavyweight concrete 6" pea gravel 2' soil	
Slab perimeter loss factor, Btu/h-ft-F	0.5	
General		
Floor area, ft ²	6000	
Internal mass, lb/ft ²	25	
Wall height, ft	32	
Number of stories	1	
Aspect Ratio	0.64	
Ratio of exterior perimeter to floor perimeter	0.85	
Design equipment gains, W/ft ²	0.2	
Design light gains, W/ft ²	0.8	
Ave. daily min. lights/equip. gain fraction	0.0	
Ave. daily max. lights/equip. gain fraction	0.9	
Sensible people gains, Btu/hr-person	250	
Latent people gains, Btu/hr-person	200	
CO ₂ people generation, L/min-person	0.3	
Design occupancy for vent., people/1000 ft ²	150	
Design ventilation, cfm/person	15	
Average weekday peak occupancy, ft ² /person	100	
Default average weekday occupancy schedule * Values given relative to average peak	Hours	Values
	1-9	0.0
	10-11	0.75
	12	0.2
	13-14	0.75
15-24	0.0	
Default average weekend occupancy schedule * Values given relative to average peak	Hours	Value
	1-24	0.0
Monthly occupancy scaling * relative to daily occupancy schedule	Month	Value
	1-5	1.0
	6-8	0.1
	9-12	1.0

Table A.8. Construction Material Properties

Inside Air Resistance	
R_inside, hr-ft ² -F/Btu	0.670
R_outside, hr-ft ² -F/Btu	0.330
R_carpet, hr-ft ² -F/Btu	2.080
Lightweight Concrete (1.25", 4", 8")	
thermal conductivity, Btu/hr-ft-F	0.208
density, lbm/ft ³	80
specific heat, Btu/lbm-F	0.200
Heavyweight Concrete (4", 6")	
thermal conductivity, Btu/hr-ft-F	1.402
density, lbm/ft ³	140
specific heat, Btu/lbm-F	0.200
Face Brick (1")	
thermal conductivity, Btu/hr-ft-F	0.758
density, lbm/ft ³	130
specific heat, Btu/lbm-F	0.220
Stone Face (1")	
thermal conductivity, Btu/hr-ft-F	1.042
density, lbm/ft ³	140
specific heat, Btu/lbm-F	0.200
Gypsum (5/8")	
thermal conductivity, Btu/hr-ft-F	0.093
density, lbm/ft ³	50
specific heat, Btu/lbm-F	0.200
Plywood (1/2 ", 3/4")	
thermal conductivity, Btu/hr-ft-F	0.067
R_ply12, hr-ft ² -F/Btu	0.625
R_ply12, hr-ft ² -F/Btu	0.937
Acoustic Tile (1/2 ")	
thermal conductivity, Btu/hr-ft-F	0.033
density, lbm/ft ³	18
specific heat, Btu/lbm-F	0.320
Built up Roof (3/8")	
thermal conductivity, Btu/hr-ft-F	0.094
density, lbm/ft ³	70
specific heat, Btu/lbm-F	0.350
Soil (2')	
thermal conductivity, Btu/hr-ft-F	1.000
density, lbm/ft ³	115
specific heat, Btu/lbm-F	0.260
Pea Gravel (6")	
thermal conductivity, Btu/hr-ft-F	1.456
density, lbm/ft ³	121
specific heat, Btu/lbm-F	0.240
Ua	
perimeter heat loss factor, Btu/h-ft-F	0.85